Chlorine and Bromine Isotopic Analyses of Groundwaters and Porewaters from the Bruce Nuclear Site

by

Yinze Wang

A thesis

presented to the University of Waterloo

in fulfillment of the

thesis requirement for the degree of

Master of Science

in

Earth Sciences

Waterloo, Ontario, Canada, 2017

I hereby declare that I am the sole author of this thesis. This is a true copy of the thesis, including any required final revisions, as accepted by my examiners.

I understand that my thesis may be made electronically available to the public.

Abstract

This study reports chlorine ($\delta^{37}Cl$) and bromine ($\delta^{81}Br$) isotopic values for groundwaters and pore fluids from early Paleozoic (Cambrian to Devonian) sedimentary rocks at the Bruce Nuclear Site near Kincardine, Ontario, Canada. The Cl and Br isotope data, in conjunction with their concentration data, are used to ascertain fluid origins as well as to identify processes responsible for isotopic fractionation.

The sampled groundwaters and porewaters (from boreholes DGR-3/4) have isotopic and geochemical signatures similar to formation fluids from the same geological units elsewhere in the Michigan Basin, based on comparison with regional sedimentary formation water databases. The Silurian Salina A1 and Guelph Formation groundwaters, sourced within the Michigan Basin, have low $\delta^{81}Br$. The Salina A1 samples appear to have been altered by halite dissolution and mixing with cold climate recharge. In contrast, the Cambrian groundwaters have high $\delta^{37}Cl$ and $\delta^{81}Br$ values that are similar to Cambrian brines found in the Appalachian Basin to the east and south. The halide isotopic signatures of the Cambrian groundwaters suggest that these fluids may be very old, and their isotopic compositions have been preserved since emplacement during basinal fluid migration events in the early Paleozoic.

In general, Devonian to Cambrian porewaters at the site have similar $\delta^{37}Cl$ and $\delta^{81}Br$ values as fluid samples from equivalent geological units listed in the combined regional database compiled from Shouakar-Stash (2008), Hobbs et al. (2011) and Skuce et al. (2015). However, some Cambrian and Ordovician porewater samples have $\delta^{37}Cl$ and $\delta^{81}Br$ values that are distinctive from regional sedimentary groundwaters found in the equivalent units.

The Early Silurian to Late Ordovician stratigraphic sequence (~400 m thick) at the site has been effectively defined as a diffusion-dominated system (Clark et al. 2013; Al et al. 2015). However, $\delta^{37}Cl$ and $\delta^{81}Br$ values of the porewater samples at the site are not easily explained by a simple diffusion process across multiple geological layers of highly variable sedimentological characteristics. The halide isotopic profiles throughout the stratigraphic sequence was potentially impacted by several fractionation mechanisms over long geologic time frames. These physical or biological processes include organic and/or microbial halide gas production and degassing, salt dissolution, diagenesis/dolomitization (early Phanerozoic), tectonically-driven fluid migration

and/or hydrothermal fluid mixing (late Phanerozoic) as well as localized diffusional migration of porewater solutes within stratigraphic units. In addition, the initial depositional environment may have influenced the $\delta^{37}Cl$ and $\delta^{81}Br$ isotopic signatures of the sedimentary porewaters from the site. This depositional influence can be tied to temporal variations in the relative fluxes of continental weathering inputs and mantle inputs (degassing from ocean volcanic sources) of Cl and Br to seawater.

This study shows that an increased understanding of transport processes, and the origin and relative ages of potential end-member fluids, can be gained through the analyses of porewater Cl and Br isotope compositions together with chemical and isotopic parameters already used to assess solute longevity.

Acknowledgements

I wish to thank all the people who have assisted and made it possible for me to accomplish this thesis. First and foremost, I would sincerely like to express my great gratitude to my supervisor, Professor Shaun K. Frape, for his enormous guidance and invaluable advice, throughout this project. Shaun, you have been the best supervisor in my life. This would not have been possible without your continued encouragement and support. Your immense help and patience were most appreciated. I am deeply honored to have had the opportunity to learn from you and wish you all the best in the future.

In addition, I am grateful to my committee members, Professor Brian Kendall and Professor Chris Yakymchuk, for their time, advice, valuable feedback and criticism throughout this project. Their advice was a great help in the development of this thesis, especially in its final stages.

I would also like to appreciate Professor Ian Clark, and his student Sarina Emma Cotroneo, from the University of Ottawa, for help with the porewater geochemical analyses that were completed over the last two years, as well as Dr. Clark's valued comments regarding the halide isotopic signatures and geochemistry.

I am also grateful for the tremendous support of Laura Kennell-Morrison, Monique Hobbs and Tammy Yang, who technically reviewed several reports and this thesis. It was especially helpful that their feedback and constructive comments made it possible to accomplish the professional NWMO reports. This project was also made possible by funding from Nuclear Waste Management Organization (NWMO).

I would especially like to extend my gratitude to Rhys Gwynne for his hard work, expertise and patience in helping me to prepare my samples in the Environmental Isotope Laboratory (EIL) at the University of Waterloo. Rhys was always more than willing to help, and for that I cannot thank him enough.

Finally, I would like to thank Mom and Dad, my fiancée Luqi and friends for their support, love, and patience during this long adventure.

Table of Contents

List of Figures

List of Tables

1. INTRODUCTION

The Nuclear Waste Management Organization (NWMO) of Canada has proposed the geological media underlying the Bruce Nuclear Site near Kincardine, Ontario (Figure 1), as a location for a Deep Geological Repository (DGR) for low- and intermediate-level nuclear waste. The Bruce Nuclear Site (herein called 'the site') is located in the Bruce structural block and lies on the eastern margin of the Michigan Basin – located west of the Algonquin Arch (Figure 1). The origin, movement and relative ages of the sedimentary formation fluids and salts found in the geological media at the site are important as a means to address both the long-term stability of the host rock and the potential for hydrochemical migration of radionuclides from the proposed repository.

The stable isotopes of Cl and Br have been used in previous studies to ascertain the origin of salts and fluids as well as to identify processes that cause isotopic fractionation (Kaufmann et al. 1992; Eggenkamp 1994; Shouakar-Stash 2008; Stotler et al. 2010; Eggenkamp 2014). This study will compare the halide isotopic signatures of groundwaters and porewaters from the sedimentary units (Devonian, Silurian, Ordovician, and Cambrian) found at the site to the halide isotopic signatures of a database consisting of regional sedimentary formation waters and evaporitic salts from southern Ontario and Michigan (Shouakar-Stash 2008; Hobbs et al. 2011; Skuce et al. 2015). This comparison will be the first attempt to use these two isotopic systems together to evaluate sources, residence times, and processes causing isotopic fractionation at a site containing such a diverse number of sedimentary units.

The chlorine isotopic values ($\delta^{37}Cl$) of sedimentary formation waters from southern Ontario and the Michigan Basin (-1.3‰ to +1.8‰; Kaufmann et al. 1992; Shouakar-Stash 2008; Skuce et al. 2015) encompass a wider range compared to fluids from crystalline environments (-0.8‰ to +1.6‰; Stotler

et al. 2010), but span a much smaller range than that of man-made compounds (-3.0‰ to +4.2‰; Kaufmann et al. 1992; van Warmerdam et al. 1995; Skitmore 1997; Rosen 1999; Eggenkamp and Coleman 2000; Frape et al. 2004; Stotler et al. 2010) (Figure 2). The range of bromine isotopic values ($\delta^{81}Br$) for sedimentary formation waters from southern Ontario and the Michigan Basin (-1.3‰ to +2.3‰; Shouakar-Stash 2008; Skuce et al. 2015) is also wider than fluids from crystalline environments (0‰ to +1.5‰; Stotler et al. 2010).

This study presents halide isotopic results from groundwater and porewater samples collected from two cored boreholes, DGR-3 and DGR-4, that intersect the entire 840 m thickness of the Paleozoic sedimentary sequence beneath the site (Figure 1 and 3). The hydrogeochemical and isotopic analyses are used to compare site-specific results against existing isotopic and chemical data from the same sedimentary formations found elsewhere in Ontario and Michigan, with a focus on Cl and Br concentrations and isotopic ratios, as well as light stable isotopes ($\delta^{18}O$, $\delta^{2}H$).

Porewater solute and isotopic profiles from the site (refer to Figure 14a) (Clark et al. 2013) show a downward decrease in Cl and Br concentrations and water isotopic signatures from the Early Silurian to the Cambrian sedimentary units. The authors attributed this trend to the slow downward diffusive migration of a hypersaline evaporative Silurian brine that mixed with the less saline pore fluids found in the older geological units. Al et al. (2015) introduced the possibility of Cambrian and even Precambrian brines entering the pore spaces of the Early Ordovician units through upward diffusion/advection and mixing with downward percolating Ordovician seawater.

Additional halide isotopic signatures ($\delta^{37}Cl$ and $\delta^{81}Br$) are used in this study to assess the origin of end-member components found in the groundwaters and pore fluids of the Ordovician and Cambrian strata at the site. One of these isotope systems ($\delta^{37}Cl$) has been used in a number of studies to assess

long-term diffusive migration in sediments and sedimentary rocks (Desaulniers et al. 1986; Gimmi and Waber 2004; Hesse et al. 2006; Le Gal La Salle et al. 2013; Rebeix et al. 2014). An increased understanding of the history of sedimentary formation water evolution and migration could be gained by measuring the halide isotopic values of groundwaters and porewaters at the Bruce site, and comparing these values to known isotopic values from similar aged formations found in the regional databases available to this study. This research would also allow an evaluation and comparison of the relationship of the halide isotopic results to previous interpretations at the site based on other geochemical and isotopic parameters (Clark et al. 2013; Al et al. 2015). The new halide isotope data are used to evaluate conceptual diffusional and fluid migration models regionally in southern Ontario and have application to interpretation of similar sites found elsewhere in the world (e.g. Desaulniers et al. 1986; Eggenkamp et al. 1994; Eggenkamp and Coleman 2009).

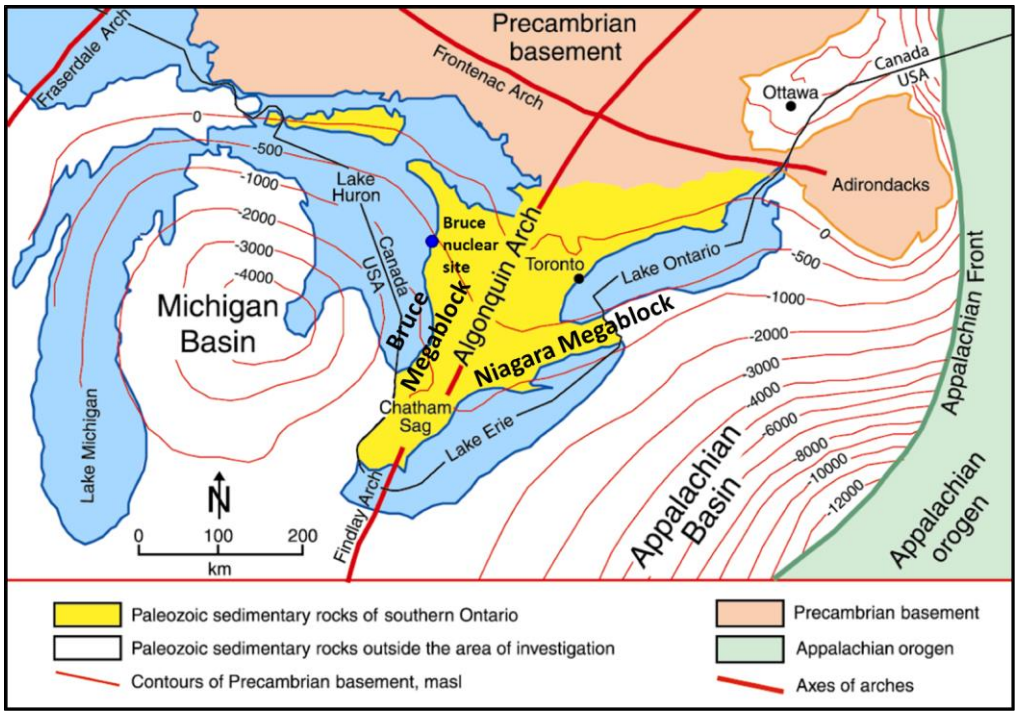

Figure 1: Large-scale tectonic elements in southern Ontario and the location of the Bruce Nuclear Site (adapted from Johnson et al. 1992, from Mazurek 2004). masl = metres above sea level.

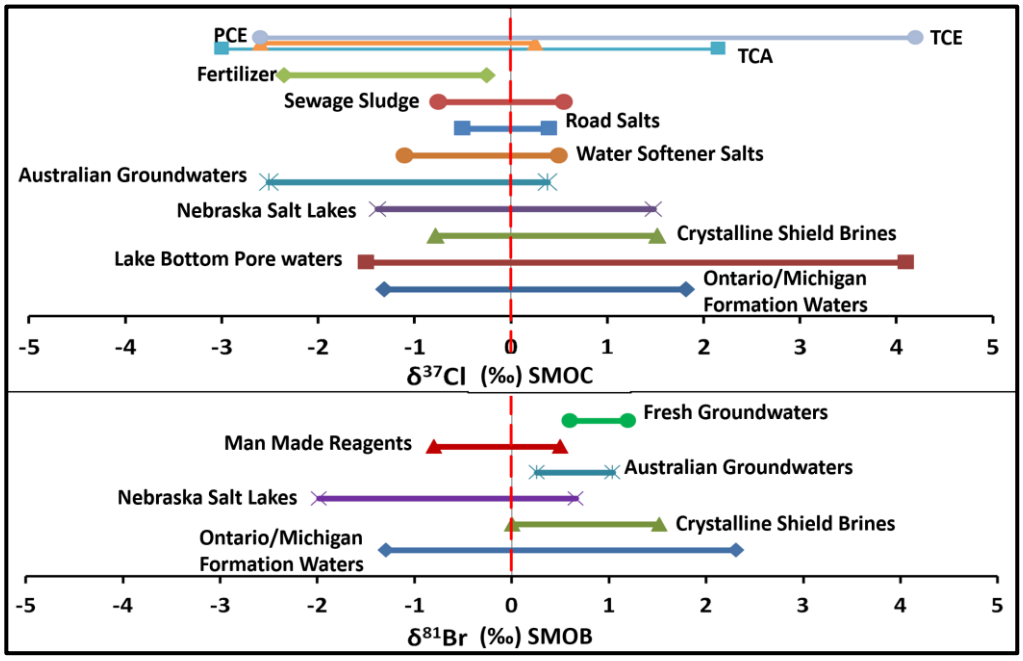

Figure 2: Examples of $\delta^{37}Cl$ and $\delta^{81}Br$ stable isotopic ranges for natural and man-made compounds (data from Dollar et al. 1988; vanWarmerdam et al. 1995; Eggenkamp et al. 1995; Drimmie and Frape 1996; Skitmore 1997; Shouakar-Stash 2008; Stotler et al. 2010; Hobbs et al. 2011; Skuce et al. 2015; Hanlon et al. 2017).

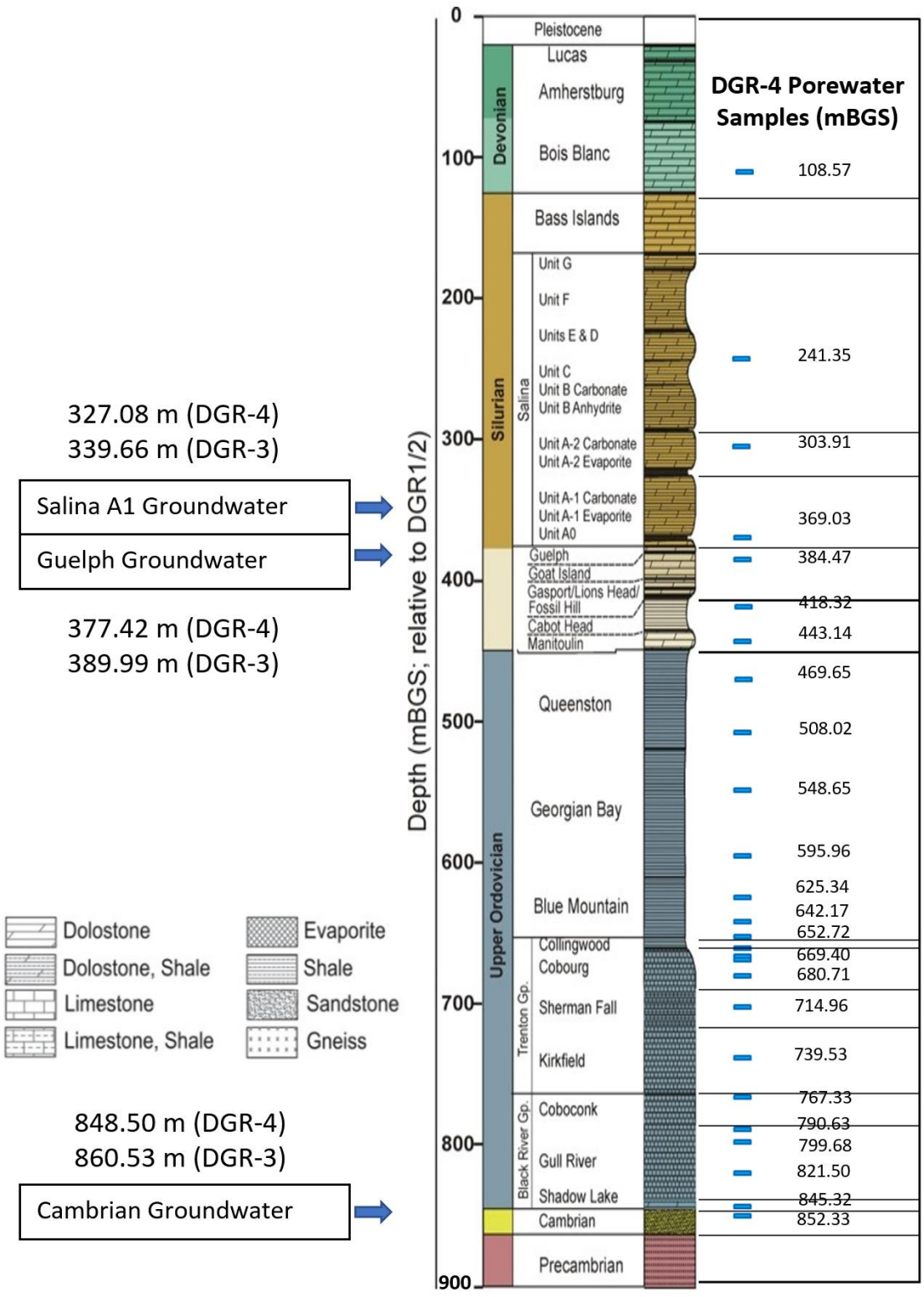

Figure 3: Lithostratigraphy of DGR-3 and DGR-4 boreholes at the Bruce Nuclear Site and locations of the groundwater and porewater samples from the DGR-4 borehole (Modified from Intera 2011).

1.1 Background

Earlier researchers have analyzed and described more than 190 samples of saline waters and brine from sedimentary formations in southern Ontario and the Michigan Basin (Dollar et al. 1991; Weaver et al. 1995; Shouakar-Stash 2008; Hobbs et al. 2011; Skuce et al. 2015). These samples were analyzed for geochemistry and a selection of isotopic parameters including $\delta^{18}O$, $\delta^{2}H$, $^{87}Sr/^{86}Sr$, $\delta^{37}Cl$ and $\delta^{81}Br$. Figure 4a and Figure 4b illustrate the locations of samples from the regional databases used for comparison with the new data from the Bruce Nuclear Site in this study. Sedimentary formation fluids in the regional database were sampled from producing oil and gas wells, as well as research boreholes drilled as part of previous hydrogeological studies in the area. These sedimentary formation fluids were taken from stratigraphic units ranging in age from Cambrian to Devonian. The majority of samples were from the Niagara Structural Block in southern Ontario (Figure 1, 4a). A comprehensive review of the chemistry and isotopic signatures of the fluids can be found in Hobbs et al. (2011), and additional information can be found in the M.Sc. thesis of Dollar (1988), the Ph.D. theses of Weaver (1994) and Shouakar-Stash (2008), and publications by McNutt et al. (1987), Dollar et al. (1991) and Weaver et al. (1995). More recently, additional regional hydrogeochemical and isotopic data was published by Skuce et al. (2015).

Several observations can be made from the regional database of $\delta^{37}Cl$ and $\delta^{81}Br$ in Shouakar-Stash (2008) (Figure 4a), and the additional data from Skuce et al. (2015) (Figure 4b). Shouakar-Stash (2008) observed that the $\delta^{81}Br$ of samples from the Appalachian Basin east of the Algonquin Arch (Figure 4a) were isotopically heavier than the seawater standard (SMOB, 0‰) (red circle, group A), but samples from the Michigan Basin west of the Algonquin Arch were almost always isotopically lighter than SMOB (blue circle, group B). However, there are not any $\delta^{37}Cl$ and $\delta^{81}Br$ data of the

Cambrian groundwaters from the Michigan Basin, thus, the assumption of a positive or negative δ^{81}Br signature for the Cambrian groundwater to the west of the Algonquin Arch cannot be stated with any certainty. The present study plans to evaluate this relationship in more detail, in particular the signatures in groundwaters and porewaters with depth throughout the geological units at the site.

Based on the concentration and isotopic ratio of helium in porewaters beneath the site, it is likely that authigenic helium within the Ordovician shale aquiclude is isolated from allochthonous helium (derived from the deep Michigan Basin) in the underlying Ordovician carbonates (Clark et al. 2013). Therefore, these authors suggest that limited transport of the Ordovician brine occurred during Paleozoic time. Clark et al. (2013) proposed a conceptual model of downward diffusive migration of fluids from the hypersaline evaporative Silurian units into older geological units. In the Early Ordovician sediments, the hypersaline fluids encountered and mixed with less saline fluids attributed to Ordovician seawater (Coniglio et al. 1994; Clark et al. 2013). The porewater signatures related to this mixing process are preserved in these units due to extremely low permeability and, in some cases, secondary halite (salt) mineralization, which occluded the pore space and minimized porosity and effective diffusion coefficients in the Ordovician shale sequence (Clark et al. 2013).

Clark et al. (2013) estimated that the probable residence time of the porewaters found in the deeper geologic system (Ordovician shale and carbonate aquiclude) was greater than 260 Ma. This was based on the helium Nobel gas component and considered diffusion to be the dominant fluid migration method in their conceptual model. Similar age calculations were made at the Tournemire site in France based on diffusive transport, using just the Cl and Br concentrations. More recently, the δ^{37}Cl of porewaters from the Tournemire site were used to further define a diffusive exchange time between end members (85±10 Ma) that was much greater than previously calculated values (53

Ma) (Le Gal La Salle et al. 2013). The $\delta^{37}Cl$ and $\delta^{81}Br$ analysis of porewaters will be used here to further investigate potential solute origins and mechanisms of solute transport and fractionation at the Bruce Nuclear site.

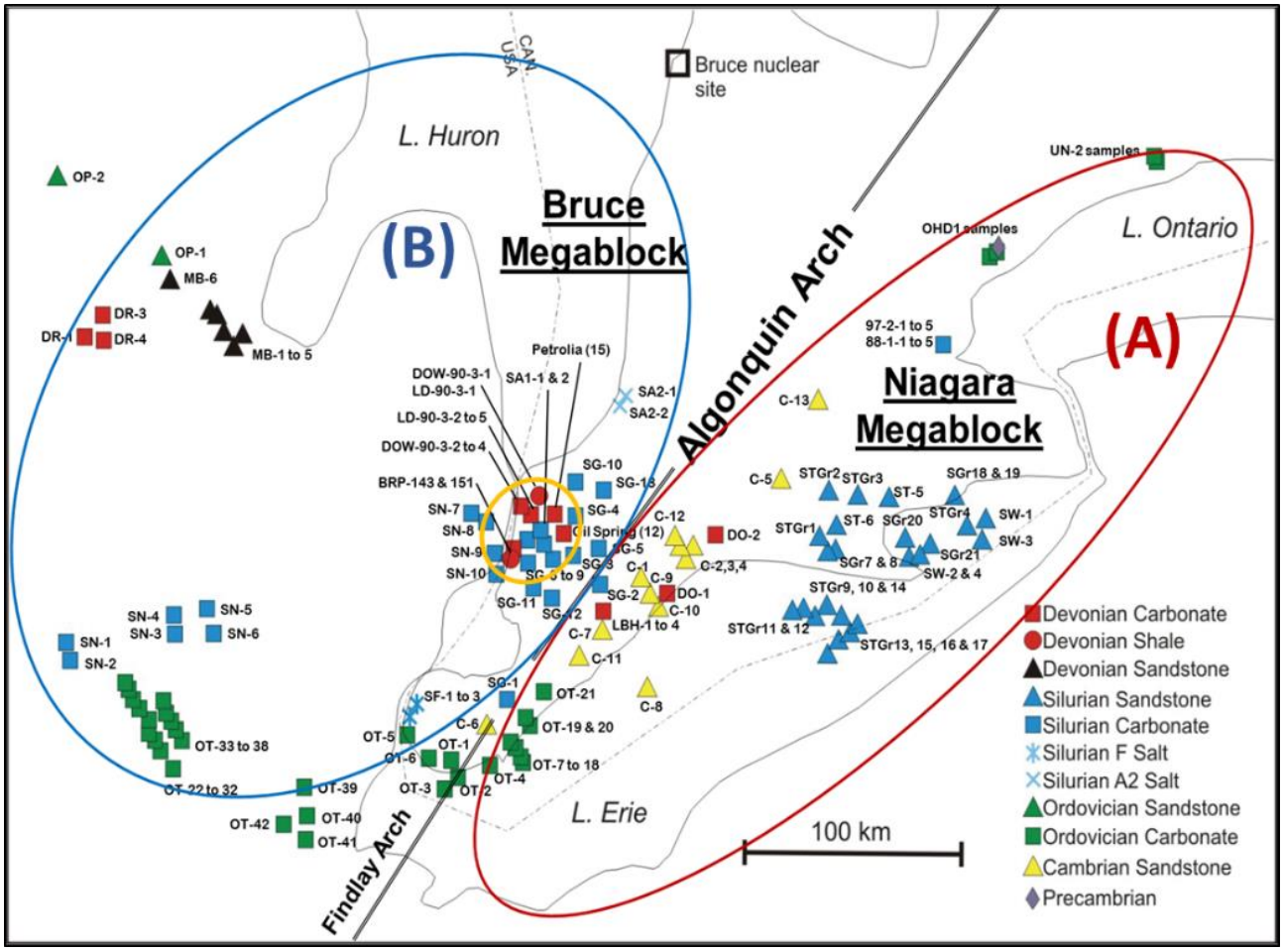

Figure 4a: Location of regional samples collected from the sedimentary formations in southwestern Ontario and in central and eastern Michigan, USA. Adapted from Hobbs et al. 2011 (from Frape et al. 1989; Shouakar-Stash 2008). The group A samples in the red circle were collected from southeast of the Algonquin Arch, while group B samples in the blue circle were from northwest of the Algonquin Arch. More dilute Devonian fluids (orange circle) were from the margin of the Michigan Basin.

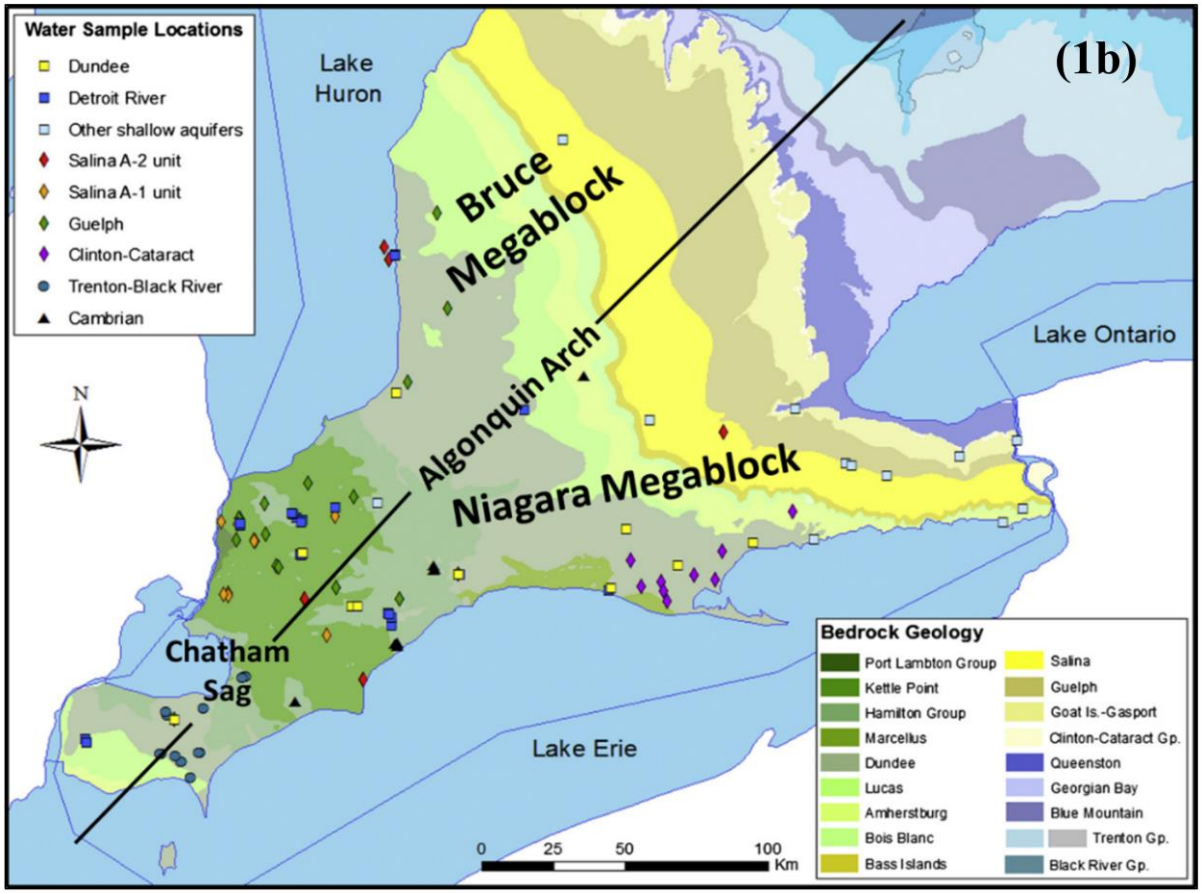

Figure 4b: Bedrock geology map of southwestern Ontario and locations of water samples collected in the study by Skuce et al. (2015).

1.2 Geology

Formation of the Michigan Basin initially started with mid-continental rifting (approximately 1,100 Ma) and was followed by tectonic subsidence of the Precambrian basement (about 580 to 500 Ma) (Klein and Hsui, 1987). With the increasing weight of sediments, the Michigan Basin experienced flexing and further subsidence (Sleep 1971; Sleep and Snell 1976; Nunn and Sleep 1984). However, other researchers (Howell and van der Pluijm 1990, 1999) primarily attributed the formation of the Michigan Basin to tectonic activities in the early Paleozoic (the Taconic and early Acadian Orogenies). For the last 200 Ma, eastern North America was in a passive margin phase (Figure 5a).

The Paleozoic sedimentary rocks within the Michigan and Appalachian basins were deposited in shallow seas (Sanford et al. 1985). The two basins represent two distinct tectonic environments. Johnson et al. (1992) concluded that two principal tectonic impacts: the orogenic activities at the eastern margin of North America and the subsequent tectonic forces, led to slightly different sedimentary rocks being deposited within the Michigan and Appalachian basins. In general, carbonates were deposited in the intracratonic Michigan Basin whereas argillaceous (clastic) sediments were deposited in the Appalachian foreland basin (Johnson et al. 1992; AECOM and ITASCA CANADA 2011).

Sanford et al. (1985) illustrated the conceptual fracture system associated with the fault framework in southern Ontario. As shown in Figure 5b, the Bruce Structural Block (Michigan Basin domain) and Niagara Structural Block (Appalachian Basin domain) are characterized by different fracture orientations (Johnson et al. 1992; Andjelkovic et al. 1998; Mazurek 2004). However, the conceptual fracture system has not been verified (Johnson et al. 1992). If it were correct, the more intensive fracture system conceptualized underneath the Niagara Megablock could enhance the migration of basinal fluids when compared to the sparser fracture system proposed for the Bruce Megablock.

Paleozoic sedimentary rocks in southwestern Ontario reflect a variety of depositional environments. In detail, the Cambrian deposits were a result of a transgressive sea that submerged the entire Algonquin Arch and extended into the subsiding Michigan Basin during the Early Cambrian (Hamblin 1999). Subsequently, the Cambrian deposits in southern Ontario were eroded over the Algonquin Arch (Bailey and Cochrane 1984a, b; Bailey 2005). Similar to the Cambrian, deposition of the Upper Ordovician Black River and Trenton groups is marked by major marine transgressions. Some researchers speculated that the collision between offshore volcanic islands and the ancient

passive Laurentian margin during the earlier Taconic Orogeny (543-440 Ma) probably had an influence on the deposition of the Trenton carbonates (Van der Voo 1982; Quinlan and Beaumont 1984; Melchin et al. 1994; Hamblin 1999). The overlying Blue Mountain Formation likely formed in an open marine depositional environment, whereas the overlying Georgian Bay Formation is considered to have formed on a shallowing storm-dominated shelf succession (Johnson et al. 1992). Subsequently, clastic sedimentary deposition in a deltaic environment in the southeastern Michigan Basin dominated during Late Ordovician time and resulted in the shale deposits of the Queenston Formation (Johnson et al. 1992).

The Silurian Period was dominated by relatively warmer temperature and higher global sea levels (Munnecke et al. 2010). The Lower Silurian Manitoulin Formation was deposited in a shallow carbonate ramp setting (Armstrong and Carter 2010), and the depositional environment of the overlying Lower Silurian Cabot Head Formation is considered to be an offshore basinal or marginal marine setting (Armstrong and Carter 2010). In general, the Middle Silurian (Gasport and Guelph Formations) is characterized by a marine transgression. The overlying Middle to Upper Salina Group and the Bass Islands Formation are interpreted as cyclical evaporite and carbonate deposits, and a relatively more open marine environment, respectively. Uyeno et al. (1982) suggested that a major marine transgression led to deposition of the Devonian carbonates, following a long period of exposure and erosion at the end of the Silurian.

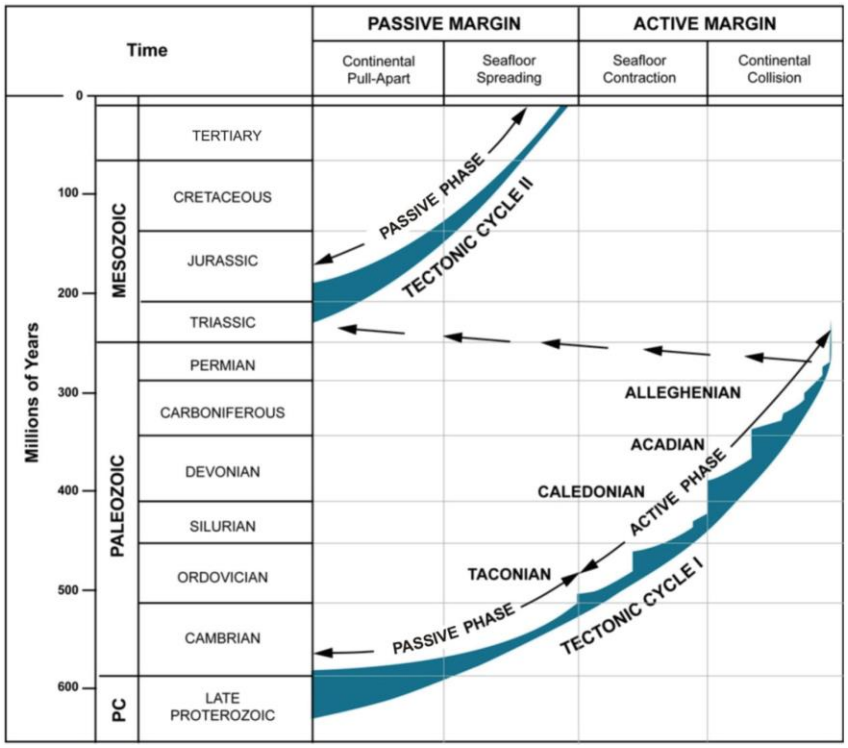

Figure 5a: Phanerozoic tectonic cycles (from Sanford et al. 1985). Note: Band widths represent relative tectonic intensity.

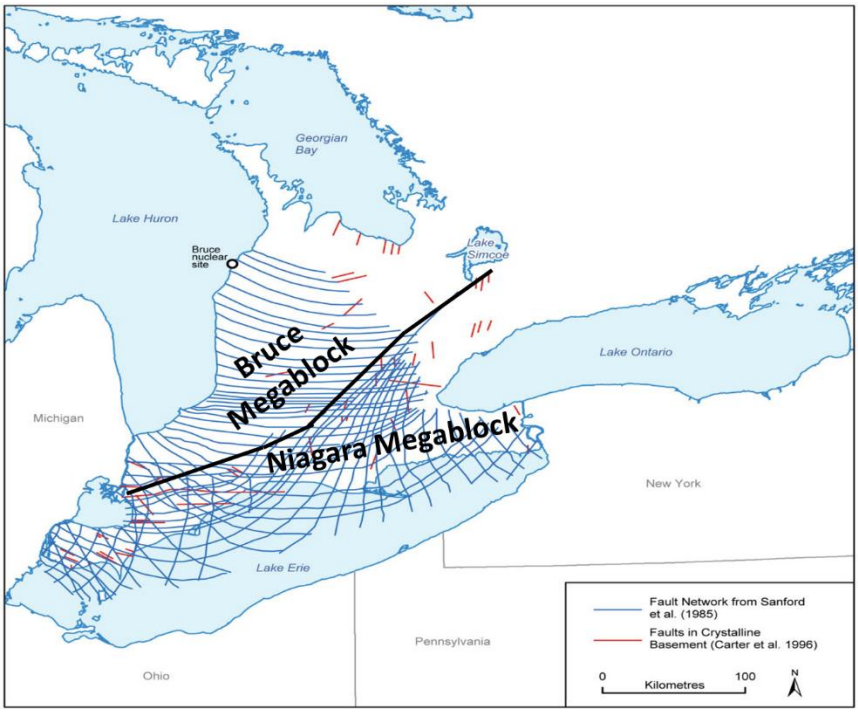

Figure 5b: Proposed fracture and fault frameworks in southern Ontario (Modified by AECOM and ITASCA CANADA (2011) from Mazurek (2004) after Carter et al. (1996) and Sanford et al. (1985)).

2. METHODOLOGY AND SAMPLE LOCATION

Geochemical and isotopic data were obtained in this study for three types of fluids: 1) regional sedimentary formation fluids, 2) Bruce Nuclear Site groundwaters, and 3) Bruce Nuclear Site pore waters. Regional sedimentary formation fluids associated with petroleum wells and deep research boreholes were analyzed in previous studies (Dollar et al. 1991; Weaver et al. 1995; Shouakar-Stash 2008; Hobbs et al. 2011; Skuce et al. 2015). These highly saline waters and brines were compared to formation groundwaters from boreholes DGR-3 and DGR-4 at the Bruce Nuclear Site. Samples consisted of archived opportunistic groundwater samples, which were chosen for analyses in consultation with NWMO personnel. Geochemical data and stable water isotope compositions have been provided by NWMO for each sample for comparison with the new $\delta^{81}Br$ and $\delta^{37}Cl$ data. This allowed the researchers to further address the relationship of the halide isotopic result to previous interpretations of other parameters from the site using the same or similar samples (Clark et al. 2013; Al et al. 2015). The data from the regional fluids and site groundwaters were compared to rock matrix pore fluids from borehole DGR-4 at the site. Pore fluid samples are University of Ottawa archival samples from the Clark et al. (2013) study. Porewater samples were prepared using the crush and leach technique described in Clark et al. (2010).

For the present study, the original porewaters are considered to be a combination of salts and matrix fluids that were trapped in the pore spaces of the rock matrix. These solutes have to be extracted from the matrix by the crush and leach technique (Clark et al. 2010). Groundwaters and/or formation fluids can freely flow through fractures and pore spaces if the opportunity arises. Therefore, when comparing the two fluid/salt reservoirs, the relative availability and ages of the potential salts for mixing as well as other processes such as diffusion must be considered.

2.1 Location of the Regional Formation Fluids

A total of 190 samples of saline waters and brines included in the Waterloo Regional Hydrogeochemistry Database (WRHD) are from Precambrian to Devonian sedimentary formations in southwestern Ontario and the Michigan Basin (Figure 4a). These samples were collected from northwest and southeast of the Algonquin Arch (Figure 1a). Sample depths range from near ground surface to almost four kilometers. Several researchers, including Dollar (1988), Sherwood-Lollar and Frape (1989), Cloutier (1994), Weaver (1994), and Husain (1996) collected the samples over the past 30 years. A more recent regional geochemical database is also available from Skuce et al. (2015).

Sampling methods described by Lico et al. (1982) and Kharaka et al. (1987) were used to collect the samples, with slight modifications in certain situations. Weaver et al. (1995) and Hobbs et al. (2011) reported the specific procedures used for sample collection and handling.

2.2 Location of the DGR Groundwater Samples

Six groundwater samples are included in this study representing the only zones of flowing water from two deep vertical bedrock boreholes at the site (DGR-3 and DGR-4). The geology of the DGR-3 and DGR-4 boreholes are described in detail by Intera (2011) and NWMO (2011) (Figure 3). The formation fluid samples in the DGR-3 borehole at 339.66 m and in DGR-4 at 327.08 m are from the Salina A1 Unit (Upper Silurian), which consists of argillaceous dolostone and anhydritic dolostone. The formation fluid samples in DGR-3 at 389.99 m and in DGR-4 at 377.42 m are from the Guelph Formation (Middle Silurian), which consists of porous dolostone and dolomitic limestone. The formation fluid samples in DGR-3 at 860.53 m and in DGR-4 at 848.50 m are from the Cambrian

Formation, which consists primarily of sandstone and dolostone.

2.3 Location of the Porewater Samples

Porewater samples were obtained by the crush and leach (CL) technique (Clark et al. 2010) on selected core samples from geological units ranging from Silurian to Cambrian in age. These samples were provided by Professor Ian Clark, University of Ottawa. Sampling was concentrated on the lower part of the Upper Ordovician strata and moved upwards and downwards incorporating splits of the available porewaters from previous studies (Clark et al. 2013). The samples were sealed and refrigerated and therefore should not have changed isotopically due to the conservative nature of Cl and Br in solution (Cecil 2001). In the event that samples for analyses from a specific stratigraphic section of interest were missing, further extractions were undertaken, depending on the availability of core material, using the same methodology as Clark et al. (2010). In such a case, unpreserved core can be used to leach Br and Cl salts as these elements remain in the pore space of the core, are highly soluble, generally do not form insoluble salts upon desiccation, and are not recorded to be volatile at lower temperatures without the influence of microbial or photolytic processes (Hanlon et al. 2017). For example, Br and Cl isotopic standards of salts and fluids under long term storage in the Environmental Isotope Laboratory, University of Waterloo, have not shown any changes in isotopic signatures with repeated analyses performed years apart.

2.4 Measurement of Stable Isotopes

The ionic concentrations and stable isotope compositions ($\delta^{18}O$, $\delta^{2}H$, $\delta^{37}Cl$, and $\delta^{81}Br$) of the sedimentary formation waters in Ontario were reported in several previous studies (Dollar 1988; Sherwood-Lollar and Frape 1989; Cloutier 1994; Weaver 1994; Weaver et al. 1995; Husain 1996;

Martini and Walter 1998; Shouakar-Stash 2008; Skuce et al. 2015).

The $\delta^{37}Cl$ and $\delta^{81}Br$ of fluids were analyzed for this study using Continuous Flow Isotope-Ratio Mass Spectrometry as described by Shouakar-Stash et al. (2005a, b). The $\delta^{37}Cl$ measurements for formation fluids were completed for a PhD thesis (Shouakar-Stash 2008), but have not been published. As part of the current research, the same samples from Shouakar-Stash (2008) were reanalyzed for comparison and were found to have statistically identical values. The $\delta^{37}Cl$ and $\delta^{81}Br$ isotopic ratios are reported as permil (‰) deviations from an isotopic standard reference material using the conventional δ notation, where:

$$\delta_s = \left(\frac{R_S - R_{STD}}{R_{STD}} \right) \times 1000\,(‰)$$

Based on these methods, the analytical precision for both $\delta^{37}Cl$ and $\delta^{81}Br$ is ±0.10‰ (STDV) for n=12 or less. Standard Mean Ocean Bromide (SMOB) and Standard Mean Ocean Chloride (SMOC) were used as the standards to calibrate the bromine and chlorine isotopic data, respectively. Two internal inter-lab standards were also used to calibrate data and test the linearity of the equipment at extreme values (with an internal precision of ±0.03‰). The methodology is summarized in Appendix A1 (Shouakar-Stash et al. 2005a, b)

3. RESULTS AND DISCUSSION (PART ONE)

3.1 Compilation of the Regional Database

The archival database for the geochemical and isotopic results of formation waters from the Michigan Basin and southern Ontario are listed in Table A1 and Table A2 in Appendix A (Shouakar-Stash 2008; Hobbs et al. 2011; Skuce et al. 2015).

In southern Ontario and some parts of the Michigan Basin, the chlorine concentrations of formation water samples range from less than 1 mg/L to almost 300,000 mg/L, while the bromine concentrations range from less than 1 mg/L to approximately 8,500 mg/L (Shouakar-Stash 2008). The weight ratio between bromine and chlorine has a range between 0.0001 and 0.0389 (Shouakar-Stash 2008). The oceanic Br/Cl weight ratio is approximately 0.0034, which can be compared to Br/Cl ratios from brines and, in some cases, can be used to determine the extent of evaporation (Figure 13) (Carpenter 1978; McCaffrey et al. 1987).

The chlorine isotopic values for groundwater samples in the Waterloo Regional Hydrogeochemistry Database (WRHD) have a range from -1.31‰ to +1.82‰ based on the isotope studies conducted by earlier researchers and those analyzed in this study, and the bromine isotopic values have a range from -0.95‰ to +2.31‰ (Shouakar-Stash 2008) (Table A1). For the regional $\delta^{37}Cl$ and $\delta^{81}Br$ isotopic data from Skuce et al. (2015), exclusive of the original WRHD, the $\delta^{37}Cl$ values range from -0.49‰ to +1.00‰ and the $\delta^{81}Br$ values range from -1.29‰ to +2.21‰, similar to the WRHD (Table A2).

The $\delta^{37}Cl$ and $\delta^{81}Br$ isotopic values of formation waters show large variations, as described by Shouakar-Stash (2008) and Hobbs et al. (2011). However, the values are within the known ranges

reported for formation waters by previous researchers (Figure 2) (Desauliners et al. 1986; Eastoe and Guilbert 1992; Kaufmann et al. 1993; Eggenkamp 1994; Liu et al. 1997; Eggenkamp and Coleman 2000; Eastoe et al. 2001; Ziegler et al. 2001; Frape et al. 2004; Stewart and Spivack 2004; Shouakar-Stash et al. 2007). In the following sections, the major findings by previous researchers will be briefly described based on the Cl and Br concentrations, $\delta^{18}O$-$\delta^{2}H$, and $\delta^{81}Br$-$\delta^{37}Cl$ results of formation waters from the Michigan Basin and southern Ontario (Shouakar-Stash 2008; Hobbs et al. 2011; Skuce et al. 2015).

3.1.1 $\delta^{18}O$ and $\delta^{2}H$ Compositions

In Figure 6, the $\delta^{18}O$ and $\delta^{2}H$ isotopic values of major formation waters from the Michigan Basin and southern Ontario have higher $\delta^{18}O$ relative to modern day meteoric water, and plot to the right of and below the Global Meteoric Water Line (GMWL). The values all fall close to the end of Holser's (1979) evolutionary curve for very concentrated brines that have undergone extreme evaporation. The most concentrated samples (brines > 100g/L) show "clustering" of isotopic signatures for a given formation, and formation waters from different Paleozoic units are characterized by distinctive $\delta^{18}O$ and $\delta^{2}H$ signatures (Dollar et al. 1991; Cloutier 1994; Weaver et al. 1995; Husain et al. 2004; Hobbs et al. 2011) (Figure 6). However, some overlap between units and mixing trends with more dilute waters (lower $\delta^{18}O$ and $\delta^{2}H$) are also observed.

Several researchers reported that formation waters from shallow Devonian carbonate units or glacial drift aquifers have lower $\delta^{18}O$ and $\delta^{2}H$, suggesting a glacial melt-water end member (Dollar et al. 1991; Cloutier 1994; Weaver et al. 1995). The higher $\delta^{18}O$ isotopic signatures of the Silurian Formation waters have been attributed to significant water-rock interaction (Clayton 1966; Sheppard 1986; Farquhar et al. 1987; Coniglio et al. 2003). The $\delta^{18}O$ and $\delta^{2}H$ isotopic signatures of many

Cambrian fluids have been attributed to mixing of Cambrian waters with brines from the underlying Precambrian crystalline rocks (Hobbs et al. 2011; Skuce et al. 2015). However, none of the sedimentary formation fluids in either the previous studies or the present study exhibited the high δ^2H values above the meteoric waterline that are typical of Shield brines (Frape and Fritz 1987; Frape et al. 2003), as shown on Figure 6.

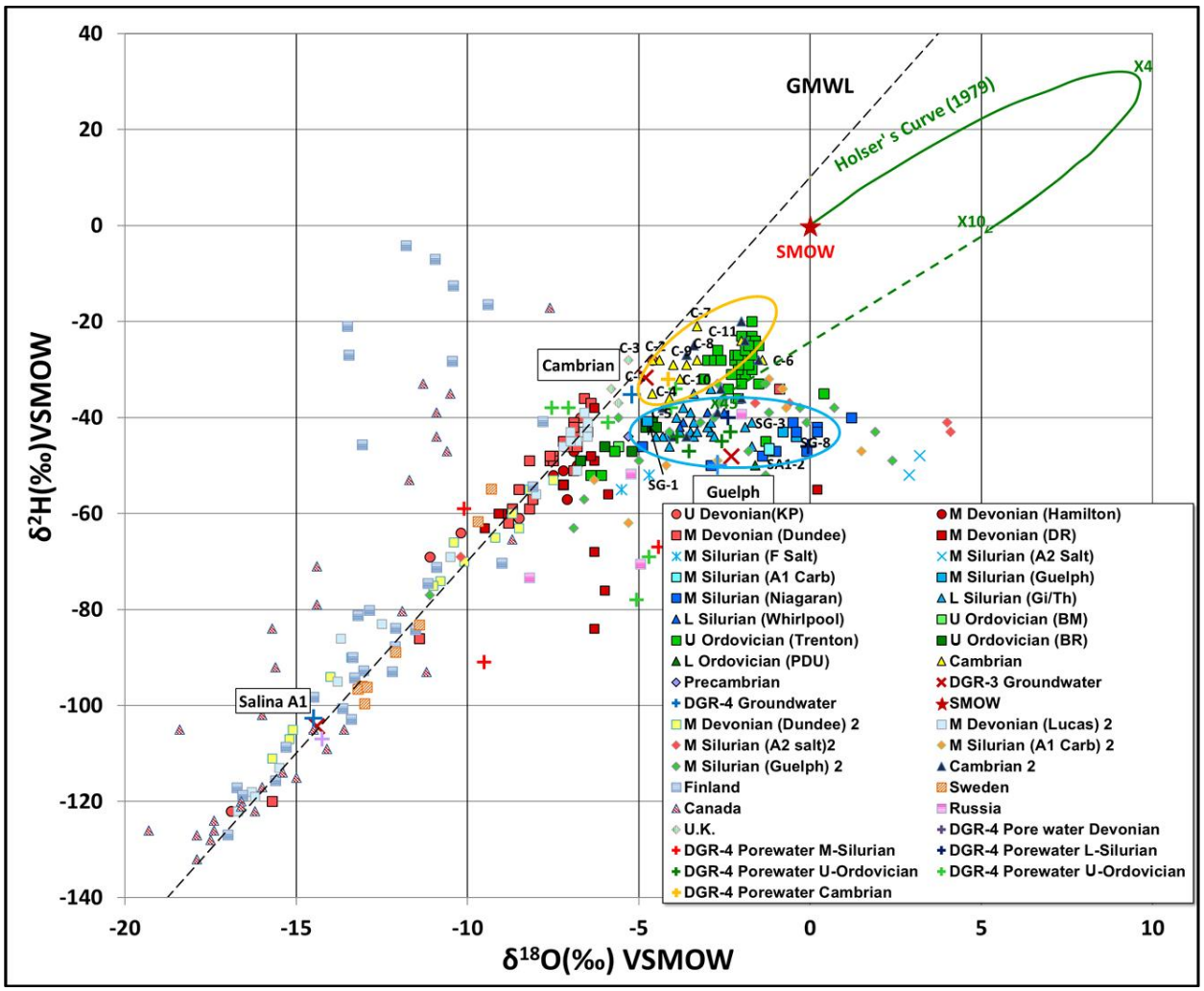

Figure 6: $\delta^{18}O$ and δ^2H of groundwater in crystalline and sedimentary rocks. The number 2 behind symbols in the legend refers to data from the Skuce et al. (2015) database. All other sedimentary data are from the WRHD. Additional data (symbols filled with lines) are from crystalline environments (Finland, Sweden, Canada, Russia and U.K.) and are from Frape et al. (2003). The Holser Evaporative Curve (1979) shows the evolutionary evaporation pathway for seawater and indicates that concentrated sedimentary formation brines in strata in the region could have a marine origin. Cambrian samples are circled by the orange line, Guelph Formation samples (SG) are circled by the blue line.

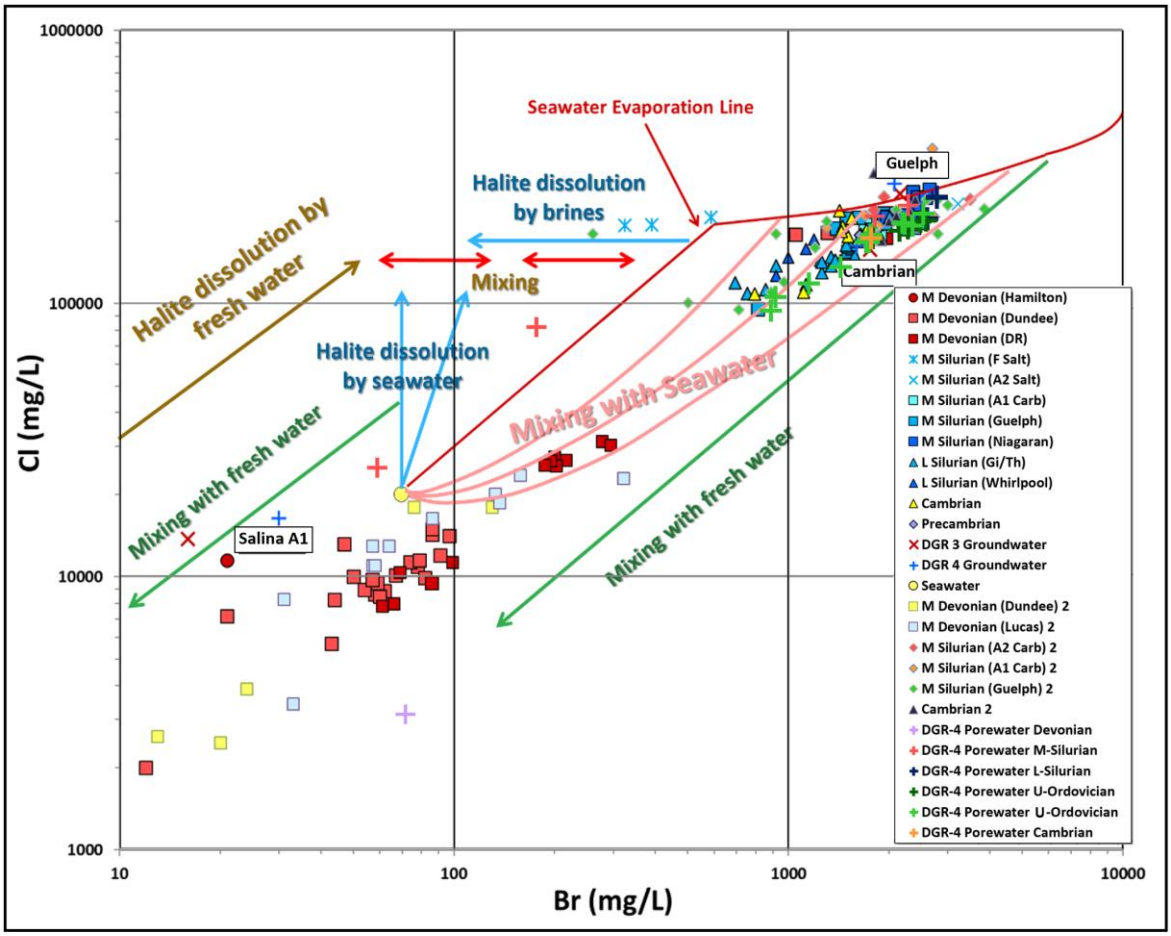

Figure 7: Trends for chloride versus bromide concentrations during the evaporation of seawater (McCaffrey et al. 1987) compared to groundwater samples from the Silurian and Cambrian strata at the site and sedimentary formation fluids. The number 2 behind symbols in the legend refers to data from the Skuce et al. (2015) database. All other data are from the WRHD. Also shown are a number of processes such as halide dissolution and mixing scenarios that would alter the primary concentrations of the formation fluids (Rittenhouse 1967; Carpenter 1978). (Modified from Shouakar-Stash 2008).

3.1.2 Cl and Br Concentrations

Figure 7 illustrates the Cl and Br concentrations of the formation waters from southern Ontario and the Michigan Basin, and compares this data to the seawater evaporation line and several potential evolutionary processes (e.g. halite dissolution, fluid mixing) that can impact the Cl and Br concentrations of sedimentary formation fluids (Rittenhouse 1967; Carpenter 1978; Kharaka and Hanor 2004; Shouakar-Stash 2008; Hobbs et al. 2011; Skuce et al. 2015). In general, most of the Cl

and Br concentrations of the formation waters fall on or just below the seawater evaporation line between the halite and sylvite precipitation stages. This suggests that formation waters have evolved from original paleo-seawater to very concentrated brines via evaporation. This aspect of the chemical signature of the sedimentary formation fluids is in agreement with high dissolved salt concentrations of the brines and the $\delta^{18}O$ and $\delta^{2}H$ evolutionary trends (Figure 6) (Shouakar-Stash 2008; Hobbs et al. 2011; Skuce et al. 2015). After initial evaporative concentration, it appears that many of the formation fluids were diluted by mixing with a less saline fluid similar to seawater or fresh water. Some of the Devonian and Silurian waters sampled from the basin margins plotted to the left and/or above the seawater evaporation line and thus would have been affected by halite dissolution with a fresh water end member (Sanford 1985; McIntosh and Walter 2005, 2006). However, due to the different mixing scenarios and diagenetic processes, it is difficult to assess the mixing proportions for most formation waters described in these studies.

3.1.3 $\delta^{81}Br$ and $\delta^{37}Cl$ Signatures

On Figure 8, all of the concentrated (> 100 g/L) formation waters from group B (northwest of the Algonquin Arch) are characterized by lower $\delta^{81}Br$ isotopic signatures in comparison to the concentrated (brine) formation waters from group A (southeast of the Arch). There is little or no overlap in $\delta^{81}Br$ values between these two groups whereas the $\delta^{37}Cl$ signatures show some overlap. Shouakar-Stash (2008) could not determine if these isotopic variations were caused by different evolutionary processes in the two basins or different origins.

On Figure 8, similar to the plot for $\delta^{18}O$ and $\delta^{2}H$, individual formations and, more generally, strata of similar geological age have similar $\delta^{37}Cl$ vs. $\delta^{81}Br$ signatures. For example, in Group A, the OT (Ordovician) fluids plot in a confined area with some overlap with the C (Cambrian) samples, similar

to what is shown for other isotopes (Figure 6). Most of the Devonian samples (orange circle) are much more dilute fluids sampled from petroleum wells near the Algonquin Arch, and have slightly higher δ^{81}Br values compared to Group B that plot in a distinctive grouping. However, these more dilute fluids have been inferred to have an origin from the deeper Appalachian Basin east of the Algonquin arch where fluids have higher δ^{81}Br signatures (Barker and Pollock 1984; Powell et al. 1984).

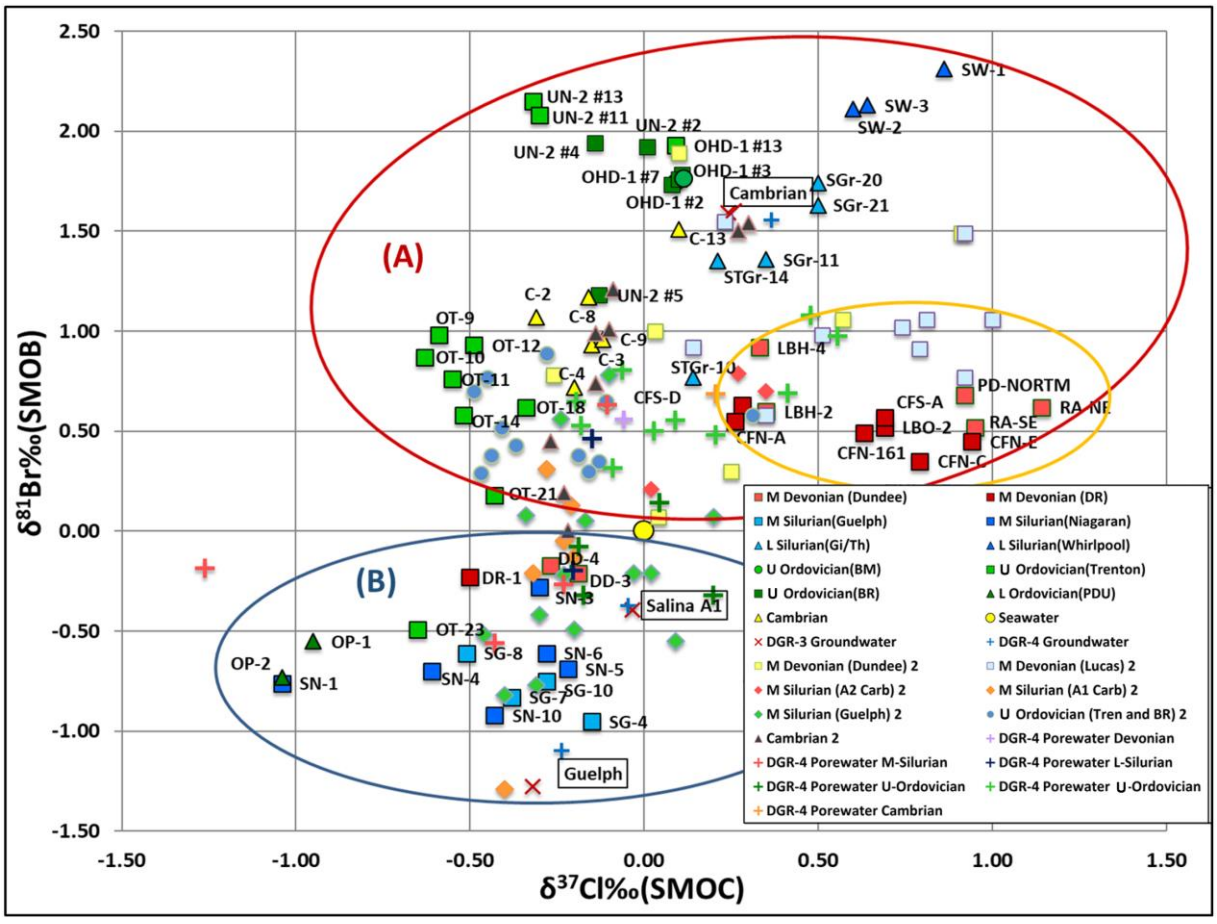

Figure 8: δ^{81}Br versus δ^{37}Cl for DGR-3, DGR-4 and regional sedimentary formation fluids. The number 2 behind symbols in the legend refers to data from the Skuce et al. (2015) database. All other data are from the WRHD. The data in the red circle (A) is from southeast of the Algonquin Arch, and data in the blue circle (B) is from northwest of the Algonquin Arch.

4. RESULTS AND DISCUSSION (PART TWO)

Results of Groundwaters (DGR-3 and DGR-4)

The geochemical data (Table 1) presented and discussed below were obtained from groundwater samples taken from two deep boreholes, DGR-3 and DGR-4, at the Bruce Nuclear Site (Figure 1). The geochemical data were compared with the combined regional sedimentary formation fluid database obtained from Shouakar-Stash (2008), Hobbs et al. (2011), and Skuce et al. (2015).

4.1 Comparison of $\delta^{81}Br$ and $\delta^{37}Cl$ between DGR groundwaters and regional sedimentary formation waters

4.1.1 Salina A1 Unit Fluids

Figure 8 also shows the isotopic results for $\delta^{81}Br$ plotted against $\delta^{37}Cl$ for the DGR-3 and DGR-4 groundwater samples relative to data from the combined regional data set. On Figure 8, the DGR-3 (327.08 m) and DGR-4 (339.66 m) groundwater samples from the Salina A1 Unit plot in an area in close proximity to the majority of Silurian Guelph and Niagaran reef (SG and SN) samples from the combined regional database. Figure 9A compares the DGR fluids to regional sedimentary brines from Silurian-aged strata. Several of the fluids from the Silurian A1-A2 carbonate units in the Skuce et al. (2015) data set plot, within analytical error, of the DGR A1 samples.

The WRHD for sedimentary formation fluids in Ontario contains two fluid samples from the Salina A1 salt (SA1-1 and SA1-2), but these samples were only analyzed for $\delta^{37}Cl$ (both have values of -0.35‰).

Table 1: Geochemical data for the formation fluids from boreholes DGR-3 and DGR-4 at the Bruce Nuclear Site. Samples were collected from three stratigraphic units (the Salina-A1 Unit, the Guelph Formation, and the Cambrian Formation).

Borehole	Depth (m)	Stratigraphic Unit	TDS	Cl (mg/L)	Br (mg/L)	Sr (mg/L)	K (mg/L)	Na (mg/L)	Ca (mg/L)	Mg (mg/L)	SO_4 (mg/L)	HCO_3 (mg/L)
DGR-3	339.66	Salina-A1 Unit	27	13745	16	18	125	7914	1014	586	2403	186
DGR-3	389.99	Guelph Formation	366	252239	2138	596	4375	103077	37918	9148	0	36
DGR-3	860.53	Cambrian Formation	225	157885	1731	876	993	35022	39156	6373	251	28
DGR-4	327.08	Salina-A1 Unit	30	16361	30	18	125	8595	1166	627	2556	316
DGR-4	377.42	Guelph Formation	375	275163	2055	491	4391	118855	15610	9467	169	27
DGR-4	848.50	Cambrian Formation	227	162512	1625	745	1017	34364	38896	6186	289	24

Borehole	Depth (m)	Stratigraphic Unit	TDS	$\delta^{37}Cl$ (SMOC) ‰	$\delta^{81}Br$ (SMOB) ‰	$\delta^{18}O$ (VSMOW) ‰	$\delta^{2}H$ (VSMOW) ‰	$^{87}Sr/^{86}Sr$
DGR-3	339.66	Salina-A1 Unit	27	-0.03	-0.39	-14.4	-104	0.708694
DGR-3	389.99	Guelph Formation	366	-0.32	-1.28	-2.3	-48	0.709096
DGR-3	860.53	Cambrian Formation	225	0.24	1.59	-4.8	-32	0.710228
DGR-4	327.08	Salina-A1 Unit	30	-0.05	-0.37	-14.5	-103	0.708596
DGR-4	377.42	Guelph Formation	375	-0.24	-1.10	-2.7	-50	0.709127
DGR-4	848.50	Cambrian Formation	227	0.36	1.56	-5.2	-35	0.710247

Note: Geochemical, $\delta^{18}O$ and $\delta^{2}H$ analyses were from Heagle and Pinder (2010), and $^{87}Sr/^{86}Sr$ analyses were from Clark et al. (2010). The analytical precision for both $\delta^{37}Cl$ and $\delta^{81}Br$ data is ±0.11‰ (stdv).

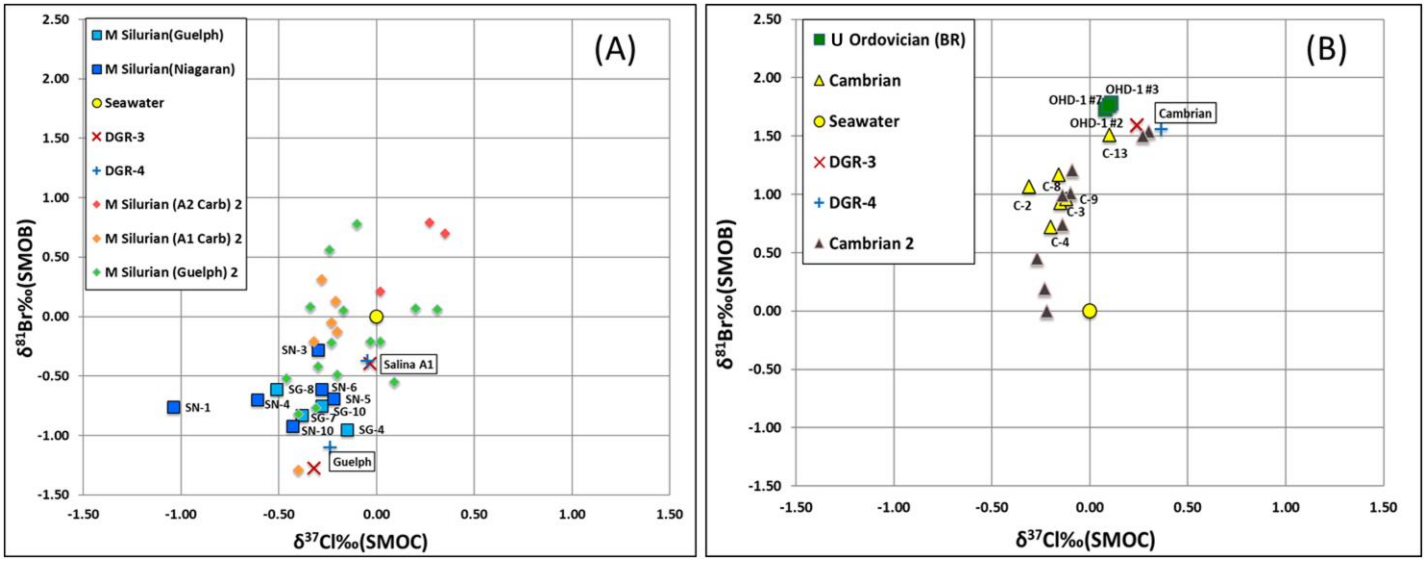

Figure 9: $\delta^{81}Br$ versus $\delta^{37}Cl$ for fluid samples (A) from Silurian strata and (B) from Cambrian and Ordovician (Black River) strata. The number 2 behind symbols in the legend refers to data from the Skuce et al. (2015) database. All other data are from the WRHD.

The $\delta^{37}Cl$ values of the two samples from the Salina A1 salts fall within the previously established range (-0.40‰ to -0.20‰) for this geological unit, as discussed in a recent study by Skuce et al. (2015). Referring to the bedrock stratigraphic column for DGR-3 and DGR-4 (Figure 3), the bedrock of the Upper Silurian Salina A1 Unit is comprised of argillaceous dolostone and anhydritic dolostone. The A1 units contain a variety of sulphate and chloride salts. Eggenkamp et al. (1994) proposed that the first salt precipitated from seawater has a higher $\delta^{37}Cl$ isotopic signature than the later precipitated salts. Salts precipitated during evaporation have lower $\delta^{81}Br$ and higher $\delta^{37}Cl$ than their corresponding residual fluids (Eggenkamp et al. 2016; Hanlon et al. 2017). Tan et al. (2009) concluded that the $\delta^{37}Cl$ value for early halite is higher than 0‰, whereas the later-formed halite has a value between -0.50‰ and 0‰. Therefore, the lower $\delta^{37}Cl$ values of the two Salina A1 salts (SA1-1 and SA1-2) suggest precipitation later in an evaporitic cycle. Therefore, halite dissolution could provide a possible source of solutes with the isotopic signature observed in the Salina A1 Unit samples from the site. Similar evolution and/or mixing/dilution processes appear to have occurred

in the Salina A1 Unit across much of southern Ontario, both in the Niagara and Bruce geological provinces (Hobbs et al. 2011).

4.1.2 Guelph Formation Fluids

The halide isotope data for the DGR-3 (389.99 m) and DGR-4 (377.42 m) fluids from the Silurian Guelph Formation plot near the Guelph Formation waters (SG-4, SG-7, SG-8, and SG-10) found in the WRHD and the equivalent Silurian Niagaran Formation waters from the Michigan Basin (Figure 9A). Referring to the stratigraphic cross-section of the site (Figure 3), the bedrock of the Guelph Formation is comprised of dolostone and dolomitic limestone. The formation waters for the SG-4, SG-7, SG-8, and SG-10 wells were collected from dolomitic limestone deposited in a reef environment west of the Algonquin Arch on the edge of the Michigan Basin (Liberty and Bolton 1971; Dollar 1988).

The $\delta^{81}Br$ values for the DGR-3 (389.99 m, -1.28‰) and DGR-4 (377.42 m, -1.10‰) Guelph Formation waters are lower than Guelph Formation samples (614-749 m, -0.95‰ to -0.61‰) from the Michigan Basin recorded in the regional database (Figure 9A). The evolution and/or mixing/dilution processes for Cl and Br in the samples from the various depths at the site appear to be identical to those for the very concentrated Guelph Formation fluids (Figure 7). The lower $\delta^{81}Br$ values (Figure 9A) are similar to Michigan Basin brines and, therefore, most likely represent fluids from a common source or evolutionary process.

4.1.3 Cambrian Formation Fluids

As shown in Figure 9B, Cambrian Formation fluids from the DGR-3 (860.53 mbgs) and DGR-4 (848.50 mbgs) boreholes have high $\delta^{81}Br$ and $\delta^{37}Cl$ values that are similar to Cambrian fluids from

regional oil wells in southern Ontario. These fluids have isotopic compositions similar to the deeper Ordovician Black River Group brines found in the Lakeview, Toronto research borehole OHD-1 (OHD-1 #2, OHD-1 #3, and OHD-1 #7), the C-13 sample from an oil well intersecting Cambrian-aged strata (from the WRHD), and two Cambrian samples from oil wells (Skuce et al., 2015 database).

The OHD-1 and Cambrian oil well samples are from the Niagara tectonic structural block, and the wells are located on the north shore of Lake Ontario and Lake Erie (Figure 4a). However, the OHD-1 samples were collected from relatively shallow depths (from 300 m to 368 m below ground surface). The Cambrian C-13 sample is from 887 m below ground surface, similar to the depth of the Cambrian samples from the DGR site. According to the bedrock lithology described by Liberty (1969), the OHD-1 #2, #3, and #7 fluids from the Lakeview, Toronto, boreholes are from craton-derived clastic rocks and impure carbonate rocks. The Cambrian Formation waters in C-13 are found in sandstones and sandy dolostone strata (Trevail 1990).

4.2 $\delta^{18}O$ and $\delta^{2}H$

The similarity of the fluids from the site to fluids in the same stratigraphic units across the region (particularly the Cambrian) needs to be confirmed using other geochemical and isotopic parameters. To this end, the $\delta^{18}O$-$\delta^{2}H$ results for groundwater samples from the site were examined and are discussed in the context of fluid origins – i.e., the concept of a sedimentary formation fluid origin versus a crystalline shield origin.

The $\delta^{2}H$-$\delta^{18}O$ data for the groundwater samples collected during site characterization activities at the Bruce Nuclear Site, obtained from NWMO (Intera 2011), is plotted in Figure 10a. The $\delta^{2}H$-$\delta^{18}O$

data in Figures 10a and 10b show that the formation waters from the Salina A1 Unit at the site plot away from the other regional data for concentrated sedimentary formation fluids in Ontario and Michigan. The significantly lower values of the Salina A1 samples from DGR-3 (327.08 m) and DGR-4 (339.66 m) indicate mixing of the original saline formation water (evaporated paleo-seawater) with fresh water from a cooler time period and/or glacial melt water.

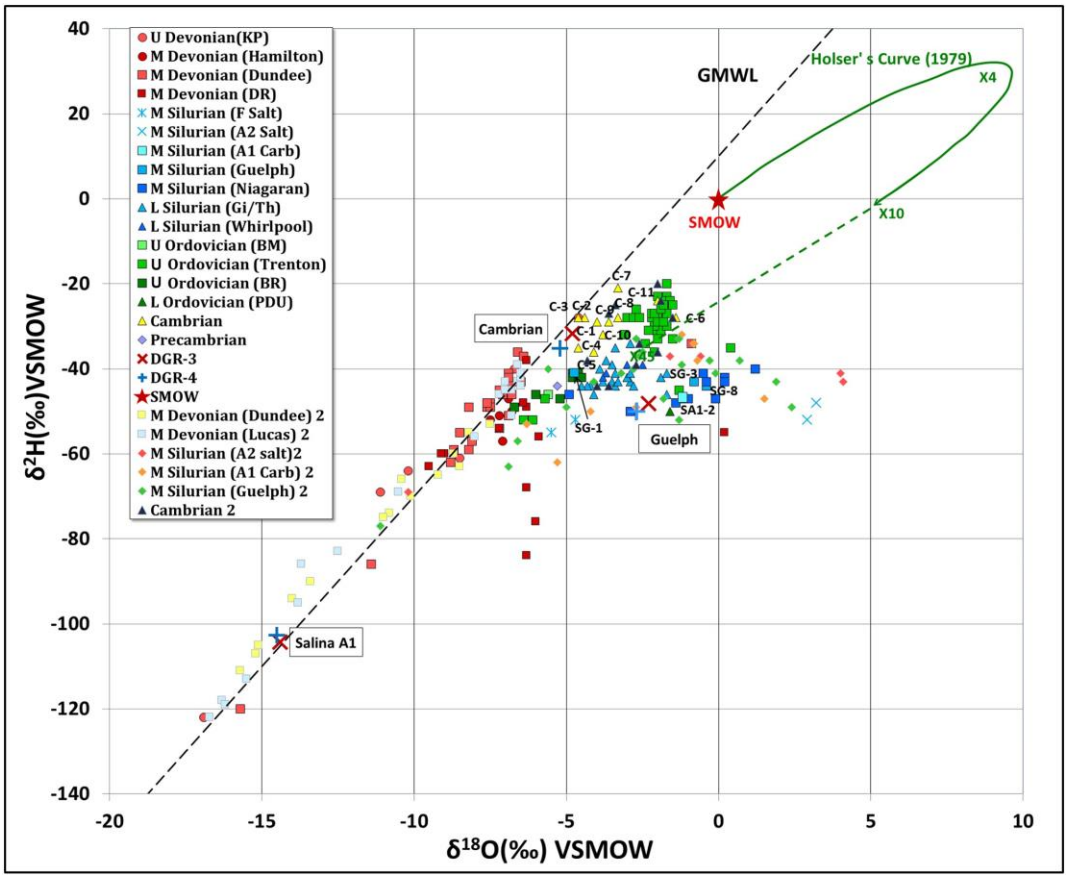

Figure 10a: $\delta^{18}O$ versus $\delta^{2}H$ for sedimentary formation fluids in the regional databases and site groundwaters from this study. The number 2 behind symbols in the figure legend refers to data from the Skuce et al. (2015) database. All other data are from the WRHD. The Holser Evaporative Curve (1979) shows the evolutionary evaporation pathway for seawater and indicates that concentrated sedimentary formation brines in strata in the region could have a marine origin.

Glacial melt water has low $\delta^{2}H$ and $\delta^{18}O$, and lower concentrations of chlorine and bromine than underlying formation waters. Hence, dilution with fresh 'glacial' water will substantially change the

Br-Cl concentration and δ^2H-$\delta^{18}O$, but will have little or no impact on the $\delta^{81}Br$ and $\delta^{37}Cl$ of the Salina A1 groundwaters from the site. A number of Devonian-sourced fluids from southwestern Ontario in the combined regional database have also had their present water isotopic signatures attributed to mixing with glacial fluids (McNutt et al. 1987; Dollar 1988; Weaver et al. 1995; NWMO 2011; Intera 2011).

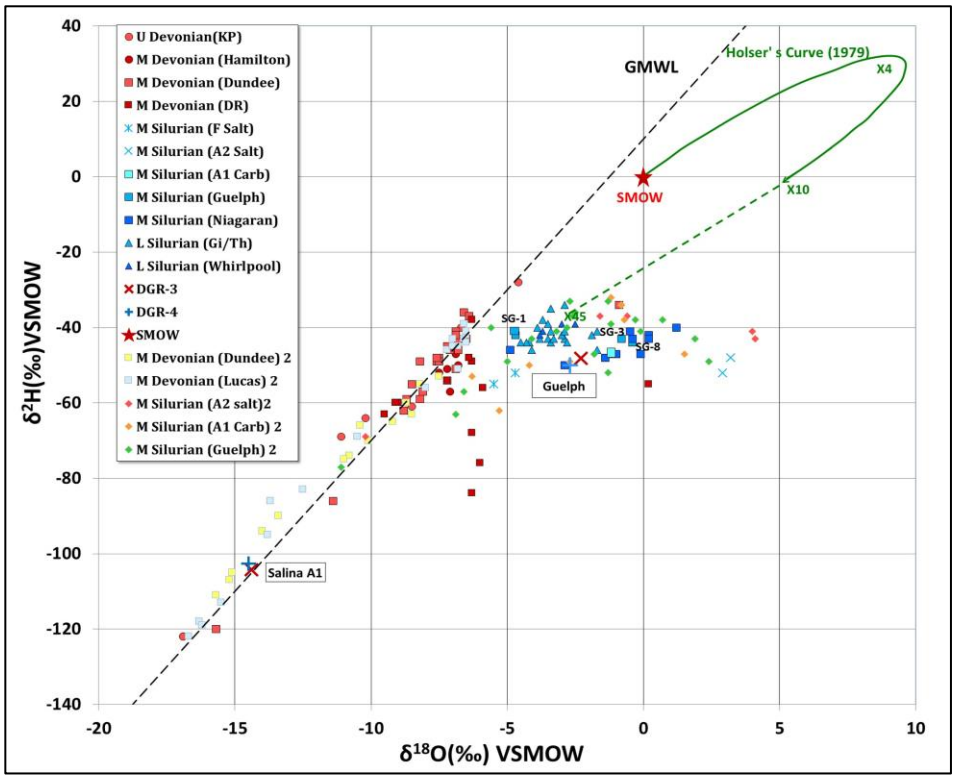

Figure 10b: $\delta^{18}O$ and δ^2H in sedimentary formation fluids from Silurian and Devonian strata in the regional databases and site groundwaters. The number 2 behind symbols in the legend refers to data from the Skuce et al. (2015) database. All other data are from the WRHD. The Holser Evaporative Curve (1979) shows the evolutionary evaporation pathway for seawater and indicates that concentrated sedimentary formation brines in strata in the region could have a marine origin.

Similar to the regional Guelph Formation waters formed elsewhere in the deeper bedrock of the Michigan Basin, the Guelph Formation water samples from the site have very high bromide and chloride concentrations and are dominated by Na-rich solutions (Table 1). Thus, the origins of the

Guelph Formation waters at both the site and regional scales are similar, based on their geochemistry. Both sets of data appear to be highly evolved and evaporated paleo-seawater, based on their locations on Figures 7 and 10b.

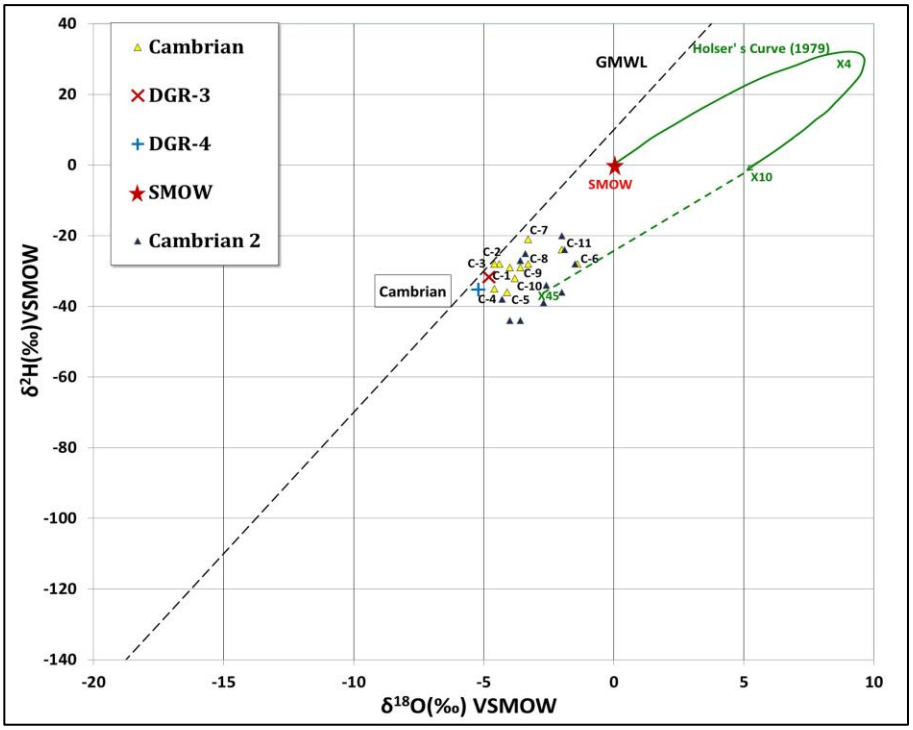

Figure 10c: $\delta^{18}O$ and $\delta^{2}H$ in sedimentary formation fluids from Cambrian strata in the regional databases and site groundwaters. Black triangles are data from the Skuce et al. (2015) database. The Holser Evaporative Curve (1979) shows the evolutionary evaporation pathway for seawater and indicates that concentrated sedimentary formation brines in strata in the region could have a marine origin.

Finally, the Cambrian samples from DGR-3 (860.53 m) and DGR-4 (848.50 m) at the site plot with the cluster of regional Cambrian samples in Ontario, and are located to the right and below the GMWL (Figure 10c). The Holser's curve (1979) evolution model indicates that the Cambrian Formation waters are derived from highly evaporated paleo-seawater. A comparison of the Cambrian data to crystalline shield brine data shows that samples with similar concentrations have very different $\delta^{18}O$-$\delta^{2}H$ values (Figure 6). The shield samples plot above and to the left of the GMWL (Frape and Fritz 1987). Although shield brines also have high $\delta^{81}Br$ values (Stotler et al.

2010), it is more likely that the Cambrian halide isotopic signatures have a sedimentary origin based on their $\delta^{18}O$-$\delta^{2}H$ signatures. The samples taken at the site from the Cambrian Formation plot close to the combined regional data sets for the same stratigraphic units east of the Algonquin Arch. Therefore, it is more probable that the Cambrian Formation fluids sampled from the site were derived from the same ancient sedimentary fluids that were present in both the Michigan and Appalachian basins during the Cambrian before the units were eroded across the present-day Algonquin Arch and became isolated in the two basins.

4.3 δ^{81}Br Isotope and $^{87}Sr/^{86}Sr$ Analysis

Figure 11 shows the relationship between $\delta^{81}Br$ and $^{87}Sr/^{86}Sr$ for samples from the site (Intera 2011) and for fluids from the combined regional data sets. The regional formation fluids and the formation fluids from the site are divided into two groups. The deeper Cambrian-sourced fluids from the site are most similar to the Ordovician, Lower Silurian and Cambrian regional formation fluids, whereas the relatively shallower fluids from the Silurian units at the site lie within an area on Figure 11 with the Upper Silurian and Devonian regional formation fluids from the Michigan Basin. The Guelph Formation fluids have similar $^{87}Sr/^{86}Sr$ as the regional Guelph Formation fluids. The Cambrian fluids from the site are slightly more radiogenic than regional Cambrian samples from the Niagara block; in particular, samples such as C-13 discussed earlier. The author does not feel this is a significant difference and may be due to slight mineralogical variations in the source rocks at the different locations. This similarity supports the hypothesis of the source (Michigan Basin origin) and evolutionary history (paleo-seawater evaporation) of the Guelph Formation fluids. Samples of the Salina A1 at the site have similar $^{87}Sr/^{86}Sr$ as the regional Salina A1 samples reported by Skuce et al. (2015). In many additional plots of chemical parameters and isotopic parameters (not shown),

this similarity between fluids from the three depths at the Bruce Nuclear Site and those from the combined regional databases by Hobbs et al. (2011) and Skuce et al. (2015) are observed.

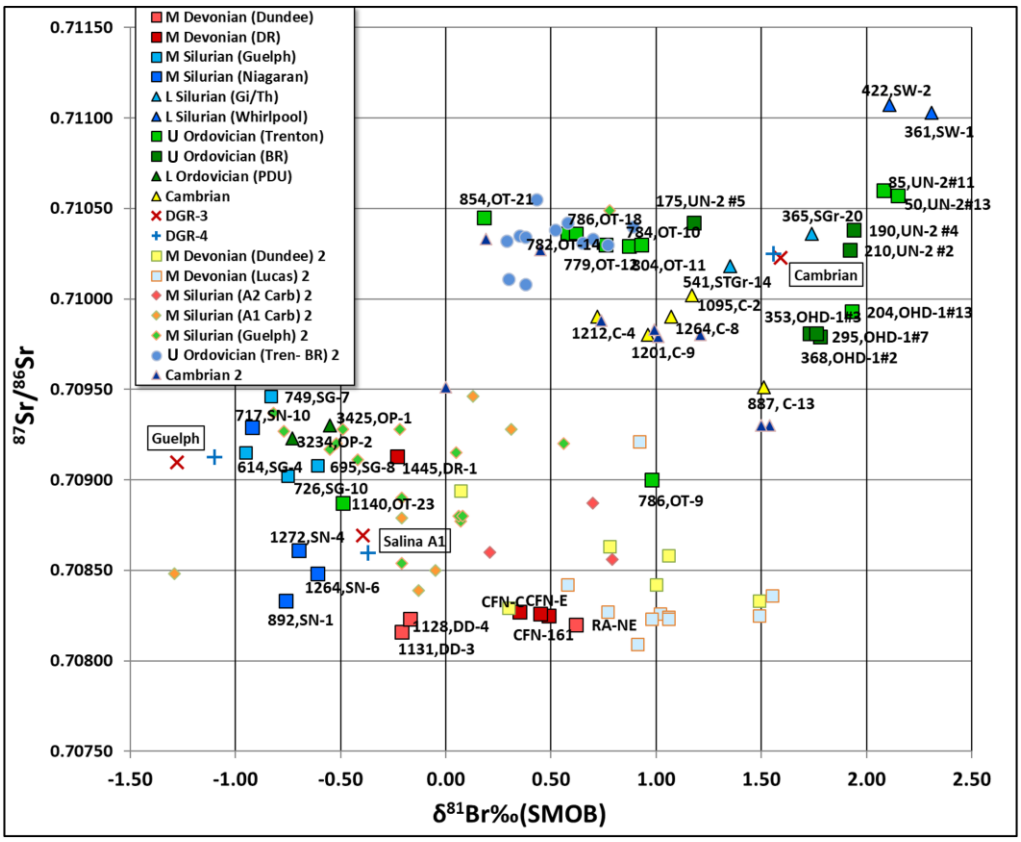

Figure 11: δ^{81}Br versus $^{87}Sr/^{86}Sr$ for sedimentary formation fluids from the regional databases vs groundwater from the site. The number 2 behind symbols in the legend refers to data from the Skuce et al. (2015) database. All other data are from the WRHD.

4.4 δ^{81}Br Versus Br Concentration

Figure 12 is a plot of δ^{81}Br versus Br concentrations for the six groundwater samples from the site (see Table 1) and the combined regional data sets. The data from the Guelph Formation waters at the site plot in proximity to the Guelph and Niagaran Formation fluids in the WRHD. The Salina A1 samples from the site plot distinctly away from both the regional Silurian samples and the Guelph Formation waters from the site. The Salina A1 samples at the site have much lower Br concentrations

than most fluids in the WRHD. As stated earlier, this is most likely the result of dilution by glacial waters, as indicated by the $\delta^{18}O$-$\delta^{2}H$ data. The glacial waters, which are assumed to have low Br concentrations, would not appreciably affect the $\delta^{81}Br$ of the groundwater samples.

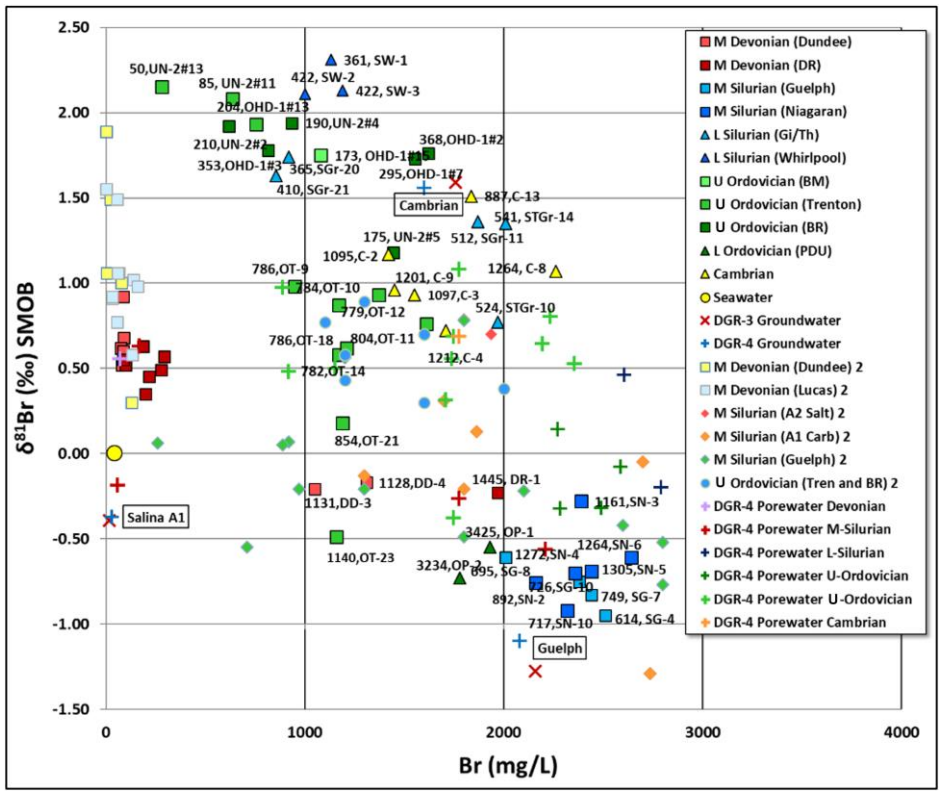

Figure 12: $\delta^{81}Br$ versus Br concentrations in samples from the Bruce Nuclear Site compared to the combined regional databases. The number 2 behind symbols in the legend refers to data from the Skuce et al. (2015) database. All other regional data are from the WRHD.

Commonly, the dilution of formation waters is higher at the margin than the center of the Michigan Basin (McIntosh and Walter 2005, 2006). Halite dissolution, especially of the Salina salts in Ontario, had a small influence on the geochemical composition and concentration of chlorine and bromine (McIntosh and Walter 2005, 2006). The data on Figure 12 illustrate that the bromide concentrations of the Salina A1 Unit waters at the site are chemically and isotopically similar to a large number of overlying dilute shallow Devonian samples that have been shown to be impacted by mixing with

cold climate glacial waters (Figures 6, 7 and 10a).

The plot of $\delta^{81}Br$ versus Br/Cl weight ratios (Figure 13) for the site groundwater samples versus the combined regional database samples supports many of the ideas discussed above. The Br/Cl weight ratios of the Guelph and Cambrian formation waters are greater than the ratio for seawater (0.0034) (Figure 13). As shown on Figure 7, the evaporation of sea water results in a rapid enrichment of Br concentration once halite (NaCl) begins to crystallize/precipitate. A residual evaporated paleo-seawater similar to the regional formation fluids appears to be the main end member of the Guelph and Cambrian groundwaters at the site (Figure 7).

The Salina A1 waters from DGR-3 and DGR-4 have a lower Br/Cl weight ratio than seawater (Figure 13). Therefore, the Salina A1 formation waters would appear to have a different end member(s) than the other groundwaters at the site. The Salina A1 samples from the site may have a non-marine water source and/or halite dissolution source based on the processes and mixing scenarios shown in Figure 7. Figure 13 shows that halite dissolution is more probable based on the low Br/Cl weight ratio (<0.002) of the samples. As halite is usually more deficient in Br relative to the fluid from which it precipitated, the dissolution of halite would significantly increase the Cl concentration relative to Br (Rittenhouse 1967; Collins 1975; Carpenter 1978; Kharaka et al. 1987; Land 1997). In addition, the Salina A1 fluids have low $\delta^{81}Br$ (-0.39‰ for DGR-3 and -0.37‰ for DGR-4). Halite salts have been shown to have low $\delta^{81}Br$ (Eggenkamp et al. 2014, 2016). Based on the $\delta^{18}O$ and $\delta^{2}H$ data (Figure 6 and 10a), the low $\delta^{18}O$ of the Salina A1 samples from the site are consistent with the $\delta^{18}O$ signature of glacial waters.

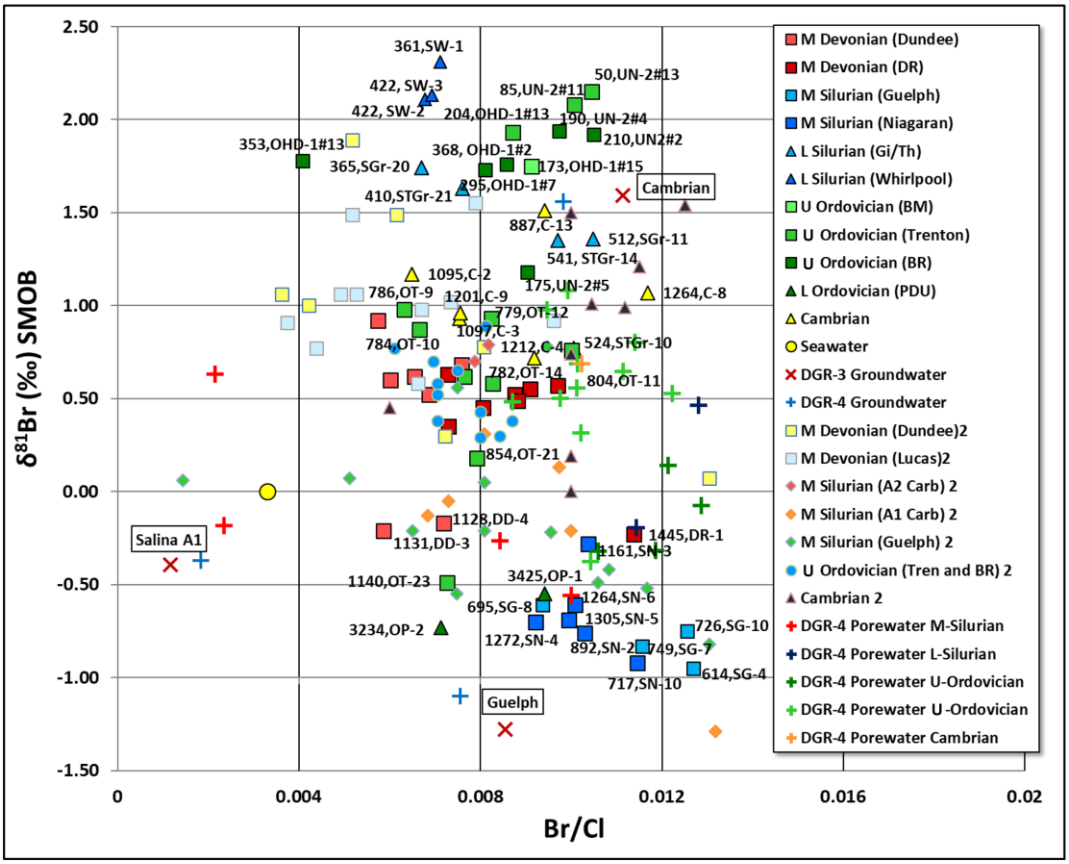

Figure 13: δ^{81}Br versus Br/Cl weight ratio for groundwaters in the Silurian and Cambrian strata at the site compared to the regional database for sedimentary formation fluids. The number 2 behind symbols in the legend refers to data from the Skuce et al. (2015) database.

5. RESULTS AND DISCUSSION (PART THREE)

5.1 Porewater Results (DGR-4)

The $\delta^{37}Cl$ values for the porewater samples from the DGR-4 borehole range from -1.26‰ to +0.55‰, and the $\delta^{81}Br$ values range from -0.56‰ to +1.08‰ (Table 2). The Cl and Br isotopic results of the porewaters from DGR-4, measured as part of this study, are listed in Table 2, and illustrated in Figures 8, 14 and 15. The isotopic values generally fall within the ranges listed for formation groundwaters in the combined regional data sets (Shouakar-Stash 2008; Hobbs et al. 2011; Skuce et al. 2015), found in Table A1 and Table A2 in the Appendix.

5.2 $\delta^{37}Cl$ and $\delta^{81}Br$ for Porewaters in DGR-4

A significant trend in porewater chemistry with depth in the DGR-4 borehole is a decrease in Cl and Br concentrations through the Lower Silurian units into the Upper Ordovician shales (Figure 14a). This is followed by a general trend to lower pore-water salinity throughout the underlying Ordovician limestones (Figure 14a) (Clark et al. 2013). At the bottom of the profile, Cl and Br concentrations increase down-section through the lower part of the Ordovician limestones and the Cambrian sandstones (Clark et al. 2013). The lower Silurian to Cambrian stratigraphic sequence at the site has been defined as a diffusion-dominated system (Clark et al. 2013; Al et al. 2015). These diffusional mixing scenarios are calculated to take millions to hundreds of millions of years (> 260 Ma) (Clark et al. 2013; Al et al. 2015). However, a simple diffusion-dominated model through the geological sequence at the site does not easily explain the $\delta^{37}Cl$ and $\delta^{81}Br$ trends for porewaters in DGR-4 (Figure 14a).

Table 2: Geochemical data for the porewaters from DGR-4 at the Bruce Nuclear Site.

Borehole	Depth rel. to DGR1/2 (m)	Stratigraphic Unit	Cl (mg/L)	Br (mg/L)	Sr (mg/L)	K (mg/L)	Na (mg/L)	Ca (mg/L)	Mg (mg/L)	SO_4 (mg/L)	HCO_3 (mg/L)	$\delta^{37}Cl$ (SMOC) ‰	$\delta^{81}Br$ (SMOB) ‰	$\delta^{18}O$ (VSMOW) ‰	$\delta^{2}H$ (VSMOW) ‰
DGR4 110.32-out-7	108.57	Lucas-Bass Islands	3310.8	70	123	164	851	1515	807	2882		-0.06	0.56	-14.2	-107
DGR4 243.44-in-4	241.36	Salina B evap	24601	58	140	1212	20484	9579	1636	42939	522	-1.26	-0.18		
DGR4 304.05-in-1	303.92	Salina A2 carb	77617	167	245	586	48923	7334	2698	19884	1243	-0.11	0.63	-10.1	-59
DGR4 369.70-2	369.03	Salina A1 evap	210307	1773	2182	13997	69591	104203	17597	222667	2863	-0.23	-0.26	-9.5	-91
DGR4 386.31-6	384.47	Guelph	220936	2209	1218	13489	63475	83643	22069	157731		-0.43	-0.56	-4.4	-67
DGR4 418.95-5	418.33	Cabot Head	203224	2604	1428	11847	40072	70016	8288	15946	159	-0.15	0.46	-2.4	-40
DGR4 442.58-3	443.14	Manitoulin	243824	2789	2865	14427	62326	146485	32326	350619	2926	-0.21	-0.20	-0.1	-46
DGR4 469.13-7	469.65	Queenston	201047	2587	1016	14740	45727	44968	13198	1825	1964	-0.19	-0.08	-2.6	-45
DGR4 508.95-2	508.03	Queenston	198799	2489	1095	13880	44233	42723	11569	3362	252	0.08		-2.3	-43
DGR4 549.21-7	548.65	Georgian Bay	191358	2269	1297	15835	50762	43966	9309	7108	928	0.20	-0.32		
DGR4 595.38-3	595.97	Georgian Bay	188149	2283	1349	12355	48923	46250	7656	13256		0.04	0.14		
DGR4 625.37-6	625.35	Blue Mountain	184306	2155	1376	10556	49038	47653	7219	13929	734	-0.03		-3.9	-44
DGR4 643.15-3	642.18	Blue Mountain	172975	1792	1183	10400	45520	40278	7316	17963		-0.18	-0.32	-3.5	-47
DGR4 654.30-4	652.73	Cobourg	135399	1434	964	17320	47267	24408	13878	55523	3442	-0.17		-5.3	
DGR4 663.25-6	661.32	Cobourg	192425	2353	1227	14818	54785	33064	16236	34197	4680	-0.18	0.53	-4.9	
DGR4 669.18-7	667.49	Cobourg	213154	2537	3601	20566	63475	268202	38572	778758		-0.18			
DGR4 671.02-7	669.40	Cobourg	195619	2232	1384	15366	57107	35068	16698	44092	547	-0.06	0.80		
DGR4 681.90-3	680.72	Cobourg	196856	2194	1490	16969	59199	40679	17645	73006		-0.20	0.65	-4.4	
DGR4 704.12-3	703.06	Sherman Fall	171766	1738	902	15561	53452	36150	12760	65897	2835	0.09	0.56	-4.7	-69
DGR4 716.15-6	714.96	Sherman Fall	167391	1746	1008	16617	56877	40479	15045	74831			-0.38	-5.1	-78
DGR4 740.63-1	739.53	Kirkfield	167207	1708	1595	14584	54992	42843	10014	72045	5079	-0.09	0.32	-8.1	
DGR4 768.52-5	767.33	Coboconk	172096	1746	1008	5005	46532	32022	13757	40537	3533	0.41	0.69	-5.9	-41
DGR4 792.29-7	790.64	Gull River	93809	888	280	5200	41612	12785	5639	43323	5269	0.55	0.98	-8.0	
DGR4 801.10-3	799.68	Gull River	118034	1153	482	6295	41865	27614	12371	70892	1807	0.03	0.50	-7.5	-38
DGR4 822.35-1	821.50	Gull River	105285	916	403	5278	38646	25570	5979	73390	1035	0.20	0.48	-7.1	-38
DGR4 845.65-1	845.33	Shadow Lake	178630	1774	832	1603	42509	43044	16819	62343	517	0.48	1.08	-3.9	-34
DGR4 852.77-5	852.34	Cambrian	173227	1773	797	2150	43635	58995		145339	721	0.20	0.69	-4.1	-32

Note: Geochemical, $\delta^{18}O$ and $\delta^{2}H$ analyses are from Clark et al. (2010). The analytical precisions for the $\delta^{18}O$, $\delta^{2}H$, $\delta^{37}Cl$ and $\delta^{81}Br$ values are ±0.15‰, ±1.50‰, ±0.11‰ and ±0.11‰, respectively.

Clark et al. (2013) attribute the stratigraphic $\delta^{18}O$ trend shown in Figure 14a to a combination of downward diffusive migration from the hypersaline Silurian units to the underlying less saline Ordovician limestones. These authors also introduce the possibility of Cambrian and even Precambrian brines entering the pore spaces of the lower part of the Ordovician units through upward diffusion/advection and mixing with the pre-existing Ordovician marine seawaters (Al et al. 2015). As shown earlier, concentrated fluids from the regional Silurian salt units have a wide range of $\delta^{18}O$ (-5.5‰ to +3.2‰). Precambrian shield brines have $\delta^{18}O$ that is significantly different from sedimentary formation fluids (Figure 6). A simple diffusion model cannot easily explain the complex fluid migration processes in the subsurface of the site suggested by the halide isotopic profiles (Figure 14b). Therefore, in the present study, the diffusive processes within the Ordovician sequence are divided into three parts to be discussed as follows: first – through the Cobourg Formation and upper Sherman Fall Formation; second – through the Coboconk Formation; and third – from the middle Gull River Formation to the Cambrian Formation.

First, there is a slight increase in halide isotopic ratios with depth in DGR-4. At the bottom of the isotopic profile (Figure 14b), there are multiple reversals in the trends for both $\delta^{37}Cl$ and $\delta^{81}Br$ throughout the lower part of the Ordovician limestones (Figure 14b). The high $\delta^{81}Br$ of porewaters in the Ordovician limestones (through the Cobourg and upper Sherman Fall Formations) appear enclosed between two zones of low $\delta^{81}Br$ in the lower Blue Mountain Formation and the lower Sherman Fall Formation. The concave-shaped $\delta^{81}Br$ profile with depth between the lower Blue Mountain Formation and the lower Sherman Fall Formation may be explained by binary bromide diffusion from the lower Cobourg Formation due to higher halide concentrations as shown on Figure 14b. This is a similar process invoked in other studies from a number of sites worldwide (Coleman et al. 2000; Hendry et al. 2000; Hesse et al. 2000; Eastoe et al. 2001; Waber et al. 2001).

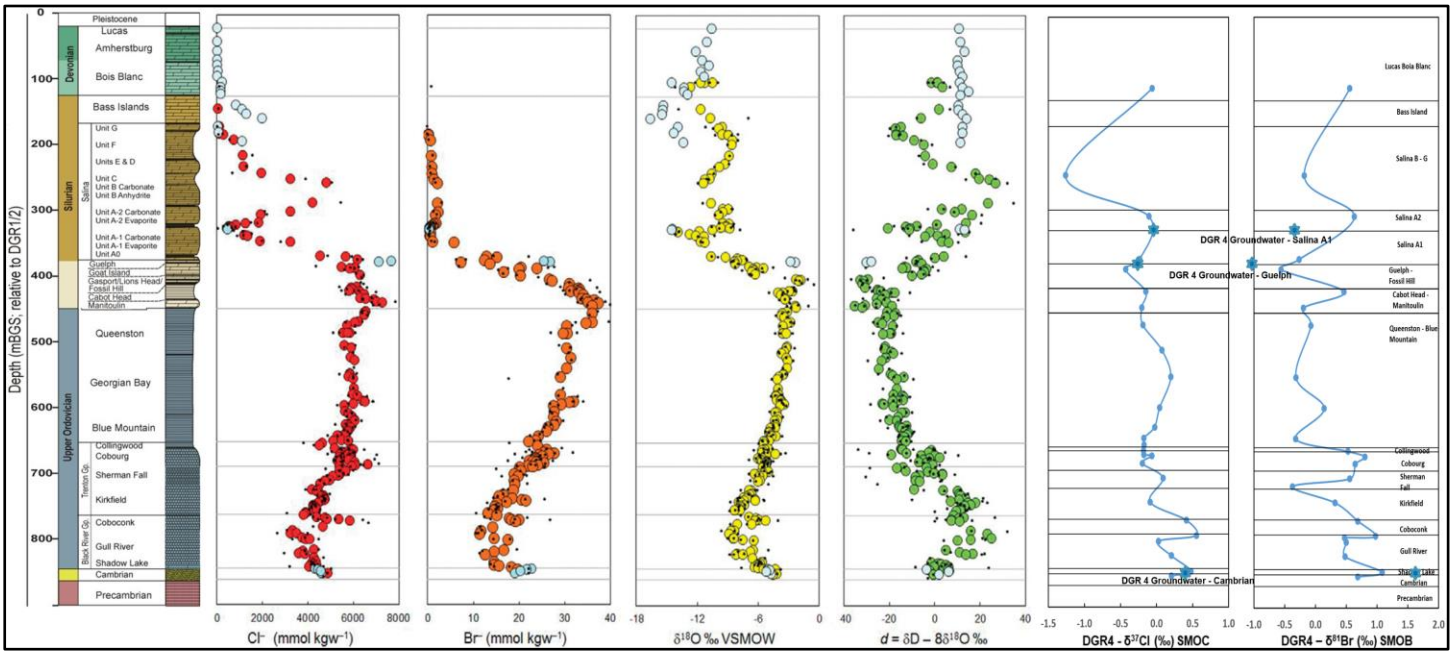

Figure 14a: Stratigraphy and porewater tracer profiles (Cl-Br concentrations, $\delta^{18}O$, d, $\delta^{37}Cl$, and $\delta^{81}Br$) from the Bruce Nuclear Site (borehole DGR-4), Ontario, Canada (Modified from Clark et al. 2013).

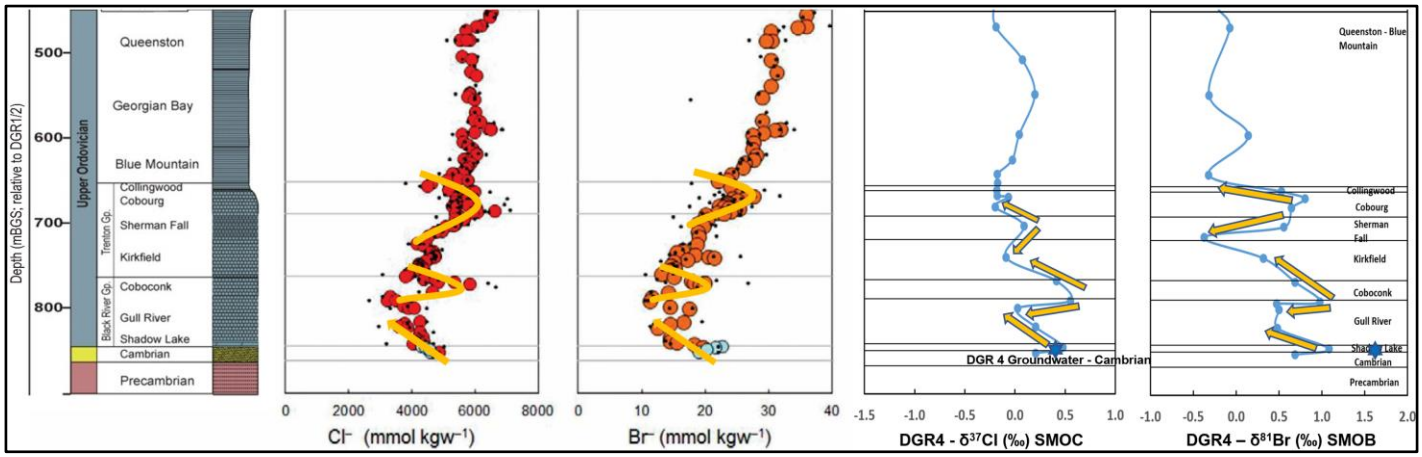

Figure 14b: Ordovician to Precambrian stratigraphy and porewater tracer profiles (Cl-Br concentrations, $\delta^{37}Cl$, and $\delta^{81}Br$) from the Bruce Nuclear Site (borehole DGR-4), Ontario, Canada (Modified from Intera 2011 and Clark et al. 2013).

Porewaters from the Coboconk Formation were characterized by a slight enrichment in the halide concentrations and slightly higher isotopic values compared with porewaters between the Kirkfield and Gull River Formations in the lower part of the Ordovician sediments (Figure 14b). A two-sided

isotopic diffusion process from the Coboconk Formation into the surrounding layers could also be invoked to explain the observed halide isotopic profile in this part of the stratigraphic sequence.

There is a reversal for the halide concentration profile at the bottom of the Ordovician limestones (Figure 14b), accompanied by higher isotopic values, with depth from the middle Gull River Formation to the Cambrian Formation. The bromide isotopic profile between the Gull River Formation and the Cambrian Formation raises the possibility of upward diffusive migration from the Cambrian Formation to the lower part of the Ordovician limestones, possibly driven by hydrothermal circulation, as suggested by other authors to explain parallel geochemical trends (Coniglio et al. 1994; Hobbs et al. 2011). In such a case, greater halide concentrations and relatively higher halide isotopic values in the Cambrian Formation at the site could be attributed to an external input from either deeper in the Michigan Basin or from the underlying Precambrian crystalline rocks whose present day δ^{81}Br has been shown to be higher than SMOB worldwide (Stotler et al. 2010). As proposed by others (Clark et al. 2013), such a process would require the Cl-Br solutes to diffuse or advect independently of the water O molecules if the underlying shield brines were invoked as a source, because shield brines have a very different δ^{18}O than the pore fluids and groundwaters in the Cambrian strata. In addition, the crystalline shield rocks have much lower porosity and therefore the volume of fluid is significantly lower than the Cambrian sedimentary rocks and insufficient to appreciably change the resident sedimentary fluid chemistry.

5.3 Porewaters Versus Groundwaters and Regional Formation Waters

In this section, porewater data are compared to the site groundwater and regional formation fluid data to identify similarities and differences in isotopic values. Regional studies have identified porewater isotopic signatures in the lower Paleozoic as most likely representing the old marine

formation signatures emplaced at or shortly after deposition of the units. As well, the $\delta^{37}Cl$ and $\delta^{81}Br$ of porewaters in the Cambrian and lower part of the Ordovician are often distinctive from each other and from other regional geological units.

It should be understood that this will be a first attempt to use the Br and Cl isotope systems together at a site where usually low permeability geological material is being assessed for potential diffusive properties. As shown on Figure 14a, the $\delta^{37}Cl$ for the three groundwater samples at the site are very close to the $\delta^{37}Cl$ of the porewater samples at the same depths. By contrast, the $\delta^{81}Br$ of the groundwaters from the DGR-4 borehole are lower for the two Silurian units (A1 and Guelph) and higher in the Cambrian sample compared to porewaters at the same depths.

Figure 15 compares porewater $\delta^{81}Br$ and $\delta^{37}Cl$ from DGR-4 and the combined regional hydrogeochemistry data set. In general, porewater fluids from DGR-4 have similar $\delta^{81}Br$ and $\delta^{37}Cl$ values as samples from the equivalent geological units in the combined regional database, even though the WRHD is compiled primarily from groundwaters associated with oil and gas wells in the Niagara tectonic structural block, located south of the Bruce tectonic block where the site is located (Figure 4a).

Porewater data from the Devonian units at the site is limited, but is isotopically similar to regional fluids (Figure 15A). Porewater fluids from the Silurian units at the site are generally isotopically similar to regional fluids in the database (Figure 15B). The halide isotopic similarity for the Silurian pore fluids from the site and the combined regional database suggests a similar origin for the fluids. As discussed before, the formation waters from the Silurian-aged zone at the site can be described isotopically as fluids sourced within the Michigan Basin based on the dominantly low $\delta^{37}Cl$ and $\delta^{81}Br$ (Shouakar-Stash 2008).

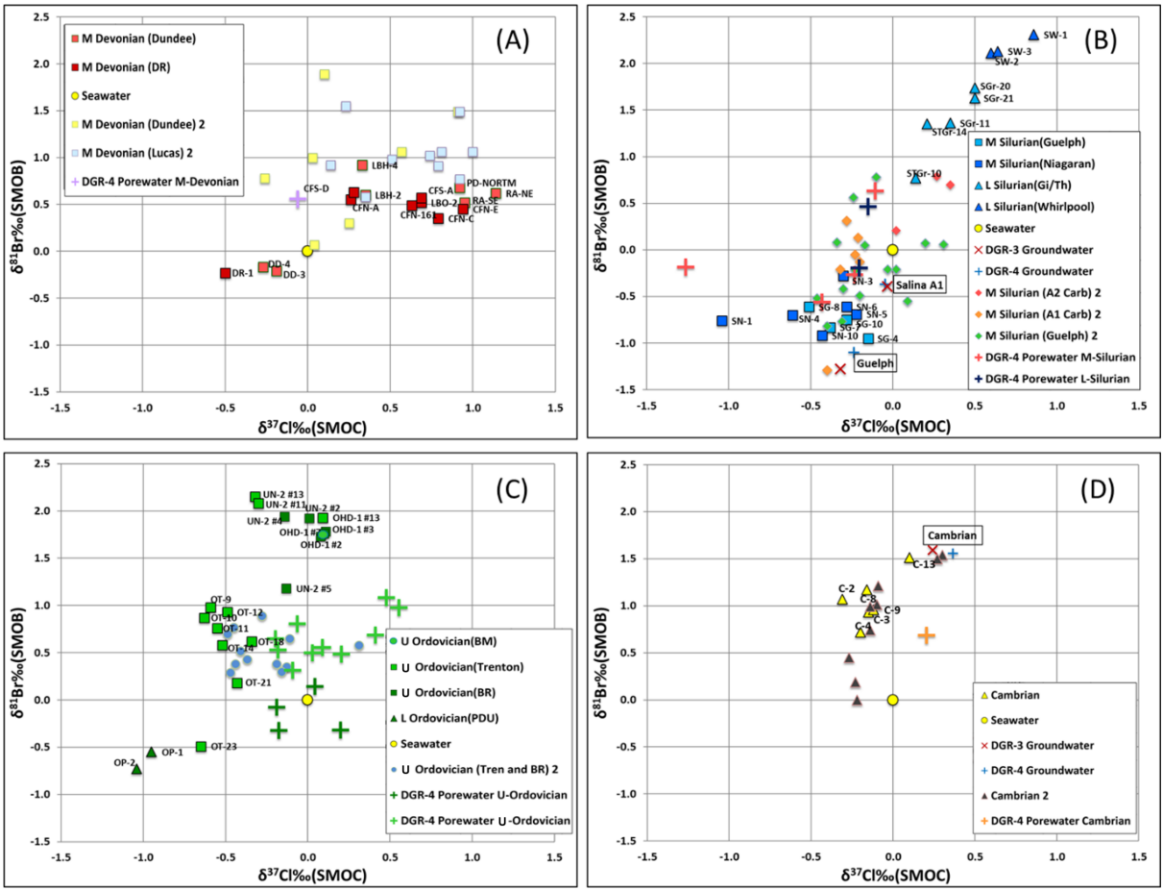

Figure 15: A comparison of $\delta^{37}Cl$ and $\delta^{81}Br$ for porewaters and groundwaters at the site versus the southern Ontario regional sedimentary formation fluid database in (A) Devonian strata, (B) Silurian strata, (C) Ordovician strata, and (D) Cambrian strata (Shouakar-Stash 2008; Skuce et al. 2015).

In general, the $\delta^{37}Cl$ of the porewaters sampled from the Ordovician units at the site are isotopically heavier than Ordovician isotopic values from the regional database (Figure 15C). As shown on Figure 15D, the $\delta^{37}Cl$ of the Cambrian groundwater fluids are similar to the porewater fluids shown on the profile, but the $\delta^{81}Br$ of the groundwater samples are slightly higher than porewater samples for similar depths at the site.

In addition, both the Lower Silurian and the top of the Upper Ordovician porewaters in DGR-4 have $\delta^{18}O$ and $\delta^{2}H$ similar to the regional formation waters from equivalent units in the regional databases (Figure 6). The Ordovician Trenton and Black River porewaters also have similar $\delta^{18}O$ and $\delta^{2}H$ as

the regional Ordovician formation waters, although two porewater samples from the Gull River Formation plot slightly to the left and above the GMWL (Figure 6). However, the $\delta^{18}O$ for these Gull River Formation fluids are not sufficiently above the GMWL (Figure 6) to be classified as having any significant component of Precambrian brine fluids. As well, the Na-Ca-Cl chemistry of these fluids are very different from Canadian Shield brines (Frape et al. 1984).

Based on the geological ages of the units at the site and tectonic events during the early Paleozoic, it is reasonable to assume that some differences in halide isotopic signatures between pore fluids and regional sedimentary formation fluid or groundwater could exist. Several processes in the past or ongoing, such as diffusion, membrane filtration and organic or microbial activity, may result in variation of the halide isotopic signatures of the porewater fluids at the site. In most cases, diffusion within the geological units was previously considered to be the main impact causing changes in stable isotopic and chemical values at the site (Clark et al. 2013; Al et al. 2015).

The $\delta^{37}Cl$ and $\delta^{81}Br$ of the porewater samples at the site are potentially impacted by a variety of fractionation mechanisms over time. The halide isotopic variations seen at the site are not easily explained by a simple diffusion process across multiple geological layers of highly-variable sedimentological media. Instead, these variations most likely are the result of multiple influencing factors that have modified the halide isotopic signatures of the porewaters at the site on numerous occasions in the geologic past.

6. DISCUSSION OF PROCESSES THAT COULD IMPACT THE Cl AND Br ISOTOPIC COMPOSITIONS OF THE POREWATERS

In natural systems, the range of $\delta^{81}Br$ is much greater than $\delta^{37}Cl$ (Figure 2). Eggenkamp (2014) suggested that bromine and chlorine stable isotopes often fractionate in opposite and independent ways from one other. There are several major mechanisms, including diffusion, mineral precipitation, and organic/microbial processes, to be considered when discussing chlorine and bromine isotopic fractionation in natural environments (Eggenkamp 2014). However, the influence of these specific mechanisms on halide isotopic fractionation, especially for bromine isotopes, are poorly known and only described in a few studies (Kaufmann et al. 1992; Eggenkamp 2009, 2014; Stotler et al. 2010; Hanlon et al. 2017).

6.1 Depositional Environment

The Paleozoic sedimentary rocks within the Michigan and Appalachian basins were deposited in a marine environment when shallow seas covered the majority of these two basins in the early Paleozoic (Sanford et al. 1985).

Schilling et al. (1978) hypothesized that the accumulation of Cl and Br in the Earth's surface reservoirs, such as the ocean, was due to continuous degassing associated with volcanic events over long geologic time periods. These authors further proposed that the degassing rate of Cl and Br by volcanic activities at approximately 1,500 Ma was almost double the present-day degassing rates (Schilling et al. 1978). Volcanic gases, which have low $\delta^{37}Cl$ and $\delta^{81}Br$ (Hesse et al. 1989; Eggenkamp et al. 2014), would have been dissolved in the oceans or deposited directly on the

continental surface (Brown et al. 1989; Graedel and Keene 1996). The chlorine isotopic composition of mantle material such as basalts and other volcanic rocks was analyzed by previous researchers (e.g. Eggenkamp and Koster van Groos 1997; Barnes et al. 2008, 2009; Bonifacie et al. 2008; Layne et al. 2009; John et al. 2010; Sharp et al. 2013). As an example, the $\delta^{37}Cl$ of the mid-ocean ridge basalts indicate that the mantle-derived rocks have lower $\delta^{37}Cl$ ($\leq$ -1.6‰, Bonifacie et al. 2008) than surface reservoirs (~0‰) (Sharp et al. 2007; Bonifacie et al. 2007, 2008). Based on such studies, there are two major input factors for Cl and Br in the natural environment that were likely relevant in the geologic past, including continental weathering and mantle degassing (volcanic activities), and these processes would affect the chlorine and bromine isotopic compositions of seawater (Shouakar-Stash 2008; Eggenkamp et al. 2014).

As discussed above, the top of the Upper Ordovician sedimentary rocks is mainly comprised of extensive clastic sediments (shale sequence) as a result of the Late Taconic Orogeny (Figure 5a), however, the extensive Hirnantian glaciation occurred during the Late Ordovician and led to an increasing mantle contribution of solutes to the marine environment as a result of reduced continental weathering inputs to the ocean (Finnegan et al. 2011). In this case, the lower $\delta^{37}Cl$ and $\delta^{81}Br$ in these rock units can be explained. In contrast, the Upper Ordovician Trenton and Black River sediments are primarily characterized by higher $\delta^{37}Cl$ and $\delta^{81}Br$. This could be due to an increasing contribution of halides to the ocean from continental weathering. The top of the Upper Ordovician clastic sediments on the other hand have lower halide isotopic values that could be mainly derived from an increased mantle input (Sharp et al. 2007; Bonifacie et al. 2007, 2008; Layne at el. 2009) compared with the isotopically heavier Ordovician limestones. Another way of evaluating the porewater data is to compare it to the isotopic compositions shown in several seawater curves constructed by others and also for this study. `

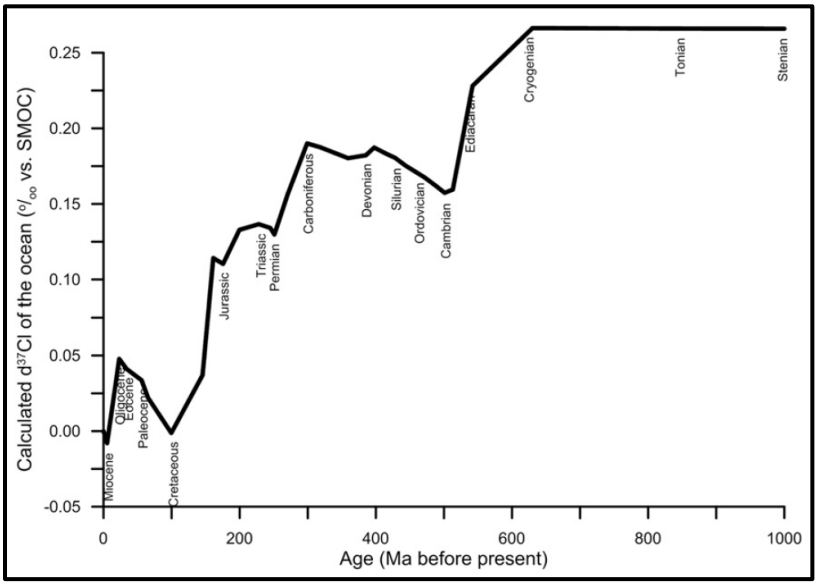

Figure 16a: Calculated evolution of seawater $\delta^{37}Cl$ (‰) (SMOC) during the last one billion years (from Eggenkamp et al. 2016). Both the extraction (precipitation of evaporites) and salt erosion data are from Hay et al. (2006).

Eastoe et al. (2007) and Eggenkamp et al. (2016) suggested that the chlorine isotopic values of paleo-seawater did not change significantly during the Phanerozoic Eon based on the small range of isotopic compositions in Phanerozoic evaporates (Figure 16a). A regional bromine isotopic study of sedimentary formation fluids from the Willston, Michigan and Appalachian Basins by Shouakar-Stash (2008) shows that the bromide concentration of seawater may have changed significantly during the Phanerozoic, which could have directly influenced seawater $\delta^{81}Br$ (Figure 16b, 16c) (Eggenkamp et al. 2015, 2016). All of the observed $\delta^{81}Br$ from this study fit the suggested range (between -1‰ and +2‰) for Phanerozoic seawater (Eggenkamp et al. 2015, 2016). Therefore, the variation in porewater $\delta^{81}Br$ (Figure 14a) at the site may be explained by variation in seawater $\delta^{81}Br$ in southern Ontario during the early Paleozoic.

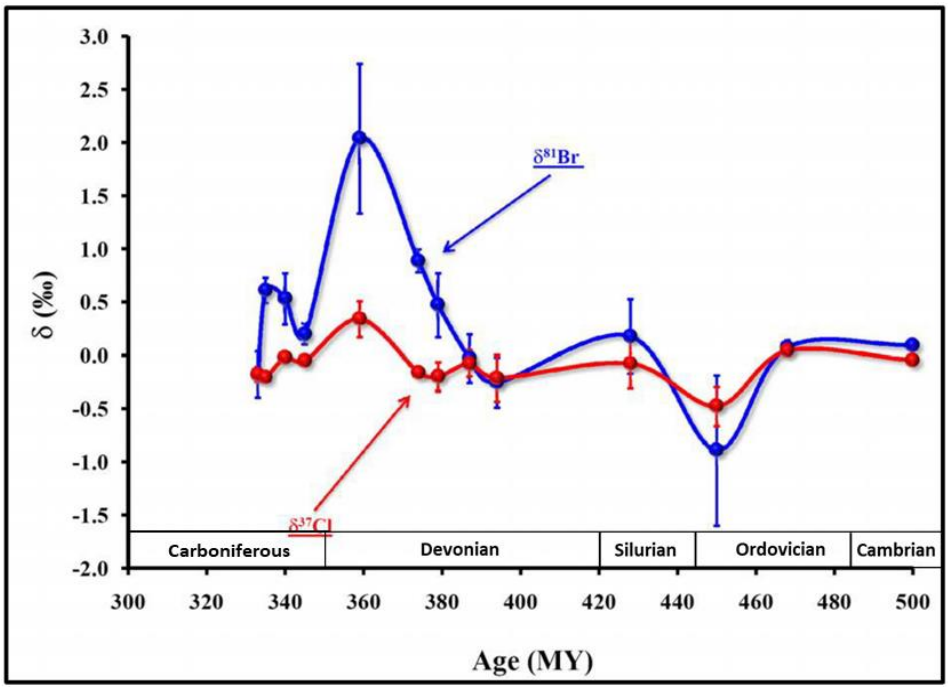

Figure 16b: δ^{81}Br (‰) (SMOB) and δ^{37}Cl (‰) (SMOC) versus Age (Ma) of the Williston Basin formation waters (Mississippian – Cambrian). The bars represent the isotopic ranges in each specific formation, and the dots represent the average isotopic values of these stratigraphic units (modified from Shouakar-Stash 2008).

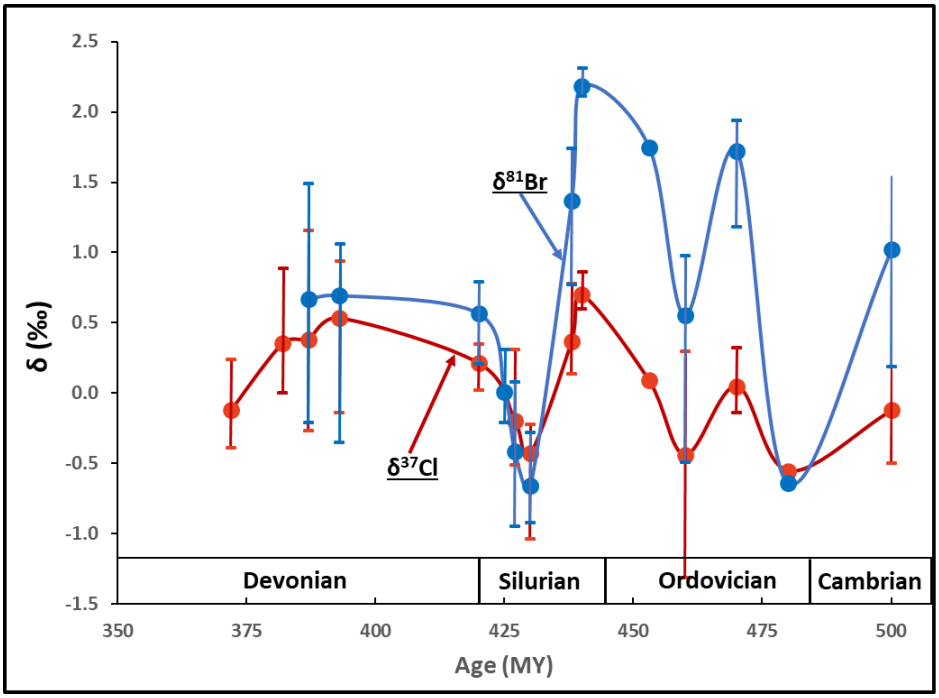

Figure 16c: δ^{81}Br (‰) (SMOB) and δ^{37}Cl (‰) (SMOC) versus Age (Ma) of the Michigan Basin and the Appalachian Basin (southern Ontario) formation waters (Devonian – Cambrian). The bars represent the isotopic ranges in each specific formation, and the dots represent the average isotopic values of these stratigraphic units. Data from WRHD (Shouakar-Stash 2008; Hobbs et al. 2011; Skuce et al. 2015).

Figure 14a shows the porewater halide isotopic variations obtained from core samples throughout the stratigraphic units of borehole DGR-4. Figure 16d was constructed to compare these porewater halide isotopic values to the average isotopic values for each unit from the WRHD. It is apparent that in some cases, the average calculated seawater values for many units are quite different from DGR-4 porewater values. Therefore, other depositional or post-depositional processes must be evaluated to aid in the interpretation of the isotopic profiles shown in Figures 14a and 16d.

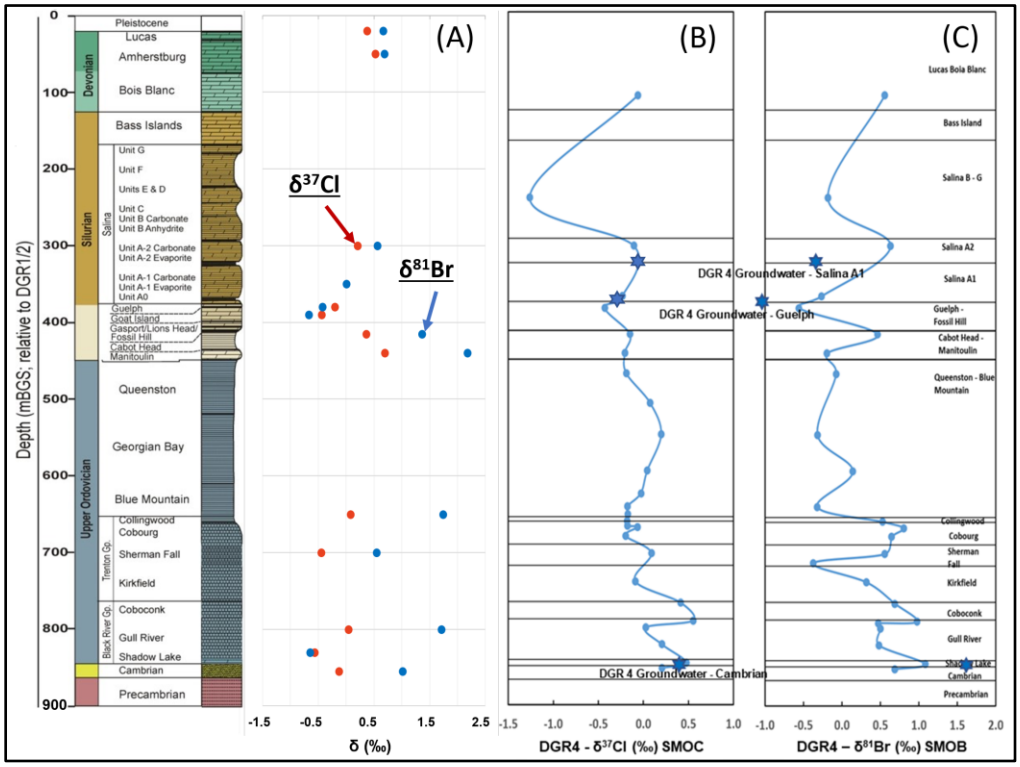

Figure 16d: (A) Stratigraphy (Devonian to Precambrian), and the $\delta^{37}Cl$ (‰) (SMOC) and $\delta^{81}Br$ (‰) (SMOB) profiles of average regional formation waters from the Michigan Basin and southern Ontario (Data from WRHD; Shouakar-Stash 2008; Hobbs et al. 2011; Skuce et al. 2015), (B) $\delta^{37}Cl$ profile of DGR-4 porewaters, and (C) $\delta^{81}Br$ profile of DGR-4 porewaters.

6.2 Processes Influencing $\delta^{37}Cl$ and $\delta^{81}Br$

There are a number of processes that could fractionate and change the halide isotopic signatures of porewater fluids during or after deposition. These physical or biological processes include: organic

and/or microbial activities, diagenesis/dolomitization (early Phanerozoic), tectonic fluid migration and/or hydrothermal activity (later Phanerozoic), and diffusional migration of porewater solutes.

6.2.1 Later Tectonics and Diffusion

For the last 200 Ma, eastern North America was in a passive margin phase (Sanford 1985). Sedimentary deposition during this time further resulted in compacting the underlying geologic layers, especially for the Ordovician shales (AECOM and ITASCA CANADA 2011). Therefore, some researchers inferred that diffusion would become the main process impacting changes in the Cl and Br concentrations and potentially halide isotopic fractionation of the porewater solutes at the site since 260 Ma (Clark et al. 2013; Al et al. 2015).

The stable isotopes of Cl and Br have been used in a variety of research projects to ascertain the origin of salts and fluids containing these elements, as well as to identify processes that cause isotopic fractionation (Kaufmann et al. 1992; Eggenkamp 1994; Shouakar-Stash 2008; Stotler et al. 2010; Eggenkamp 2014). Previous studies suggested that diffusion is the most important physical process to facilitate halide isotopic fractionation in porous media (Desaulniers et al. 1986; Eggenkamp et al. 1994; Eggenkamp et al. 1997), as lighter halide isotopes are transported faster than the heavier isotopes. Desaulniers et al. (1986) were the first to discuss the relationship of Cl concentration and $\delta^{37}Cl$ in a natural porous media and attribute the resulting depth profiles to diffusive processes. In their case, the chloride concentration and $\delta^{37}Cl$ both increased with depth. This was attributed to the upward diffusive migration of the lighter isotope (^{35}Cl) into an original chloride-free glacial till from the underlying chloride-rich bedrock. Several studies have used $\delta^{37}Cl$ profiles to assess long term diffusive migration in low permeability sediments and sedimentary rocks (Desaulniers et al. 1986; Eggenkamp et al. 1994; Eggenkamp et al. 1997; Gimmi and Waber 2004; Lavastre et al. 2005; Hesse

et al. 2006; Le Gal La Salle et al. 2013; Rebeix et al. 2014).

Several examples of the use of halide isotopes in diffusional studies are available and were chosen for comparison to the results in the present study. One of these is the case study in the eastern part of the Paris Basin (France) using chlorine isotopes to investigate long-term transport processes

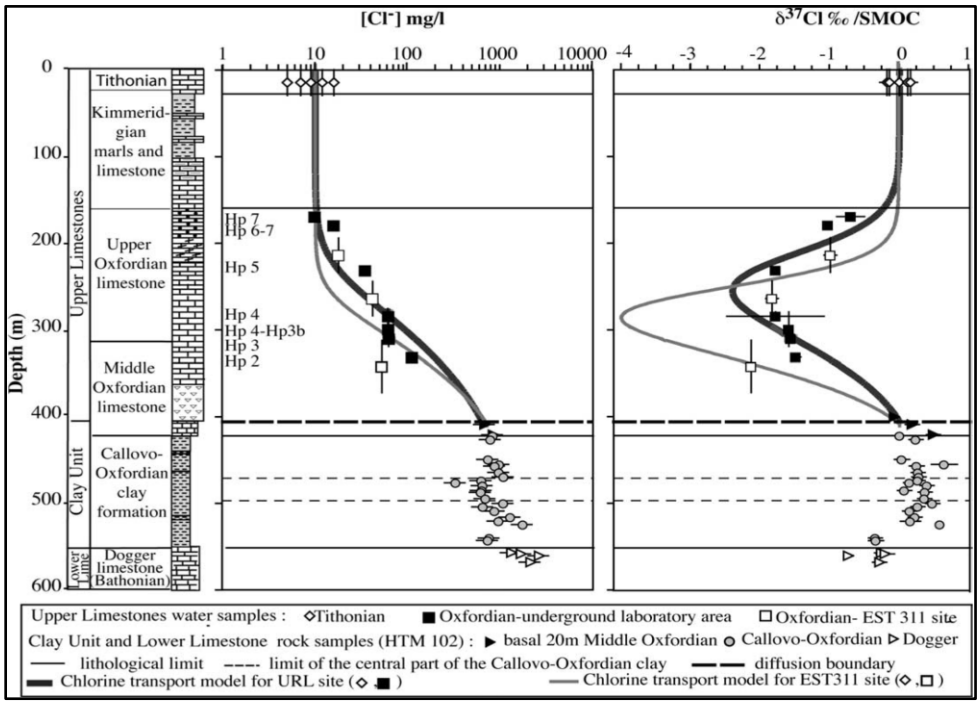

Figure 17a: Model of chlorine transport in Upper Limestones, Paris Basin, France. Lower Limestone, Clay Unit and Upper Limestones in the laboratory area, with from left to right: a simplified log, water chlorine concentrations and $\delta^{37}Cl$ (from Lavastre et al. 2005).

through a very low permeability clay sequence (Callovo-Oxfordian Formation) (Lavastre et al. 2005). The researchers suggested that the chloride concentration and $\delta^{37}Cl$ depth profiles (Figure 17a) reflect an early upward diffusion process from the Callovo-Oxfordian clay formation that was subsequently erased partially by a later chloride input from Trias evaporites below the section (as shown on Figure 17a) into the lower portion of the profile (Dogger-Callovo-Oxfordian clay) (Lavastre et al. 2005). Modelling results also illustrated that diffusion was the main process

transporting the chloride out of the Callovo-Oxfordian clay layer into the units above this layer (Middle-Upper Oxfordian limestone). In this example, a slight increase in $\delta^{37}Cl$ occurs in the clay unit, and lower $\delta^{37}Cl$ and lower Cl concentrations are observed in the overlying Oxfordian limestones.

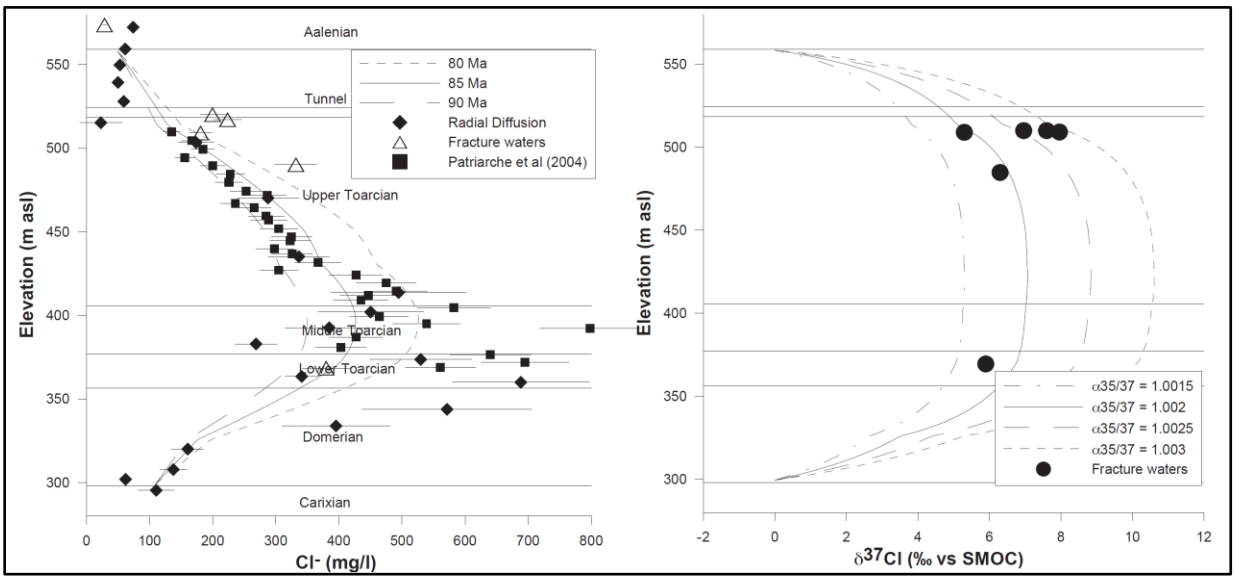

Figure 17b: (a) Experimental chloride profile compared to modelled curves of a diffusive exchange between seawater and freshwater since aquifer activation. (b) Comparison of $\delta^{37}Cl$ values in fracture water with model curves obtained for a diffusive exchange (from Le Gal La Salle et al. 2013).

In another case from Tournemire, France, a 250 m thick low permeability argillite layer (of Toarcian age) containing saline water is enclosed between two freshwater aquifers (Figure 17b). The chloride concentration (decreases away from the argillite) and isotopic values (higher $\delta^{37}Cl$ in the argillite than SMOC) of porewaters from the Tournemire site were used to model the diffusive transport process. These authors calculated a diffusive travel time between end members (85±10 Ma), which was much greater than the initially proposed time (53 Ma) by Patriarche et al. (2004) based on the Pyrenean orogeny as the driving force for diffusion (Le Gal La Salle et al. 2013). Le Gal La Salle et al. (2013) suggested a two-sided diffusion model to explain the concave shape of the Cl concentration

and isotope profiles for porewaters across the Toarcian/Domerian argillite at Tournemire.

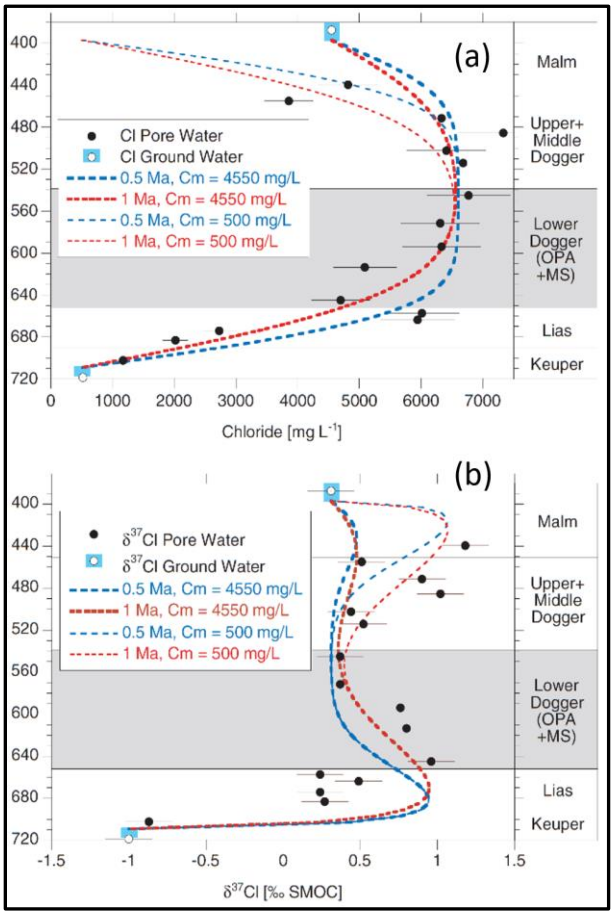

Figure 17c: Calculated profiles of (a) chloride and (b) $\delta^{37}Cl$ for the base case and for a constant, lower Cl concentration at the Malm boundary (from Gimmi and Waber 2004). Y-axis represents the depth (mbgs) below ground surface.

However, not every case involving a deep geologic sequence can be explained by a simple diffusive mechanism. In the deep borehole at Benken (northeastern Switzerland), a sequence of aquifers and argillaceous aquitards was investigated (Gimmi and Waber 2004). In this case, the Dogger aquitard is surrounded by the Malm and the Keuper aquifers, in a similar arrangement to the Tournemire site. In this case, the chloride concentration profile (Figure 17c – a) appears to be a two-sided diffusion profile from the Dogger aquitard to the Malm and Keuper aquifers. However, the chloride isotopic

profile was not interpreted as a simple two-sided diffusion process (Figure 17c – b). In particular, it was concluded that there must have been multi-diffusional reversals over time, or some other older processes occurring during burial, for example, which would have modified the chlorine isotopic signatures of porewaters before or after the diffusive transport process was fully developed. In this example, Gimmi and Waber (2004) ran multiple mathematical simulations in an attempt to duplicate the geochemical and isotopic results from the site. Figure 17c is one of the better simulations that most closely models the observed data.

From the above examples, it is apparent that applying a simple diffusional scenario to a multi-layered porous media may not always reproduce the observed geochemical results. Therefore, other processes must be considered to explain the data at the Bruce Nuclear Site.

6.2.2 Diagenesis / Fluid Migration

In the present study, the halide isotopic and concentration trends (Figure 14) do not necessarily agree and are much more complicated than the examples discussed above. In some cases, the $\delta^{37}Cl$ and $\delta^{81}Br$ depth profiles trend in opposite directions from each other and the concentration data. These complex halide isotopic trends cannot be explained by a simple diffusion mechanism similar to those shown for the Paris Basin (France) and Benken (Switzerland).

An altered zone occurs beneath the Precambrian/Cambrian unconformity, and is comprised of secondary chlorite, illite and K-rich feldspar (Carter and Easton 1990). This zone was formed by interaction between the host crystalline rock and regional brine that migrated westward from the Appalachian Basin into southern Ontario in response to the Taconic Orogeny (543-440 Ma) (Ziegler and Longstaffe 2000a, b). The present halide isotopic signatures of the porewaters in the lower part

of the Upper Ordovician limestones and the Cambrian sandstones may thus have been modified by mixing with external fluids, which contained different halide isotopic signatures compared to the host fluids.

6.2.3 Dolomitization

Diagenetic fluids/brines are inferred to have migrated through the underlying Cambrian sandstones in the Michigan and Appalachian Basins during the Paleozoic (Sanford et al. 1985; Middleton et al. 1990; Davies and Smith 2006). During the late Paleozoic and early Mesozoic, the southern Ontario region probably underwent substantial surficial erosion, resulting in the removal of up to 1000 m of ca. 325-260 Ma rocks (Sanford et al. 1985; Wang et al. 1994; Dickinson et al. 2010). Erosion may have caused compaction pressure release and could have enhanced the upward migration of underlying Precambrian brines (with high salinity, $\delta^{37}Cl$ and $\delta^{81}Br$) into the overlying Cambrian sandstones and Ordovician limestones.

There were numerous diagenetic events and processes that altered the Paleozoic rocks (Coniglio and Williams-Jones 1992). Among these, dolomitization is the most significant process that affected the stratigraphy and permeability (Sanford et al. 1985; Middleton et al. 1993; Conglio et al. 1994). The higher homogenization temperatures (from approximately 100 to 200 °C) found in fluid inclusions in secondary dolomites points to hydrothermal fluid flow during the Ordovician to Late Silurian (Legall et al. 1981; Coniglio et al. 1994). Therefore, these authors attributed the porous and permeable zones within the Ordovician limestones in southern Ontario to hydrothermal dolomitization.

During the Ordovician to Late Paleozoic, it was speculated that most dolomitization events occurred

after marine carbonate deposition corresponding to peak burial compaction (Morrow 1990). Fracturing/faulting significantly increased porosity and permeability within the deeper Paleozoic formations of the Niagara Block (Sanford et al. 1985; Carter 1991; Middleton et al. 1993; Coniglio et al. 1994; Carter et al. 1996). Hence, the dolomitized fluids could have migrated upward along discrete faults and fracture systems south of the site through the Cambrian sandstones that underlie the Ordovician limestones of the Trenton and Black River groups (Frape et al. 1989; Budai et al. 1991; Ziegler and Longstaffe 2000a, b; Bailey 2005). The driving force for the transport of dolomitizing fluids within the Ordovician units in southern Ontario could either be the compaction-driven force, which forces the deep basinal brines to migrate from deeper in the Michigan Basin to the margin (Coniglio and Williams-Jones 1992), or hydrothermally-driven brines forced by a heat source in the Precambrian basement associated with tectonic events during the Paleozoic and early Mesozoic (Sanford et al. 1985; Middleton et al. 1993; Conglio et al. 1994; Carter et al. 1996). Both driving forces could have caused the Cambrian brines, and even Precambrian brines, to migrate upward into the overlying, lower part of the Ordovician limestones of the Niagara Block during the Alleghenian Orogeny between approximately 350 and 250 Ma (Hobbs et al. 2011). However, at the site, fracturing of the Ordovician carbonates is sparse and fracturing of the Cambrian is moderate. The relatively sparse fracturing of these units (e.g., when compared to other regions of southern Ontario) make it difficult to comment on the extent of dolomitization processes in the Bruce block in the context of this thesis. U-Pb geochronology of the Devonian and Upper Silurian calcite veins at the Bruce Nuclear Site yields an age of 318 ± 10 Ma (ID-TIMS method) for the Silurian Salina A1 unit (DGR-4, 344.18 m) (Davis et al. 2016). This age suggested that the geologic timeframe (318 ± 10 Ma) for post-depositional fluid mobility above Upper Silurian Salina salts is consistent with the Alleghenian Orogeny in the Appalachian Basin. Therefore, it supports the hypothesis that the

Alleghenian Orogeny is the driving force for hydrothermal dolomitization during the Late Devonian in southern Ontario.

Due to hydrothermal dolomitization in southern Ontario, the $\delta^{37}Cl$ and $\delta^{81}Br$ of the Silurian and Ordovician formation waters at the site may be affected by the migrated fluids from the underlying Precambrian shield or the deeper Appalachian basin, both containing fluids with enriched halide isotopic signatures (Shouakar-Stash 2008; Stotler et al. 2010). As previously discussed, invoking Precambrian Shield brines requires unreasonably large volumes of fluid and hence is not a viable scenario to explain the halide isotopic compositions of Silurian and Ordovician formation waters. Previous researchers attributed the Cambrian halide isotopic signatures to an external input, including either the hydrothermal fluids from the underlying Precambrian crystalline shield or regional fluids from the Appalachian Basin that migrated through faults and fracture systems in southern Ontario (Frape et al. 1989; Budai et al. 1991; Ziegler and Longstaffe 2000a, b; Bailey 2005). Under these post-depositional tectonic scenarios, the Cambrian Formation waters may not preserve their original chemical or isotopic characteristics during burial diagenesis. However, to completely understand the halide isotopic variations within the porewaters of the Ordovician sequence, other processes than hydrothermal dolomitization need to be considered.

6.2.4 Salt Precipitation

Apart from the dolomitization process mentioned above, salt dissolution has been proposed to influence the salinity in many fluids found in southern Ontario and Michigan (Sanford et al. 1985; Dollar et al. 1988; Frape et al. 1992). Such a process would have an influence on the halide concentrations and isotopic values in the site samples. The majority of salt dissolution would have occurred along regional fractures and faults through the Silurian salt-rich units primarily at the

margin of the Michigan Basin during the Late Caledonian Orogeny (425-400 Ma) and subsequent Acadian Orogeny (375-325 Ma) (Sanford et al. 1985). As halite is usually more deficient in Br relative to the fluid from which it precipitated, the dissolved halite would increase the Cl concentration relative to Br after dissolution, as seen on Figure 7.

Eggenkamp et al. (1994) proposed that the first salt precipitated from the seawater has higher $\delta^{37}Cl$ than later precipitated salts. Recent studies have speculated that salt dissolution could increase $\delta^{37}Cl$ while decreasing $\delta^{81}Br$ in a fluid (Eggenkamp 2015; Hanlon et al. 2017) because precipitated salts have isotopically heavier chlorine and isotopically lighter bromine than the residual fluids (Stotler et al. 2010; Eggenkamp 2014, 2015; Hanlon et al. 2017). However, the bromide concentration in salts such as halite (NaCl) is proportionally less than the chloride concentration compared to the fluid that precipitates the salt. Therefore, fractionation due to adsorption or occlusion during salt precipitation might be a minor process affecting the bromine isotopic system (Eggenkamp 2014).

As discussed previously, the Salina A1 groundwater samples from the DGR site could be inferred as having a glacial water source that caused halite dissolution during recharge – based on chemical and isotopic results shown earlier (Figure 6, 7, 13). The evaporites in parts of the Salina Formation may have influenced halide isotopic signatures. Therefore, the lower $\delta^{37}Cl$ and $\delta^{81}Br$ of the fluids found in Silurian-aged strata at the site could be derived at least partially from halite dissolution.

Chloride and bromide are involved in different molecular reactions during diagenesis. In brief, chloride preferentially goes into mineral precipitates (evaporites). Bromide will participate in inorganic reactions such as salt precipitation, but often it is also involved in organic and/or biologic activities due to its redox behavior (Manley 2002; Blei et al. 2010, 2012; Leri and Myneni 2012; Leri et al. 2010, 2014; Eggenkamp et al. 1998, 2015). Therefore, not only the diagenetic processes but

also organic/microbial activities should be considered in order to fully understand the halide isotopic fractionations.

6.2.5 Organic and Microbial Activities

Organic and microbial activities have also been invoked to explain higher $\delta^{81}Br$ of sedimentary formation waters over long geological time periods (Eggenkamp 2014, 2015). Eggenkamp (2015) stated that the impact of organic and microbial activities on bromine isotopes are larger than those affecting chlorine isotopes due to the differences in redox behavior and the role of each element in biological processes (Manley 2002; Blei et al. 2010, 2012; Leri and Myneni 2012; Leri et al. 2010, 2014; Eggenkamp et al. 1998, 2015). Bromine isotopes are more effectively used than chlorine isotopes during organic or microbial activities, as it takes less energy (organic and/or inorganic) to oxidize the bromide ion than to oxidize the chloride ion (Eggenkamp 2015). Leri et al. (2010) demonstrated the effect of organic carbon on bromine in marine sediments. The organobromine tends to be highly associated with organic carbon in marine sediments due to covalent bonding between them, even though bromine is often treated as a conservative element in marine environments (Leri et al. 2010, 2014).

As the lighter isotope of bromine is preferentially removed from brine into organic matter and is also released as gases (HBr, CH_3Br), residual brines should have isotopically heavier Br (Horst et al. 2014; Eggenkamp 2015; Hanlon et al. 2017). Such processes could occur both in the early depositional environment before burial and in the post-depositional environment, and would alter either an initial paleo-seawater signature or a sedimentary formation fluid signature.

Total organic carbon (TOC) contents in the DGR-4 borehole porewaters was presented by Jackson

(2009) in the NWMO Technical Report (TR-08-29). As shown on Figure 18, TOC contents have a parallel trend in many cases to the bromine isotopic profile. Several higher $\delta^{81}Br$ values are associated with higher TOC within a specific geologic unit (shown by red arrows, Figure 18). It is apparent that the TOC content increases from the Upper Ordovician shales and reaches the highest value in the Collingwood Member of the Cobourg Formation (Figure 18). Similarly, a large increase in TOC in the Coboconk Formation correlates with higher $\delta^{81}Br$. The organic-rich zones provide an environment that is ideal for organobromine reactions to preferentially remove the lighter Br isotope during deposition or diagenesis.

The enriched $\delta^{81}Br$ isotopic values of the Cobourg and Coboconk Formation waters are associated with relatively high TOC contents. Organic matter bromination was proposed to change the $\delta^{81}Br$ of waters via isotopic fractionation during biologically-mediated bromide oxidation (Manley 2002; Blei et al. 2010, 2012; Leri and Myneni 2012; Leri et al. 2010, 2014; Horst et al. 2014; Eggenkamp et al. 1998, 2015; Hanlon et al. 2017). Therefore, the organic and microbial activities could further modify the $\delta^{81}Br$ isotopic signatures of the brines from the Ordovician limestones at the site after, or parallel with, other diagenetic processes discussed in the previous sections. Apart from two-sided diffusive transport, the organic and/or microbial activities provide another possible explanation for the higher $\delta^{81}Br$ of the porewaters in TOC-rich parts of the DGR-4 borehole.

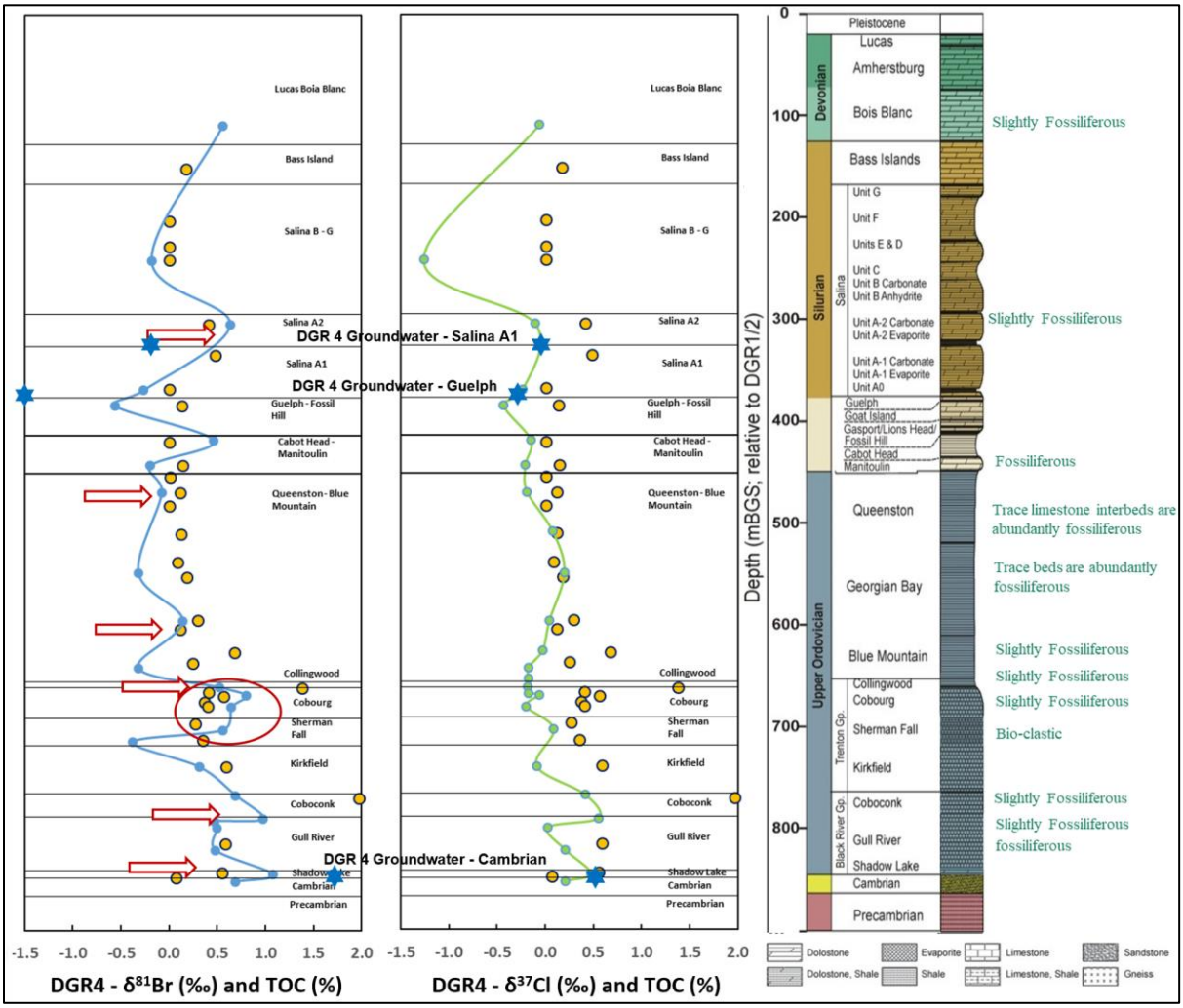

Figure 18: $\delta^{37}Cl$ - $\delta^{81}Br$ (green and blue lines) and total organic carbon (TOC) profiles (orange dots) of DGR-4 porewater samples, and accompanying lithostratigraphy of the DGR-4 borehole at the Bruce Nuclear Site (TOC data from Jackson 2009).

6.2.6 Microbial and Photolytic Conversion to Gas Phase

Previous researchers observed the degassing processes of volatile halide gases (e.g., HBr, CH_3Br, CH_3Cl, BrO, etc.) through microbial, vegetative, or photolytic processes above and near high-salinity lakes and salt flats (e.g., Hönninger et al. 2004; Monks 2005; Huset 2007; Blei et al. 2012; Pratt et al. 2013). There are very few studies concerning the microbial use of chloride, though some researchers have found that microbial activities can lead to higher $\delta^{37}Cl$ in residual soils and salts

after microbial reduction of chlorinated organic compounds (e.g., Numata et al. 2002; Sturchio et al. 2003; Abe et al. 2009; Wiegert et al. 2013; Palau et al. 2013). In general, volatile HBr and CH_3Br gases are produced from carbon macromolecules that reacted with bromide ions and protons, as shown in Figure 19 below. Analogously, bromine isotopic fractionation also resulted in higher $\delta^{81}Br$ of the residual solution following microbial reduction of brominated phenols or the release of methyl bromides (Bernstein et al. 2013; Zakon et al. 2013; Horst et al. 2014). Methyl halide gases are characterized as having lower $\delta^{37}Cl$ and $\delta^{81}Br$ than the organic material and residual brine source materials (Horst et al. 2014). Most likely, the release of volatile brominated compounds from surficial reservoirs was a result of either photolytic processes or microbial activity (Eggenkamp 2015; Hanlon et al. 2017) and most likely has occurred over long periods of geological time. Therefore, degassing of methyl halide gases also needs to be considered when explaining the distinctive isotopic features of porewaters over geological time scales at the site.

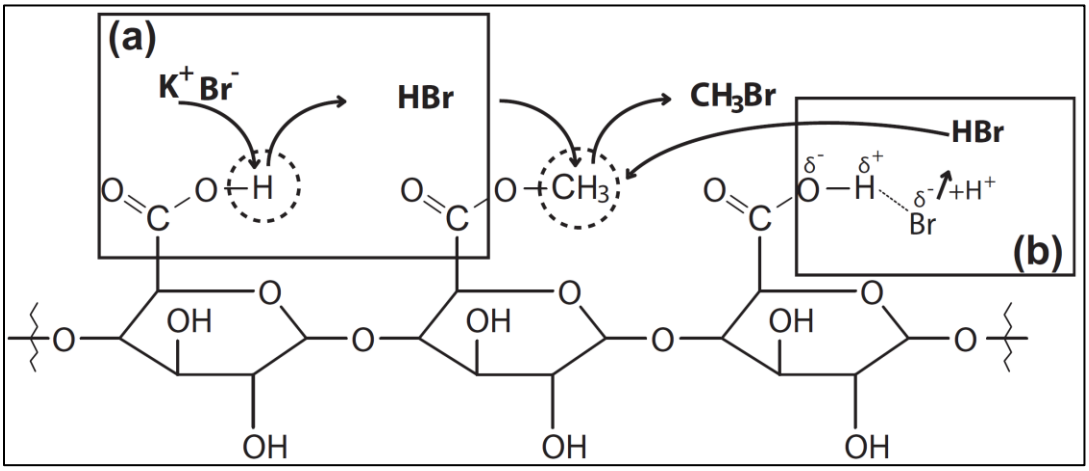

Figure 19. The microbial reduction of bromine to HBr and CH_3Br (Horst et al. 2014).

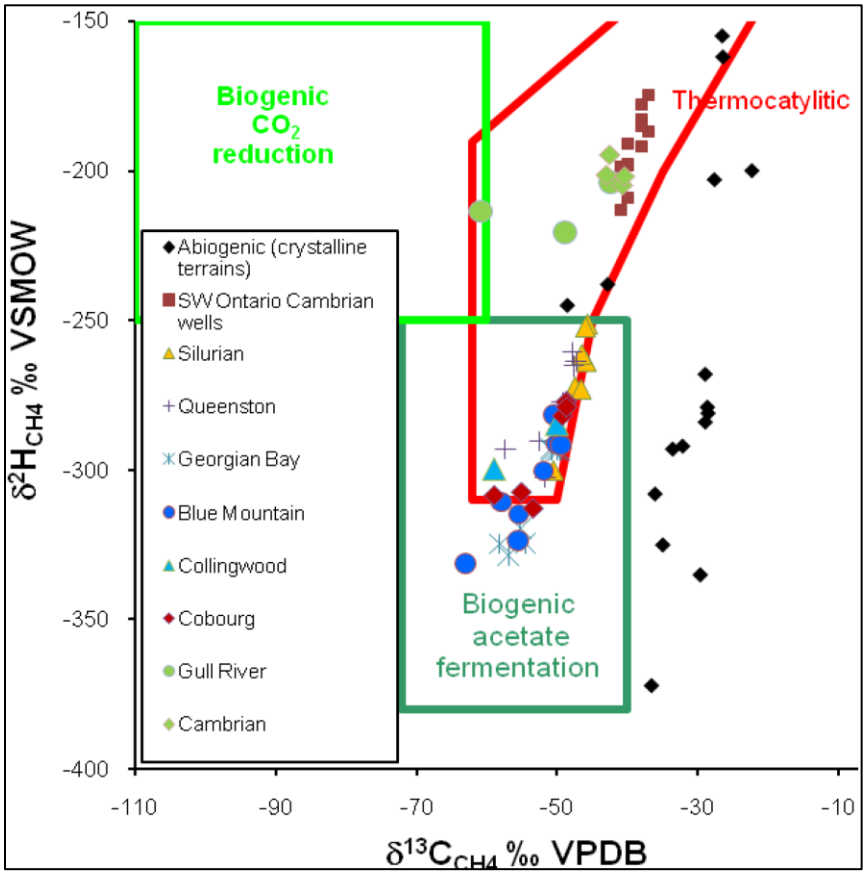

Figure 20: Isotopes of CH_4 in cores from the Bruce Nuclear Site (from Jackson 2009).

Barker and Pollack (1984) and Sherwood-Lollar et al. (1994) characterized the natural gases sampled from the Silurian, Ordovician and Cambrian strata in southwestern Ontario. These researchers suggested the possibility of gas formation and migration within the geological units in southwestern Ontario. Sherwood-Lollar et al. (1994) proposed that the pore gases from the Gull River and Cambrian Formations are characterized by thermogenic methane. However, some pore gases sampled from the Blue Mountain Formation and Collingwood Member had $\delta^{13}C$ and $\delta^{2}H$ outside the thermo-catalytic zone, and instead represent a biogenic origin (Sherwood-Lollar et al. 1994; Jackson 2009) (Figure 20). The isotopic composition of pore gases between the Upper Ordovician shales and Cambrian point to mixing of the biogenic and thermogenic endmembers (Jackson 2009).

Therefore, the carbon and hydrogen isotope evidence for biogenic and thermogenic methane production raises the possibility that gas generation and migration influenced the halide isotopic signatures of the porewaters within the Ordovician limestones at the site.

The extensive volcanic activities induced by the Taconic Orogeny and the relatively high subsurface temperatures during the Ordovician could have significantly facilitated the degassing processes of methyl halides, which could have resulted in preferential accumulation of heavier Br isotopes on the surface of the continents and/or shallow marine areas (primarily within the paleo-Appalachian region).

7. SUMMARY

The six groundwater samples from the Bruce Nuclear Site analyzed in this study were pumped from three zones: the Silurian Salina A1 Carbonate, the Silurian Guelph Formation, and the Cambrian Formation. For the many combinations of isotopic and geochemical parameters examined, including $\delta^{81}Br$ and $\delta^{37}Cl$, the site groundwaters were, for the most part, found to be similar to regional sedimentary formation fluids from the same geological units found in the Niagara tectonic structural block to the south of the site (Figure 4a). The WRHD is compiled primarily from oil and gas wells in the Niagara tectonic structural block, which is south of the Bruce tectonic block where the study site is located (Figure 1).

Groundwaters sampled from the Salina A1 Carbonate unit at the site have low Br/Cl weight ratios (Figure 13), which are less than the seawater ratio, and are also unique in having low $\delta^{81}Br$ (Figures 9A, 11, 12), $\delta^{18}O$, and $\delta^{2}H$ (Figures 6 and 10a). Based on these isotopic characteristics, the Cl-Br source for the Salina A1 Carbonate samples at the site appears to have been derived from halite

dissolution (Figure 7), most likely by cold climate recharge (Figure 6). Weaver et al. (1995) describe a very similar situation to the south of the site involving the same Silurian stratigraphic units.

Groundwater fluids from the Guelph Formation at the site have low $\delta^{81}Br$ and $\delta^{37}Cl$ (Figure 9a, 11, 12), similar to fluids from the Guelph/Niagaran petroleum-producing wells in southern Ontario and the Michigan Basin. The $\delta^{81}Br$, $\delta^{37}Cl$ (Figure 8), and Br/Cl ratios (Figure 13) of the groundwaters from the Salina A1 Unit and the Guelph Formation in both DGR boreholes are consistent with previous hypotheses that Michigan Basin fluids have low $\delta^{81}Br$ (Figure 8) (Shouakar-Stash 2008). Thus, the groundwaters from the two Silurian-aged rock units at the site can be described as fluids with similar geochemical and isotopic characteristics as many of the fluids found within stratigraphic units of the Michigan Basin.

The halide isotopic similarity for the Cambrian groundwaters from the site with Cambrian fluids from the regional database suggests a similar origin for these fluids. Both the $\delta^{81}Br$ and $\delta^{37}Cl$ of the groundwaters are high and similar to fluids sourced in the Appalachian Basin (Figure 8) from petroleum wells to the east and south of the site. This suggests that Cambrian samples from the site, located west of the Algonquin Arch, may have the same origin as the Cambrian fluids east of the Algonquin Arch, but a different origin from the Silurian groundwater samples at the site. This would further suggest that the fluids within the Cambrian may be old and have maintained some aspects of their isotopic signatures since they were emplaced by a regional fluid event at a time when Cambrian sediments were continuous across the Michigan and Appalachian basins before sea-level fall and the Algonquin Arch rise created the present stratigraphic boundaries. Several authors have invoked large-scale basinal fluid movements at various times in the geologic past that resulted in dolomitization and the emplacement of hydrothermal mineral and petroleum resources in southern

Ontario (Frape et al. 1989; Middleton et al. 1990; Budai et al. 1991; Coniglio et al. 1992; Ziegler and Longstaffe 2000a, b; Bailey 2005). In addition, the dolomitized fluids are hypothesized to have migrated along faults and fracture systems through the Cambrian sandstones underlying the Ordovician limestones of the Trenton and Black River groups (Frape et al. 1989; Middleton et al. 1990; Budai et al. 1991; Coniglio et al. 1992; Ziegler and Longstaffe 2000a, b; Bailey 2005).

Understanding the timing of events at the site, such as large-scale mixing, hydrothermal fluid circulation, and dissolution of halite by fluid recharge, is limited and based on only three groundwater fluid-producing zones in the Silurian and Cambrian. In an attempt to expand our knowledge base of the distribution of halide isotopes at the site, a pore fluid sampling study was conducted.

The porewater samples from the Bruce Nuclear Site analyzed in this study were extracted from Devonian to Cambrian stratigraphic units in the DGR-4 core. However, the $\delta^{37}Cl$ and $\delta^{81}Br$ of site porewaters from the Cambrian and the lower part of the Upper Ordovician units (i.e., Shadow Lake, Gull River and Coboconk) are often distinctive from the equivalent geological units in the combined regional database compiled from Shouakar-Stash (2008), Hobbs et al. (2011) and Skuce et al. (2015) (Figure 15). Based on the geological ages of the units at the site and the tectonic events during the Paleozoic, it is reasonable to assume that some differences in isotopic signatures between pore fluids and sedimentary formation fluids could exist. The $\delta^{37}Cl$ values of the groundwater samples from the site are very close to the $\delta^{37}Cl$ values of the porewater samples at similar depths. However, the $\delta^{81}Br$ values of two Silurian groundwaters from the DGR-4 are more depleted and the $\delta^{81}Br$ values of the Cambrian groundwaters from the DGR-4 are more enriched compared to the porewaters at the same depths (Figure 14a).

Previous studies suggested that diffusion of a hypersaline brine from the lower part of the Upper

Silurian through the stratigraphic sequence to be the primary process causing changes in the water isotopic values and Cl-Br concentrations of the pore fluids (Clark et al. 2013). The modified conceptual model by Al et al. (2015) suggests that high-salinity brines with high $\delta^{37}Cl$ and $\delta^{81}Br$ pervaded the entire shale units prior to peak consolidation of the sediments. This process would have occurred over many millions of years, particularly during restricted basin conditions with high-salinity brines moving in during the Late Silurian (Al et al. 2015). After peak compaction and burial, the high salinity brines reached the Cobourg Formation, but not stratigraphically underlying units, and diffusion remained the only potential active process (Al et al. 2015). Diffusional transport downward below the Cobourg Formation is presumed to have been very slow, possibly even minimal, and is used to explain the trends only in the Trenton Group and some of the Black River Group carbonates (Al et al. 2015). However, the halide isotopic variations seen in this study are not easily explained by a simple downward density-driven diffusion process across multiple sedimentologically variable layers (Figure 16d, 18). Instead the observed stratigraphic trends (Figure 14a) are most likely the result of multiple factors that modified the halide isotopic signatures of the porewaters on numerous occasions in the geologic past. These physical or biological processes include organic and/or microbial halide gas production and degassing, salt dissolution, diagenesis/dolomitization (early Phanerozoic), tectonically-driven fluid migration and/or hydrothermal fluid mixing (late Phanerozoic), and localized diffusional migration of porewater solutes within stratigraphic units.

The sedimentary geologic units from the DGR-4 borehole are characterized by distinctive and variable depositional environments. The initial $\delta^{37}Cl$ and $\delta^{81}Br$ of the pore fluids would have been impacted initially by each different depositional environment. The earliest diagenesis processes, such as lithification and geochemical reactions, likely altered the halide isotopic signatures of the

pore fluids. Fluid migration, mixing and diffusion during diagenesis could also impact the halide isotopic signatures of pore fluids at the site.

To evaluate the potential influence of seawater halide isotopic compositions from different depositional environments, data from the regional databases was averaged to produce a potential paleo-sea water curve for southern Ontario and the Michigan Basin (Figure 16d). This approach ignores the origin of the formational fluids (primarily petroleum-producing wells) used to produce the curve. However, the curve can be used to compare with the porewater values from the site. It is apparent that the average calculated seawater values (Figure 16d) are quite different in some cases from those of the DGR-4 porewater values (Figure 16d). Therefore, other depositional or post-depositional processes were evaluated and considered to aid in the interpretation of the isotopic profiles seen in Figure 14a and 16d.

In the present study, the halide isotope and concentration trends (Figure 14) are often complicated and cannot be explained by a simple diffusion mechanism along the geologic sequence. Instead, the heat source in the Appalachian Basin induced by the Taconic Orogeny (543-440 Ma) forced external fluids, with high $\delta^{37}Cl$ and $\delta^{81}Br$, to migrate into the Cambrian units in southern Ontario (Ziegler and Longstaffe 2000a, b). As shown in Figure 16d, there are different bromine isotopic signatures for the Cambrian Formation groundwater and porewater. Phanerozoic tectonic cycles (Sanford et al. 1985) illustrated that southern Ontario was impacted by several tectonic orogenies between the Middle and Late Paleozoic; as a result, it is necessary to consider the impact of diagenesis, especially hydrothermal dolomitization, on the halide isotopic signatures and concentrations of pore fluids at the site.

In the geologic past, the removal of up to 1000 m of Paleozoic rock (325 to 260 Ma) in southern

Ontario (Sanford et al. 1985; Wang et al. 1994; Dickinson et al. 2010) could have enhanced the upward migration of underlying Precambrian brines containing high salinity and high $\delta^{81}Br$ into the overlying Cambrian and the lower part of the Upper Ordovician units along discrete faults and fracture systems in southern Ontario. This provides an alternative explanation to the similarities between Cambrian groundwaters at the site and regional fluids. The problem with this scenario is the lack of similarity between crystalline shield water isotopic signatures ($\delta^{18}O$-$\delta^{2}H$) and the Cambrian formation fluid isotopic signatures and the groundwater values from the site (Figure 6). As well, the porosity differences and volumes of available fluid from the crystalline rocks are orders of magnitude lower than the Cambrian rocks, such that the impact of a Precambrian fluid input during mixing would most likely be a negligible change in the geochemical composition of fluids in the overlying units.

Salt dissolution also has an influence on the halide concentrations and isotopic values (Sanford et al. 1985; Dollar et al. 1988; Frape et al. 1992) during the Late Silurian to Devonian, possibly induced by events such as the Caledonian Orogeny (425-390 Ma) and subsequent Acadian Orogeny (375-325 Ma) (Sanford et al. 1985). Dissolution of evaporites in parts of the Salina Formation may have influenced the halide isotopic signatures. Therefore, the lower $\delta^{37}Cl$ and $\delta^{81}Br$ of the fluids found in Silurian-aged strata at the site could be derived, at least partially, from halite dissolution (Eggenkamp 2014, 2016).

For the last 200 Ma, eastern North America was in a passive margin phase (Sanford 1985) and the Ordovician shales had significantly low permeability due to their fine grain size and high pressure from the overlying sedimentary deposits. To date, some researchers attributed diffusion as the main process causing changes in the Cl and Br concentrations and potentially halide isotopic compositions

of the porewater solutes at the site since 260 Ma (Clark et al. 2013; Al et al. 2015). However, the halide isotopic variations in porewaters in the DGR-4 core at the site are not easily explained by a simple diffusion process across multiple geological layers of highly variable sedimentological media (Figure 14a). Therefore, diffusive processes within the Ordovician sequence have been discussed in terms of three separate stratigraphic sections of the borehole: first – through the Cobourg Formation and upper Sherman Fall Formation; second – through the Coboconk Formation; and third –from the middle Gull River Formation to the Cambrian Formation (Figure 14b). Diffusion in the geologic sequence is believed to be an ongoing process. In addition, other physical and biological processes likely affected the halide isotopic signatures and concentrations of the pore fluids in DGR-4 at the site.

Another interesting correlation observed in the study was the relationship of total organic content (TOC) in some geological units with the bromine isotopic values (Figure 18). In Figure 18, the TOC contents have a similar stratigraphic trend as the $\delta^{81}Br$ profile. Several high $\delta^{81}Br$ values are associated with higher TOC contents within a specific geologic unit (Figure 18). The variation in $\delta^{81}Br$ is larger than $\delta^{37}Cl$ within the same geological units, which can be explained by their different redox behavior and biological processes (Manley 2002; Blei et al. 2010, 2012; Leri and Myneni 2012; Leri et al. 2010, 2014; Eggenkamp et al. 1998, 2015). Therefore, organic and/or microbial factors could further explain the apparent two-sided diffusive transport model and be invoked to account for the $\delta^{81}Br$ trends seen in the Collingwood-Cobourg-Sherman Fall, Kirkfield-Coboconk-Gull River, and Gull River-Shadow Lake-Cambrian profiles on Figure 18. The potential mobilization of bromine as gas by organic and/or microbial activities associated with the zones of higher TOC provide another possible explanation for the higher $\delta^{81}Br$ of the porewaters in DGR-4 at the site. Such processes may have occurred during deposition (before burial and consolidation)

and diagenesis, and thus may have altered the halide isotopic signatures (particularly Br) of either an initial paleo-seawater signature or a sedimentary formation fluid signature. Furthermore, the carbon and hydrogen isotopic composition of pore gases between the Upper Ordovician shales and Cambrian sandstones? indicate mixing of biogenic and thermogenic methane (Jackson 2009). Therefore, the combination of biogenic and thermal activities further confirms that complex processes potentially impacted and changed the halide isotopic signature of the porewaters within the Ordovician carbonates at the site.

This study is the first attempt to use $\delta^{37}Cl$ and $\delta^{81}Br$ together to evaluate sources, residence times, and processes causing isotopic fractionation at a site involving a large number of different sedimentary units and ages of deposition (ranging from Cambrian to Devonian). The present study was forced to use archived samples that were limited in numbers for many of the key stratigraphic sequences where processes such as diffusion and/or microbial redox reactions may have changed, or are changing, isotopic porewater values. This was a major limitation and hence a more detailed scientific study of the $\delta^{37}Cl$ and $\delta^{81}Br$ of the porewater samples is needed to better define stratigraphic trends and understand the geologic processes that occurred at the Bruce Nuclear Site in southern Ontario.

REFERENCES

Abe, Y., R. Aravena, J. Zopfi, O. Shouakar-Stash, E. Cox, J.D. Roberts, and D. Hunkeler, 2009. Carbon and chlorine isotope fractionation during aerobic oxidation and reductive dechlorination of vinyl chloride and cis-1, 2-dichloroethane. Environmental Science and Technology, 43: 101-107.

AECOM and ITASCA CANADA. 2011., Regional Geology – Southern Ontario. AECOM Canada Ltd. and Itasca Consulting Canada, Inc. report for the Nuclear Waste Management Organization, NWMO DGR-TR-2011-15 R000. Toronto, Canada.

Al, T., I.D. Clark, L. Kennell, J. Mark and K.G. Raven., 2015. Geochemical Evolution and Residence Time of Porewater in Low Permeability Rocks of the Michigan Basin, Southwest Ontario, Chemical Geology, doi: 10.1016/j. chemgeo. 2015.03.005

Armstrong, D.K. and T.R. Carter., 2010. The subsurface Paleozoic stratigraphy of Southern Ontario. Ontario Geological Survey, Special Volume 7.

Bailey Geological Services Ltd. and R.O. Cochrane., 1984a. Evaluation of the Conventional and Potential Oil and Gas Reserves of the Cambrian of Ontario. Ontario Geological Survey Open File Report 5499.

Bailey Geological Services Ltd. and R.O. Cochrane., 1984b. Evaluation of the Conventional and Potential Oil and Gas Reserves of the Ordovician of Ontario. Ontario Geological Survey Open File Report 5498.

Bailey, S.M.B., 2005. A comparison of Cambrian reservoir rocks onlapping the S.E. and N.W. sides of the Algonquin Arch in SW Ontario. A regional correlation project. Presented at: The Ontario Petroleum Institute 44th Annual Oil and Gas conference, Technical Paper 5.

Barnes, J.D., Sharp, Z.D. and Fischer, T.P., 2008. Chlorine isotope variations across the Izu-Bonin-Mariana arc. Geology, 36: 883-886.

Barnes, J.D., Sharp, Z.D., Fischer, T.P., Hilton, D.R. and Carr, M.J., 2009. Chlorine isotope variations along the Central American volcanic front and back arc. Geochem, Geophys, Geosyst, 10.

Barker, J.F. and Pollock, S.J., 1984. The geochemistry and origin of natural gases in southern Ontario. Bulletin of Canadian Petroleum Geology, 32: 313-326.

Bernstein, A., Z. Ronen, E. Levin, L. Halicz, and F. Gelman, 2013. Kinetic bromine isotope effect:

example from the microbial debromination of brominated phenols. Analytical and Bioanalytical Chemistry, v. 405: 2923-2929.

Brown, J., Colling, A, Park, D., Phillips, J., Rothery, D. and Wright, J., 1989. Seawater: Its composition, properties and behavior. In: Bearman, G. (Ed.). The Open University, S330, vol. 2. Pergamum Press. 165pp.

Budai, J.M. and J.L. Wilson., 1991. Diagenetic history of the Trenton and Black River Formations in the Michigan Basin. In: Catacosinos, P.A. and P.A. Daniels, Jr. (Eds.). Early sedimentary evolution of the Michigan Basin. Geological Society of America Special Paper 256: 73-88.

Blei, E., Hardacre, C.J., Mills, G.P., Heal, K.V. and Heal, M.R., 2010. Identification and quantification of methyl halide sources in a lowland tropical rainforest. Atmospheric Environment, 44: 1005-1010.

Blei, E., Heal, M.R., Heal, K.V., 2012. Long-term CH_3Br and CH_3Cl flux measurements in temperate salt marshes. Bio-geosciences, 7: 3657- 3668.

Bonifacie, M., Jendrzejewski, N., Agrinier, P., Coleman, M., Pineau, F. and Javoy, M., 2007. Pyrohydrolysis-IRMS determination of silicate chlorine stable isotope compositions. Application to oceanic crust and meteorite samples. Chemi Geol, 242: 187-201.

Bonifacie, M., Jendrzejewski, N., Agrinier, P., Humler, E., Coleman, M. and Javoy, M., 2008. The chlorine isotope composition of Earth's mantle. Science, 319: 1518-1520.

Carpenter, A.B., 1978. Origin and chemical evolution of brines in sedimentary basins. Oklahoma Geological Survey Circular, 79: 60-77.

Carter, T.R. and Easton, R.M., 1990. Extension of Grenville basement southwestern Ontario: Lithology and tectonic subdivisions. In Geology of Southwestern Ontario (Core Workshop) (pp. 9-28). American Association of Petroleum Geologists 1990 Eastern Section Meeting, London, Ontario.

Carter, T.R., 1991. Dolomitization Patterns in the Salina A-1 and A-2 Carbonate Units, Sombra Township, Ontario. Proceedings 30th Annual Ontario Petroleum Institute Conference Technical Paper 4. London, Canada.

Cecil, L.D., 2000. Origin of Chlorine-36 in the eastern Snake River Plain aquifer, Idaho: implications for describing ground water contamination near a nuclear facility. Ph.D. Dissertation, University of Waterloo, Waterloo, Ontario, Canada.

Clark, I. D., T. Al, M. Jensen, L. Kennell, M. Mazurek, R. Mohapatra and K.G. Raven., 2013. Paleozoic-

aged brine and authigenic helium preserved in an Ordovician shale aquiclude. Geol, 41: 951-954.

Clark, I., I. Liu, H. Mohammadzadeh, P. Zhang, R. Mohapatra and M. Wilk., 2010. Porewater and Gas Analyses in DGR-3 and DGR-4 Core. Intera Engineering Ltd. Report TR-08-19. Ottawa, Canada.

Cloutier, V., 1994. Stable Isotopes of Chlorine as Indicators of the Source and Migrational Paths of Solutes within Glacial Deposits and Bedrock Formations, Lambton County, Southwestern Ontario. M.Sc. Thesis. University of Waterloo. Canada.

Coleman, M.L., T.J. Shepherd, J.J. Durham, J.E. Rouse and G.R. Moore., 1982. Reduction of water with Zinc for hydrogen isotope analysis. Analytical Chemistry, vol. 54: 993-995.

Collins, A.G. 1975., Geochemistry of Oil-Field Waters. Elsevier, New York, USA.

Coniglio, M. and A.E. Williams-Jones., 1992. Diagenesis of Ordovician carbonates from the northeast Michigan Basin, Manitoulin Island area, Ontario: evidence from petrography, stable isotopes and fluid inclusions. Sedimentology 39: 813-836.

Coniglio, M., R. Sherlock, A.E. Williams-Jones, K. Middleton and S.K. Frape., 1994. Burial and hydrothermal diagenesis of Ordovician carbonates from the Michigan Basin, Ontario, Canada. Special Publications of the International Association of Sedimentologists 21: 231-254.

Davies, G. R. and L.B. Smith., 2006. Structurally controlled hydrothermal dolomite reservoir facies: An overview. American Association of Petroleum Geologists Bulletin 90: 1641-1690.

Davis, D. W., 2016. Continued application of U-Pb geochronology methods to the absolute age determination of secondary calcite: 2014-2016. NWMO-TP-2016-07. Toronto. Canada.

Desaulniers D.E, Kaufmann R.S, Cherry J.A, Bentley H.W., 1986. ^{37}Cl-^{35}Cl variations in a diffusion controlled groundwater system. Geochem et Cosmochim Acta, 50: 1757–1764.

Dickinson, W.R., G.E. Gehrels and J.E. Marzolf., 2010. Detrital zircons from fluvial Jurassic strata of the Michigan basin: Implications for the transcontinental Jurassic paleo river hypothesis. Geol 38: 499-502.

Dollar, P.S., 1988. Geochemistry of Formation Waters, Southwestern Ontario, Canada and Southern Michigan, U.S.A. Implications for Origin and Evolution. M.Sc. Thesis. University of Waterloo, Canada.

Eastoe C.J, Long A, Land L.S and Kyle J.R., 2001. Stable chlorine isotopes in halite and brine from the Guld Coast Basin: brine genesis. Chem Geol 176:343–360

Eastoe C.J, Peryt T.M, Petrychenko O.Y and Geisler-Cussey D., 2007. Stable chlorine isotopes in Phanerozoic evaporites. Appl Geochem 22:575–588.

Eggenkamp, H.G.M., 1994. The geochemistry of chlorine isotopes. Ph.D. Thesis. University of Utrecht, the Netherlands. 150pp.

Eggenkamp, H.G.M., and Koster van Groos, A.F., 1997. Chlorine stable isotopes in carbonatites: evidence for isotopic heterogeneity in the mantle. Chem Geol. 140: 137-143.

Eggenkamp H.G.M, and Coleman M.L., 2000. Rediscovery of classical methods and their application to the measurement of stable bromine isotopes in natural samples. Chem Geol 167:393–402.

Eggenkamp H.G.M and Coleman M.L., 2009. The effect of aqueous diffusion on the fractionation of chlorine and bromine stable isotopes. Geochim Cosmochim Acta 73:3539–3548.

Eggenkamp, H.G.M., 2014. The geochemistry of stable chlorine and bromine isotopes. Berlin: Springer. 73-153

Eggenkamp, H.G.M., 2015. Why are variations in bromine isotope compositions in the Earth's history larger than chlorine isotope compositions? Annales UMCS, Sectio AAA 70: 183–194.

Eggenkamp, H.G.M., Bonifacie, M., Ader, M. and Agrinier, P., 2016. Experimental determination of stable chlorine and bromine isotope fractionation during precipitation of salt from a saturated solution. Chem Geol, 433: 46-56.

Epstein, S. and T.K. Mayeda., 1953. Variation of the 18O content of waters from natural sources. Geochemical ET Cosmochimica Acta. vol. 4, 213-224.

Finnegan, S., Bergmann, K., Eiler, J.M., Jones, D.S., Fike, D.A., Eisenman, I., Hughes, N.C., Tripati, A.K. and Fischer, W.W., 2011. The magnitude and duration of Late Ordovician–Early Silurian glaciation. Science, 331: 903-906.

Frape, S.K. and P. Fritz., 1987. Geochemical trends for groundwaters from the Canadian Shield. In: Saline water and gases in crystalline rocks. P. Fritz and S.K. Frape (Eds.). Geological Association of Canada Special Paper 33: 19-38.

Frape, S.K., P.S. Dollar, B. Sherwood Lollar and R.H. McNutt., 1989. Mixing of saline basinal fluids in southern Ontario: Implications of rock-water interaction, hydrocarbon emplacement and Canadian Shield brines. Proceedings 6th International Water-Rock Interaction Conference, Malvern, U.K. Miles (ed.), Bathema, Roterdam: 223-226.

Frape, S.K., Blyth, A.R., Jones, M.G., Blomqvist, R., Tullborg, E.L., McNutt, R.H., McDermott, F. and Ivanovich, M., 1992, July. A comparison of calcite fracture mineralogy and geochemistry for the Canadian and Fennoscandian Shields. In 7th International Symposium on Water Rock Interaction, Vol. 1: 787-791.

Frape, S.K., Blyth, A., Blomqvist, R., McNutt, R.H. and Gascoyne, M., 2003. Deep fluids in the continents: II. Crystalline rocks. Treatise on geochemistry, 5: 541-580.

Gimmi, T. and Waber, H.N., 2004. Modelling of tracer profiles in porewater of argillaceous rocks in the Benken borehole: Stable water isotopes, chloride, and chlorine isotopes. Nagra, National Cooperative for the Disposal of Radioactive Waste. 47-85.

Graedel, T.E. and Keene, W.C., 1996. The budget and cycle of Earth natural chlorine. Pure & Applied Chemistry. 68: 1689-1697.

Hamblin, A.P., 1998a. Upper Cambrian Strata of Southwestern Ontario: Summary of Literature. Geological Survey of Canada Open File 3663.

Hamblin, A.P., 1998b. The Middle Ordovician Shadow Lake Formation of Southwestern, Ontario. Geological Survey of Canada Open File 3662.

Hanlon, C., Stotler, R., Frape, S.K. and Gwynne, R., 2017. Comparison of $\delta^{81}Br$ and $\delta^{37}Cl$ composition of volatiles, salt precipitates, and associated water in terrestrial evaporative saline lake systems. Isotopes in Environmental and Health Studies: 1-20.

Hendry M. J., Wassenaar L. I., and Kotzer T., 2000. Chloride and chlorine isotopes (^{36}Cl and ^{37}Cl) as tracers of solute migration in a thick, clay-rich aquitard system. Water Res. Res. 36: 285–296.

Hesse R., Frape S. K., Egeberg P. K., and Matsumoto R., 2000. 12-Stable isotope studies (Cl, O and H) of interstitial water from site 997, Blake ridge hydrate field, West Atlantic. Proc. Ocean Drill. Program. Sci. Res. 164: 129–137.

Hesse R, Egeberg P.K, Frape S.K., 2006. Chlorine stable isotope ratios as a tracer for pore-water advection rates in a submarine gas-hydrate field: implication for hydrate concentration. Geofluids 6:1–7.

Heagle, D. and L. Pinder., 2010. Opportunistic groundwater sampling in DGR-3 and DGR-4, TR-08-18, Intera Engineering Ltd. Report TR-08-18. Revision 1, June 18, Ottawa.

Hobbs, M.Y., S.K. Frape, O. Shouakar-Stash and L.R. Kennell., 2011. Regional Hydrogeochemistry - Southern Ontario. Nuclear Waste Management Organization Report NWMO DGR-TR-2011-12 R000. Toronto, Canada.

Horst, A. H. Holmstrand, P. Andersson, B.F. Thornton, A. Wishkerman, F. Keppler and Ö. Gustafsson, 2014. Stable bromine isotopic composition of methyl bromide released from plant matter. Geochem et Cosmochim Acta, 125: 186-195.

Holser, W.T., 1979. Trace elements and isotopes in evaporites. In: Burns, R.G. (Ed.), Reviews in Mineralogy, In: Marine Minerals, vol. 6. Mineralogical Society of America, Washington, DC: 295-346.

Howell, P.D. and van der Pluijm, B.A., 1990. Early history of the Michigan basin: Subsidence and Appalachian tectonics. Geology, 18: 1195-1198.

Hönninger, G., Bobrowski, N., Palenque, E.R., Torrez, R. and Platt, U., 2004. Reactive bromine and sulfur emissions at Salar de Uyuni, Bolivia. Geophysical research letters, 31(4).

Husain, M.M., 1996. Origin and persistence of Pleistocene and Holocene water in a regional clayey aquitard and underlying aquifer in part of southwestern Ontario. Ph.D. Thesis, University of Waterloo, Canada.

Huset, R.A., 2007. Methyl halides: Concentrations, fluxes and stable carbon isotope ratios measured in the atmosphere, coastal waters, and soils.

Intera Engineering Ltd., 2010. Bedrock Formations in DGR-1, DGR-2, DGR-3 and DGR-4, TR-08-12, Revision 1, March 2010, Ottawa.

Intera Engineering Ltd., 2011. Descriptive Geosphere Site Model, report for the Nuclear Waste Management Organization NWMO DGR-TR-2011-24, Revision R000, March 2011, Toronto, Canada.

Jackson, R., 2009. Organic geochemistry and clay mineralogy of DGR-3 and DGR-4 core. DGR site characterization document Intera Engineering project 08-200. Intera TR-08-29. Ottawa: Intera.

Johnson, M.D., D.K. Armstrong, B.V. Sanford, P.G. Telford and M.A. Rutka., 1992. Paleozoic and

Mesozoic Geology of Ontario. In: Geology of Ontario; Ontario Geological Survey, Special Volume 4, Part 2. Ministry of Northern Development and Mines. Chapter 20: 907-1008.

John, T., Layne, G.D., Haase, K.M. and Barnes, J.D., 2010. Chlorine isotope evidence for crustal recycling into the Earth's mantle. Earth and Planetary Science Letters, 298(1): 175-182.

Kaufmann, R. S., McNutt, R., Frape, S. K. and Eastoe, C., 1992. Chlorine stable isotope distribution of Michigan Basin and Canadian Shield formation waters. In: Kharaka, Y.K. and Maest, A.S. (eds., International Symposium on); 7th International Symposium on Water-Rock Interaction, Park City, Utah, USA. Balkema, Rotterdam, Brookfield. vol. 2: 943-946.

Kharaka, Y.K., A.S. Maest, W.W Carothers, L.M. Law, P.J. Lamothe and T.L. Fries., 1987. Geochemistry of metal-rich brines from central Mississippi Salt Dome Basin, U.S.A. Appl Geochem 2: 543-561.

Land, L.S., 1997. Mass transfer during burial diagenesis in the Gulf of Mexico sedimentary basin: an overview. Society for Sedimentary Geology 57: 29-39.

Lavastre, V., Jendrzejewski, N., Agrinier, P., Javoy, M. and Evrard, M., 2005. Chlorine transfer out of a very low permeability clay sequence (Paris Basin, France): ^{35}Cl and ^{37}Cl evidence. Geochem et Cosmochim Acta, 69: 4949-4961.

Layne, G.D., Kent, A.J. and Bach, W., 2009. $\delta^{37}Cl$ systematics of a backarc spreading system: The Lau Basin. Geology, 37: 427-430.

Legall, F.D., Barnes, C.R. and Macqueen, R.W., 1981. Thermal maturation, burial history and hotspot development, Paleozoic strata of southern Ontario-Quebec, from conodont and acritarch colour alteration studies. Bulletin of Canadian Petroleum Geology, 29(4): 492-539.

Le Gal La Salle C, Matray JM, Bensenouci F, Michelot JL, Dauzères A, Wittebroodt C, Frape S, Shouakar Stash O, Rebaix R, Lancelot J., 2013. Modelling Cl-concentration and δ37Cl profiles in porewater across a 250 m-thick indurated clayrock at the tournemire URL (France). Proc Earth Planet Sc 7:471–474.

Leri, A.C., Hakala, J.A., Marcus, M.A., Lanzirotti, A., Reddy, C.M. and Myneni, S.C., 2010. Natural organobromine in marine sediments: New evidence of biogeochemical Br cycling. Global Biogeochemical Cycles, 24(4).

Leri, A.C. and Myneni, S.C., 2012. Natural organobromine in terrestrial ecosystems. Geochim et Cosmochim Acta, 77: 1-10.

Leri, A.C., Mayer, L.M., Thornton, K.R. and Ravel, B., 2014. Bromination of marine particulate organic matter through oxidative mechanisms. Geochim et Cosmochim Acta, 142: 53-63.

Liberty, B.A., 1969. Paleozoic geology of the Lake Simcoe area, Ontario, Geological Survey of Canada, Memoir 335, 201pp.

Liberty, B.A. and T.E. Bolton. 1971. Paleozoic geology of the Bruce Peninsula area, Ontario, Geological Survey of Canada, Memoir 360, 163pp.

Lico, M.S., Y.K. Kharaka, W.W. Carothers and V.A. Wright., 1982. Methods for collection and analysis of geopressured geothermal and oil field waters. US Geological Survey Water-Supply Paper, Report W 2194.

Martini, A.M., L.M. Walter, J.M. Budai, T.C.W. Ku, C.J. Kaiser and M. Schoell., 1998. Genetic and temporal relations between formation waters and biogenic methane: Upper Devonian Antrim Shale, Michigan Basin, USA. Geochim et Cosmochim Acta 62(10): 1699-1720.

Manley, S.L., 2002. Phytogenesis of halomethanes: a product of selection or a metabolic accident. Biogeochemistry, 60: 163-180.

Mazurek, M., 2004. Long-term Used Nuclear Fuel Waste Management - Geoscientific Review of the Sedimentary Sequence in Southern Ontario. University of Bern Technical Report TR 04-01. Bern, Switzerland.

Melchin, M.J., M.E. Brookfield, D.K. Armstrong and M. Coniglio., 1994. Stratigraphy, sedimentology and biostratigraphy of the Ordovician rocks of the Lake Simcoe area, south-central Ontario; Geological Association of Canada–Mineralogical Association of Canada, Joint Annual Meeting, Waterloo, Ontario, Guidebook for Field Trip A4.

McCaffrey, M.A., B. Lazar and H.D. Holland., 1987. The evaporation path of seawater and the coprecipitation of Br^- and K^+ with halite. Journal of Sedimentary Petroleum 57: 928-937.

McIntosh, J.C. and L.M. Walter., 2006. Paleowaters in Silurian-Devonian carbonate aquifers: Geochemical evolution of groundwater in the Great Lakes region since the late Pleistocene. Geochim et Cosmochim Acta 70: 2454-2479.

McIntosh, J.C. and L.M. Walter., 2005. Volumetrically significant recharge of Pleistocene glacial meltwaters into epicratonic basins: Constraints imposed by solute mass balances. Chem Geol 222: 292-309.

McNutt, R.H., S.K. Frape and P. Dollar., 1987. A strontium, oxygen and hydrogen isotopic composition of brines, Michigan and Appalachian Basins, Ontario and Michigan. Appl Geochem 2: 495-505.

Middleton K., M. Coniglio and S.K. Frape. 1990. Diagenetic History of Dolomitized Ordovician and Devonian Oil and Gas Reservoirs in Southwestern Ontario. Part B: Fracture-related Diagenesis of Middle Ordovician Carbonate Reservoirs, Southwestern Ontario. Ontario Geological Survey Miscellaneous Paper 150: 134-142.

Middleton, K., 1991. Fracture-related diagenesis of Middle Ordovician Carbonate reservoirs, southwestern Ontario. M.Sc. Thesis, University of Waterloo, Canada.

Middleton, K., M. Coniglio, R. Sherlock and S.K. Frape., 1993. Dolomitization of Middle Ordovician carbonate reservoirs, southwestern Ontario. Bulletin of Canadian Petroleum Geology 41: 150-163.

Moser, H. (ed.). 1977. Jahresbericht 1977. Internal reports of the Institute for radiohydrometrie GSF Munich, vol. 169: 70–71.

Monks, P.S., 2005. Gas-phase radical chemistry in the troposphere. Chemical Society Reviews, 34: 376-395.

Morrow, D.W., 1990. Dolomite- Part 2: Dolomitization Models and Ancient Dolostones. Diagenesis. Geoscience Canada Reprint Series 4: 125-139.

Munnecke, A., Calner, M., Harper, D.A. and Servais, T., 2010. Ordovician and Silurian sea-water chemistry, sea level, climate: a synopsis. Paleogeography, Paleoclimatology, Paleoecology, 296: 389-413.

Numata, M., N. Nakamura, H. Koshikawa, and Y. Terashima, 2002. Chlorine isotope fractionation during reductive dechlorination of chlorinated ethenes by anaerobic bacteria. Environmental Science and Technology, 36: 4389-4394.

Nunn, J.A. and Sleep, N.H., 1984. Thermal contraction and flexure of intracratonal basins: a three-dimensional study of the Michigan basin. Geophysical Journal International, 76: 587-635.

NWMO. 2011. Geosynthesis. Nuclear Waste Management Organization Report NWMO DGR-TR-2011-11. Toronto, Canada.

Patriarche, D., Michelot, J.L., Ledoux, E. and Savoye, S., 2004. Diffusion as the main process for mass

transport in very low water content argillites: 1. Chloride as a natural tracer for mass transport—Diffusion coefficient and concentration measurements in interstitial water. Water Resources Research, 40.

Palau, J., O. Shouakar-Stash, and D. Hunkeler, 2014. Carbon and chlorine isotope analysis to identify abiotic degradation pathways of 1, 1, 1-trichloroethane. Environmental Science and Technology, 38: 14400-14408.

Pratt, K.A., Custard, K.D., Shepson, P.B., Douglas, T.A., Pöhler, D., Zielcke, J., Simpson, W.R., Platt, U., Tanner, D.J., Huey, L.G. and Carlsen, M., 2013. Photochemical production of molecular bromine in Arctic surface snowpacks. Nature Geoscience, 6: 351.

Powell, T.G., Macqueen, R.W., Barker, J.F. and Bree, D.G., 1984. Geochemical character and origin of Ontario oils. Bulletin of Canadian Petroleum Geology, 32: 289-312.

Quinlan, G. and C. Beaumont., 1984. Appalachian thrusting, lithospheric flexure and the Paleozoic stratigraphy of the Eastern Interior of North America. Canadian Journal of Earth Sciences 21: 973-996.

Rebeix, R., La Salle, C. L. G., Jean-Baptiste, P., Lavastre, V., Fourré, E., Bensenouci, F., Michelot, J. L., 2014. Chlorine transport processes through a 2000 m aquifer/aquitard system. Marine and Petroleum Geology, 53: 102-116.

Rittenhouse, G., 1967. Bromine in oil-field waters and its use in determining possibilities of origin of these waters. American Association of Petroleum Geology Bulletin 51: 2430-2440.

Sanford, B.V., F.J. Thompson and G.H. McFall., 1985. Plate tectonics – A possible controlling mechanism in the development of hydrocarbon traps in southwestern Ontario. Bulletin of Canadian Petroleum Geology 33: 52-71.

Schilling, J.G., Unni, C.K. and Bender, M.L., 1978. Origin of chlorine and bromine in the oceans. Nature, 273: 631-636.

Sharp, Z.D., Barnes, J.D., Brearley, A.J., Chaussidon, M., Fischer, T.P. and Kamenetsky, V.S., 2007. Chlorine isotope homogeneity of the mantle, crust and carbonaceous chondrites. Nature, 446: 1062.

Sharp, Z.D., Mercer, J.A., Jones, R.H., Brearley, A.J., Selverstone, J., Bekker, A. and Stachel, T., 2013. The chlorine isotope composition of chondrites and Earth. Geochim et Cosmochim Acta, 107: 189-204.

Sherwood Lollar, B. and S.K. Frape., 1989. Report on hydrogeochemical and isotopic investigations at Ontario Hydro UN-2 and OHD-1 boreholes. Contract # GHED 88-1. Ontario Hydro Report.

Sherwood Lollar, B., S.M. Weise, S.K. Frape, J.F. Barker., 1994. Isotopic constraints on the migration of hydrocarbon and helium gases of southwestern Ontario. Bull. Can. Petrol. Geol., 42, 283-295.

Shouakar-Stash, O., 2008. Evaluation of stable chlorine and bromine isotopes in sedimentary formation fluids. Ph.D. Thesis, University of Waterloo, Canada.

Shouakar-Stash, O., S.K. Frape and R.J. Drimmie., 2005a. Determination of bromine stable isotopes using continuous-flow isotope ratio mass spectrometry. Anal Chem. 77: 4027-4033.

Shouakar-Stash, O., R.J. Drimmie and S.K. Frape., 2005b. Determination of inorganic chlorine stable isotopes by Continuous Flow Isotope Ratio Mass spectrometry. Rapid Communication in Mass Spectrometry, 19: 121-127.

Shouakar-Stash, O., S.V. Alexeev, S.K. Frape, L.P. Alexeeva and R.J. Drimmie., 2007. Geochemistry and stable isotopic signatures, including chlorine and bromine Isotopes, of the deep groundwaters of the Siberian Platform, Russia. Applied Geochemistry, 22: 589-605.

Skuce, M., 2014. Isotopic Fingerprinting of Shallow and Deep Groundwaters in Southwestern Ontario and its Applications to Abandoned Well Remediation. M.Sc. Thesis, the University of Western Ontario, London, Ontario, Canada.

Skuce, M., F.J. Longstaffe, T.R. Carter and J. Potter., 2015. Isotopic fingerprinting of groundwaters in southwestern Ontario: Applications to abandoned well remediation. Appl Geochem, 58: 1-13.

Sleep, N.H., 1971. Thermal effects of the formation of Atlantic continental margins by continental break up. Geophysical Journal International, 24(4), pp.325-350.

Sleep, N.H. and Snell, N.S., 1976. Thermal contraction and flexure of mid-continent and Atlantic marginal basins. Geophysical Journal International, 45: 125-154.

Sturchio, N.C., P.B. Hatzinger, M.D. Arkins, C. Suh, and L.J. Heraty, 2003. Chlorine isotope fractionation during microbial reduction of perchlorate. Environmental Science and Technology, 37: 3859-3863.

Stotler, R.L., S.K. Frape and O. Shouakar-Stash., 2010. An isotopic survey of δ^{81}Br and δ^{37}Cl of dissolved

halides in the Canadian and Fennoscandian Shields. Chemical Geology 274: 38-55.

Tan, H.B., H.Z. Ma, X.Y. Zhang, J.X. Xu and Y.K. Xiao., 2009. Fractionation of chlorine isotope in salt mineral sequences and application: research on sedimentary stage of ancient salt rock deposit in Tarim Basin and western Qaidam Basin. Acta Petrol Sinica 25: 955–962.

Tanweer, A. and L.F. Han., 1996. Reduction of microliter amounts of water with manganese for D/H isotope ratio measurement by mass spectrometry. Isotopes in Environmental and Health Studies. 32: 97-103.

Trevail, R.A., 1990. Cambro-Ordovician shallow water sediments, London area, southwestern Ontario; In: Subsurface Geology of Southwestern Ontario: a core workshop. Ontario Petroleum Institute. American Association of Petroleum Geologists. 1990 Eastern Meeting: 29-50.

Uyeno, T.T., P.G. Telford and B.V. Sanford., 1982. Devonian conodonts and stratigraphy of southwestern Ontario. Geological Survey of Canada Bulletin 332.

Van der Voo, R., 1982. Pre-Mesozoic paleomagnetism and plate tectonics. Annual Review of Earth and Planetary Sciences 10: 191-220.

van Warmerdam, E. M., Frape, S. K., Aravena, R., Drimmie, R. J., Flatt, H. and Cherry, J. A., 1995. Stable chlorine and carbon isotope measurements of selected chlorinated organic solvents. Appl Geochem. 10: 547-552.

Waber, H. N., Frape S. K., and Gautschi A., 2001. Cl-isotopes as indicator for a complex paleohydrogeology in Jurassic argillaceous rocks, Switzerland. Water Rock Interaction Meeting, 2001. Abstract volume: 1403–1406.

Wang, H.F., K.D Crowley and G.C. Nadon., 1994. Thermal History of the Michigan Basin from Apatite Fission-Track Analysis and Vitrinite Reflectance. In basin Compartments and Seals P.J. Ortoleva (Ed), AAPG Memoir 61. American Association of Petroleum Geologists. Tusla, Oklahoma, USA.

Wang, Y and Frape S.K, 2015. Chlorine and Bromine isotopic analyses of groundwaters: DGR-3 and DGR-4. NWMO Report. TR-2015-20.

Weaver, T.R., 1994. Groundwater flow and solute transport in shallow Devonian bedrock formations and overlying Pleistocene units, Lambton County, southwestern Ontario. Ph.D. Thesis, University of Waterloo, Canada.

Weaver, T.R., S.K. Frape and J.A. Cherry., 1995. Recent cross-formational fluid flow and mixing in the shallow Michigan Basin. Geological Society of America Bulletin 107: 697–707.

Wiegert, C., M. Mandalakis, T. Knowles, P.V. Polymenakou, C. Aeppli, J. Macháčková, H. Holmstrand, R.P. Evershed, R.D. Pancost, and Ö. Gustafsson, 2013. Carbon and chlorine isotope fractionation during microbial degradation of tetra- and trichloroethene. Environmental Science and Technology, 47: 6449—6456.

Zakon, Y., L. Halicz, and F. Gelman, 2013. Bromine and carbon isotope effects during photolysis of brominated phenols. Environmental Science and Technology, 47: 14147-14153.

Ziegler, K. and F.J. Longstaffe., 2000a. Multiple episodes of clay alteration at the Precambrian/Paleozoic unconformity, Appalachian Basin: Isotopic evidence for long-distance and local fluid migrations. Clays and Clay Minerals 48: 474-493.

Ziegler, K. and F.J. Longstaffe., 2000b. Clay mineral authigenesis along a mid-continental scale fluid conduit in Paleozoic sedimentary rocks from southern Ontario, Canada. Clays and Clay Minerals 35: 239-260.

APPENDIX A: Br-Cl Isotopic Analysis Methods and Regional Geochemical and Isotopic Data

A.1 Br-Cl Isotopic Analysis Methods

Continuous Flow Isotope Ratio Mass Spectrometry (CF-IRMS) method with gas chromatography (GC) was used to analyze the $\delta^{37}Cl$ and $\delta^{81}Br$ isotopes from the Bruce Nuclear Site at the University of Waterloo (Shouakar-Stash et al. 2005a, b).

a) Brief procedure for Bromine isotope analysis

1) Bromide Separation

- Solution is separated in the special distillation apparatus to isolate Bromine gas from impure solution, which depends on the differences of oxidation-reduction behavior of different halogens (Figure 1A). Separation technique is described in the CF-IRMS paper by Shouakar-Stash et al. (2005a).

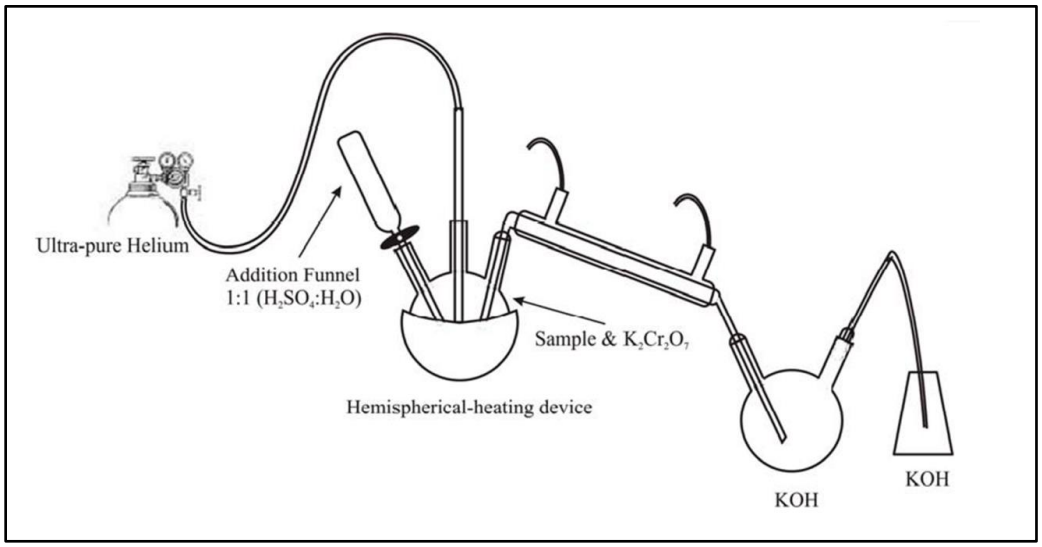

Figure 21: Bromine Distillation Apparatus (from Shouakar-Stash 2005a).

2) Silver Bromide Preparation

- The solution is first acidified to pH ~ 2 by adding ultra-pure concentrated nitric acid (HNO_3).
- 18 g of potassium nitrate (KNO_3) is added to the solution to increase the ionic strength.
- 2 mL of silver nitrate ($AgNO_3$) solution (0.2 M) is added to precipitate AgBr.
- Stored in a dark environment (24 hours) during AgBr settling.
- Then rinsed twice with 5% HNO_3.

- Placed into an oven at 80°C overnight to dry.

3) Methyl Bromide Preparation

- 0.5 mg AgBr samples are moved into 20 mL amber crimp vials to react with methyl iodide (CH_3Br) completely. The whole process is conducted in a glove bag under helium flow.
- CH_3Br (100 μL) is added to the samples, and then vials (4-6) are sealed.
- Place vials in an oven for 56 ± 5 hours at 80°C for the reaction to complete.

4) Isotope analysis

- The first step is sample injection, which is done automatically via an autosampler (CombiPAL).
- The second step is gas separation via the gas chromatograph (GC).
- The third step is the analysis of the CH_3Br by mass spectrometer.

The internal precision using pure methyl bromide gas is less than 0.03‰ (STDV), while the external precision using seawater standard could be 0.06‰ (STDV) for n =12 or less (Shouakar-Stash et al., 2005a).

b) Brief procedure for Chlorine isotope analysis

1) Silver Chloride Preparation

- Adding ultra-pure water, or evaporate the solution, to get desired concentration.
- Solution is acidified to pH~2 with ultra-pure nitric acid (HNO_3) and heated at 80°C for a few minutes to drive off CO_2.
- Then, 0.4 M potassium nitrate (KNO_3) solution is added to reach a high ionic strength.
- Anhydrous sodium phosphate dibasic (Na_2HPO_4) and citric acid monohydrate ($HOC(CH_2CO_2H)_{2CO2H.H2O}$) (0.0004 and 0.0098 mol, respectively) are added to buffer pH at ~2 and to remove small amounts of sulfide, phosphate and carbonate from the precipitate.
- 1 mL silver nitrate ($AgNO_3$) solution (0.2 M) is added to the residual solution to separate the AgCl from solution.
- 24 hours' storage in a dark cabinet for AgCl settling, and then placement into an oven at 80°C overnight to dry.

2) Methyl Chloride Preparation

- 0.2 mg AgCl samples are moved into 20 mL amber crimp vials to react with methyl iodide (CH_3I) completely. The whole process is conducted in a glove bag under helium flow.
- CH_3I (100 mL) is added to the samples and then vials (3-4) are sealed.
- Place vials in an oven for 48 hours at 80°C for the reaction to complete.

3) Isotope analysis

- Sample analysis is conducted under three protocols including CombiPAL (sample injection), the Agilent 6890 GC setup (gas separation), and the mass spectrometry method (chlorine isotope analysis).

The internal precision using pure CH_3Cl gas is less than 0.04‰ (STDV), while the external precision using seawater standard could be 0.07‰ (STDV) for n =12 or less (Shouakar-Stash et al. 2005b).

A.2 Geochemical and Isotopic Data from Southern Ontario and Michigan

Table A1: Geochemical data and stable water isotopic data for the formation waters from southern Ontario and Michigan (from Shouakar-Stash 2008). The samples and data presented in this table were compiled from various authors: [1] Dollar 1988; [2] Walter, Pers. Comm.; [3] Cloutier 1994; [4] Husain 1996; [5] Weaver 1994; [6] Sherwood-Lollar and Frape 1989.

Author	Sample Name	Rock Type	Water Type	Depth m	Ca mg/L	Na mg/L	Mg mg/L	K mg/L	Sr mg/L	Cl mg/L	Br mg/L	SO_4 mg/L	HCO_3 mg/L	F mg/L	Br/Cl	$\delta^{18}O$ (VSMOW) (‰)	$\delta^{2}H$ (VSMOW) (‰)	$\delta^{37}Cl$ (SMOC) (‰)	$\delta^{81}Br$ (SMOB) (‰)	$^{87}Sr/^{86}Sr$	TDS mg/L
Late Devonian (Ketlle Point Antrim)																					
[3]	LD-90-3-5	Shale	Na-Cl	52	127	5410	120	31	5	8600	7	1	1210		0.000814	-11.1	-69	1.82			15511
[3]	DOW-90-3-4	Shale	Na-Cl	44	8.41	189	0.1	*11*	0.5	164	0.7	42	164		0.004268	-8.5	-61				641
[4]	BRP-143	Shale	Na-Cl	44	39.6	278	14	5	0.8	393	0.4	10	194		0.001018	-16.9	-122	0.01			934
[4]	BRP-151	Shale	Na-Cl	46	26.5	338	12	*9*	0.5	390	0.3	6	202		0.000769	-16.9	-122	0.24			984
[2]	SP A2-32	Shale	Na-Cl		6770	82600	3590	667	323	147000	307	<5	5		0.002088	-4.6	-28	-0.39		0.71000	241262
[2]	WSMC2-10	Shale	Na-Cl		7700	63700	4690	487	424	128200	454		16		0.003541	-6.7	-40	-1.11			205671
[2]	HGR D4-6	Shale	Na-Cl		3280	42400	2140	370	221	74300	179		24		0.002409	-10.2	-64	-0.35			122914
Late Devonian (Hamilton)																					
[3]	LD-90-3-4	Shale	Na-Cl	68	122	3K40	68	29	3	5800	5	349	200		0.000862	-7.5	-52	0.89			10415
[3]	LD-90-3-3	Shale	Na-Cl	89	104	2590	59	47	4	3530	5	783	376		0.001416	-7.2	-51	0.67			7499
[3]	LD-90-3-2	Shale	Na-Cl	131	200	4230	137	41	14	7260	0	324	724		0.000000	-6.9	-47	0.18			12930
[3]	DOW-90-3-3	Shale	Na-Cl	77	164	3760	75	47	3	6080	6	379	214		0.000987	-7.1	-57	0.00			10728
[3]	DOW-90-3-2	Shale	Na-Cl	106	367	5940	208	67	8	11500	21	572	404		0.001826	-6.8	-50	0.03			19086
Middle Devonian (Dundee)																					
[3]	DOW-90-3-1	Carbonate	Na-Cl	142	127	2920	70	48	3	3880	9	819	504		0.002320	-6.9	-51	-0.72			8380
[3]	LD-90-3-1	Carbonate	Na-$S0_4$-Cl	142	92	1510	28.9	136	2	793	4	1830	470		0.005044	-7.2	-54				4866
[1]	DD-1	Carbonate	Na-Cl	108	660	3690	632	85	29	10000	50	795	293		0.005000	-11.4	-86	0.05		0.70852	15940
[1]	DD-2	Carbonate	Ca-Na-Cl	97	623	414	83	19	12	2000	12	98	<7		0.006000	-15.7	-120			0.70949	3260
[1]	DD-3	Carbonate	Na-Ca-Cl	1131	31500	70600	5410	3030	750	179000	1050	166	<7	17	0.005866			-0.19	-0.21	0.70816	291500
[1]	DD-4	Carbonate	Na-Ca-Cl	1128	40300	56600	6990	3370	1120	182200	1310	150	90	10	0.007190	-0.9	-34	-0.27	-0.17	0.70823	292000
[5]	PD-COCH	Carbonate	Na-Ca-Mg-Cl		1180	3470	715	91	23	8650	58	I700	264		0.006705	-7.5	-48			0.70822	16155
[5]	PD-NORTH	Carbonate	Na-Ca-Cl		I5K0	4830	898	115	29	12000	91	2200	325		0.007583	-6.9	-41	0.92	0.68		22073
[5]	PD-RAL	Carbonate	Na-Ca-Mg-Cl		1580	4390	908	117	30	10900	78	2000	158		0.007156	-6.8	-43			0.70820	20166
[5]	PD-WEST	Carbonate	Na-Ca-Mg-Cl		1400	3870	793	105	26	9920	82	1940	258		0.008266	-7.1	-46				18399
[5]	RA-N	Carbonate	Na-Ca-Mg-Cl		1140	3420	675	85	24	8870	62	I380	348		0.006990	-7.6	-49				16008
[5]	RA-NE	Carbonate	Na-Ca-Cl		1410	4360	808	105	28	11300	74	1810	499		0.006549	-6.8	-46	1.14	0.62	0.70820	20145
[5]	RA-SE	Carbonate	Na-Ca-Cl		1490	4530	858	111	28	11500	79	1920	320		0.006870	-7.2	-45	0.95	0.52		20S40
[5]	RA-SW	Carbonate	Na-Ca-Cl		1320	3970	758	100	25	10100	67	1690	308		0.006634	-7.5	-49				18342
[5]	LAI-1	Carbonate	Na-Mg-Ca-Cl		1270	3670	818	103	25	9500	59	1790	589		0.006211	-6.6	-36				I7828

Author Sample Name		Rock Type	Water Type	Depth m	Ca mg/L	Na mg/L	Mg mg/L	K mg/L	Sr mg/L	Cl mg/L	Br mg/L	SO_4 mg/L	HCO_3 mg/L	F mg/L	Br/Cl	$\delta^{18}O$ (VSMOW) (‰)	$\delta^{2}H$ (VSMOW) (‰)	$\delta^{37}Cl$ (SMOC) (‰)	$\delta^{81}Br$ (SMOB) (‰)	$^{87}Sr/^{86}Sr$	TDS mg/L
Middle Devonian (Dundee)																					
[5]	LAI-2	Carbonate	Na-Mg-Ca-Cl		1300	3520	803	102	26	8980	54	2010	548		0.006013	-6.5	-43	1.02		0.70821	17346
[5]	LAI-3	Carbonate	Na-Mg-Ca-Cl		1220	3430	773	107	23	8240	44	2110	561		0.005340	-6.4	-37				16512
[5]	WB-11	Carbonate	Na-Mg-Ca-Cl		736	2100	450	62	51	5700	43	751	572		0.007544	-8.5	-55	1.16		0.70813	10470
[5]	WB-2	Carbonate	Na-Mg-Ca-Cl		918	2620	593	76	21	7190	21	787	599		0.002921	-8.2	-49				12829
[5]	WB-7	Carbonate	Na-Mg-Ca-Cl		1100	3090	6XK	8S	22	8450	60	1320	512		0.007101	-7.6	-48	1.25			15334
[5]	WB-8	Carbonate	Na-Mg-Ca-Cl		1240	3590	843	III	27	9750	57	1230	536		0.005846	-6.9	-42			0.70820	17388
[5]	LBH-1	Carbonate	Na-Mg-Ca-Cl		1700	4450	1170	152	32	13200	47	1400	157		0.003561	-8.7	-59				22314
[5]	LBH-2	Carbonate	Na-Mg-Ca-Cl		2000	4950	1320	156	34	14300	86	2340	5		0.006014	-8.8	-62	0.35	0.60		25194
[5]	LBH-3	Carbonate	Na-Mg-Ca-Cl		1940	4900	1340	169	36	14100	97	2140	5		0.006879	-8.2	-59			0.70827	24731
[5]	LBH-4	Carbonate	Na-Mg-Ca-Cl		1760	5150	1300	171	36	15000	86	1220	112		0.005733	-8.1	-57	0.33	0.92		24839
Middle Devonian (Detroit River)																					
[5]	LBO-2	Carbonate	Na-Mg-Ca-Cl		1530	4030	940	131	34	11300	99	448	40		0.008761	-7.5	-53	0.69	0.52		18556
[5]	LBO-3	Carbonate	Na-Ca-Mg-Cl		1640	3130	920	125	35	10400	69	630	113		0.006635	-7.2	-54				17066
[5]	CFN-14	Carbonate	Na-Ca-Mg-Cl		1310	2390	608	85	29	7990	66	796	219		0.008260	-9.5	-63	0.50		0.70833	13500
[5]	CFN-A	Carbonate	Na-Ca-Mg-Cl		1570	3170	830	123	35	9460	86	916	171		0.009091	-9.0	-60	0.26	0.55		16365
[5]	CFN-B	Carbonate	Na-Ca-Mg-Cl		1190	2590	673	98	27	7810	61	398	297		0.007810	-9.1	-60				13148
[5]	CFN-161	Carbonate	Na-Ca-Mg-Cl		5990	10900	2750	445	100	31400	277	1240	328		0.008822	-6.3	-84	0.63	0.49	0.70825	53400
[5]	CFN-C	Carbonate	Na-Mg-Ca-Cl		3830	8690	2430	307	70	27400	200	760	221		0.007299	-6.3	-38	0.79	0.35	0.70827	43912
[5]	CFN-E	Carbonate	Na-Ca-Mg-Cl		4020	8090	2270	288	67	26800	216	1220	328		0.008060	-5.9	-56	0.94	0.45	0.70826	43304
[5]	CFS-A	Carbonate	Na-Ca-Mg-Cl		4320	9330	2330	311	70	30300	294	1390	345		0.009703	-6.0	-76	0.69	0.57		48694
[5]	CFS-B	Carbonate	Na-Ca-Mg-Cl		4240	9700	2270	325	67	25500	202	1350	148		0.007922	-6.3	-49	0.49			43805
[5]	CFS-C	Carbonate	Na-Ca-Mg-Cl		3800	8910	2160	309	67	26600	195	941	206		0.007331	-6.4	-48	0.72			43192
[5]	CFS-D	Carbonate	Na-Mg-Ca-Cl		3500	8320	2150	299	67	25700	187	808	421		0.007276	-6.3	-68	0.28	0.63		41456
[1]	DR-1	Carbonate	Ca-Na-Cl	1445	64900	23400	7960	8320	2060	173100	1970	205	258	14	0.011381	0.2	-55	-0.50	-0.23	0.70913	281900
Midddle Silurian (F Salt)																					
[1]	SF-1	Salt	Na-Cl	150	8200	100000	2850	2600	214	207000	587	750			0.002836	-5.5	-55	-0.20		0.70866	322200
[1]	SF-2	Salt	Na-Cl	150	10300	94500	3100	2780	197	194100	390	510	73		0.002009						305900
[1]	SF-3	Salt	Na-Cl	150	9630	94400	3370	2600	158	192900	325	595	76		0.001685	-4.7	-52				304000
Middle Silurian (A2 Salt)																					
[1]	SA2-1	Salt	Ca-Na-Mg-Cl	250	48400	33400	16600	5000	1620	232000	3220	110			0.013879	2.9	-52			0.70853	340400
[1]	SA2-2	Salt	Ca-Na-Mg-Cl	250	46800	33600	16200	6400	1620	232000	3214	106			0.013853	3.2	-48			0.70866	340000
Middle Silurian (A1 Carbonate)																					
[1]	SA1-1	Carbonate	Ca-Na-Cl	645	52000	37700	11400	4520	740	176000	1880	167	76		0.010682			-0.35			284400
[1]	SA1-2	Carbonate	Ca-Na-Cl	649	54700	37900	10900	4760	969	195300	1700	193	18		0.008705	-1.1	-47	-0.35		0.70849	306400
Middle Silurian (Guelph)																					
[1]	SG-1	Carbonate	Na-Ca-Cl	354	15000	41200	3780	1430	263	95500	810	810	127	164	0.008482	-4.7	-42			0.71029	158800
[1]	SG-2	Carbonate	Na-Ca-Cl	448	31300	65500	7770	1880	436	189100	1390	250	69	8	0.007351					0.70931	297600
[1]	SG-3	Carbonate	Na-Ca-Cl	553	44500	61300	9000	2740	599	206900	1620	127	43		0.007830	-0.8	-43	-0.40			326800
[1]	SG-4	Carbonate	Ca-Na-Cl	614	60300	46600	8250	3040	1220	197800	2510	119	<7		0.012690			-0.15	-0.95	0.70915	319800

Author	Sample Name	Rock Type	Water Type	Depth m	Ca mg/L	Na mg/L	Mg mg/L	K mg/L	Sr mg/L	Cl mg/L	Br mg/L	SO_4 mg/L	HCO_3 mg/L	F mg/L	Br/Cl	$\delta^{18}O$ (VSMOW) (‰)	$\delta^{2}H$ (VSMOW) (‰)	$\delta^{37}Cl$ (SMOC) (‰)	$\delta^{81}Br$ (SMOB) (‰)	$^{87}Sr/^{86}Sr$	TDS mg/L
Middle Silurian (Guelph)																					
[1]	SG-5	Carbonate	Na-Ca-Cl	571	29000	70000	8200	2040	449	189100	1390	259	84	8	0.007351					0.70934	300400
[1]	SG-6	Carbonate	Ca-Na-Cl	646	53700	42100	9520	3240	744	186300	1780	227	<7	8	0.009554					0.70889	297600
[1]	SG-7	Carbonate	Ca-Na-Cl	749	66000	42300	8440	3270	1120	210900	2440	239	<7	8	0.011569			-0.38	-0.83	0.70946	334700
[1]	SG-8	Carbonate	Ca-Na-Cl	695	61500	46000	10600	3400	997	214600	2010	61	<7		0.009366	-0.4	-44	-0.51	-0.61	0.70908	339200
[1]	SG-9	Carbonate	Ca-Na-Cl	770	53100	42900	13300	2150	580	205500	1490	203	<7	8	0.007251					0.70929	319200
[1]	SG-10	Carbonate	Ca-Na-Cl	726	57200	39400	8670	3340	1220	189500	2380	172	<7		0.012559			-0.28	-0.75	0.70902	301900
[1]	SG-11	Carbonate	Ca-Na-Cl	518	52600	49900	9500	4840	702	213700	1920	170	245		0.008985					0.70893	333300
[1]	SG-I 2	Carbonate	Na-Ca-Cl	597	34700	53200	7080	2390	572	155200	1510	300	<7	27	0.009729					0.70931	255000
[1]	SG-13	Carbonate	Ca-Na-Cl	670	50200	54800	8230	2810	684	208200	1920	170	77	8	0.009222					0.70907	327000
Middle Silurian (Niagaran)																					
[1]	SN-1	Carbonate	Ca-Na-Cl	892	62000	40800	8680	6080	1270	209700	2160	79	<7	319	0.010300	0.2	-42	-1.04	-0.76	0.70833	330800
[1]	SN-2	Carbonate	Ca-Na-Cl	895	61300	40300	8530	5920	1270	208500	1880	79	<7	295	0.009017	-1.4	-48				327800
[1]	SN-3	C arbonate	Ca-Cl	1161	73800	24800	17900	8560	2040	230400	2390	59	<7		0.010373	-2.9	-50	-0.30	-0.28		359900
[1]	SN-4	Carbonate	Ca-Cl	1272	78500	25300	17900	9280	2170	256200	2360	38	<7		0.009212	-4.9	-46	-0.61	-0.70	0.70861	391700
[1]	SN-5	Carbonate	Ca-Na-Cl	1305	77300	31000	11900	10300	2040	245300	2440	42	<7		0.009947	1.2	-40	-0.22	-0.69		380300
[1]	SN-6	Carbonate	Ca-Cl	1264	79500	25200	15500	9820	2500	261800	2640	49	<7		0.010084	-1.0	-47	-0.28	-0.61	0.70848	397000
[1]	SN-7	Carbonate	Ca-Na-Cl	1010	62900	45300	8550	4320	1160	210700	2270	94	<7	8	0.010774	0.2	-43	-0.30		0.70935	335300
[1]	SN-8	Carbonate	Ca-Na-Cl	1001	61900	45100	8080	3900	1190	187800	2240	105	<7	11	0.011928	-0.5	-41	-0.30		0.70939	310300
[1]	SN-9	Carbonate	Ca-Na-Cl	713	54900	46000	9600	3560	919	207100	1970	89	<7		0.009512	-0.4	-43			0.70909	324100
[1]	SN-10	Carbonate	Ca-Na-Cl	717	62600	42600	8530	3370	1060	202500	2320	89	<7	8	0.011457	-0.1	-47	-0.43	-0.92	0.70929	323100
[2]	Cold Srings WHI-29	Carbonate	Ca-Cl		88643	26275	10176	18285	3661	244975	2570	36			0.010491			-0.39			394620
Early Silurian (Grimsby/Thorhold)																					
[1]	STGr-1	Sandstone	Na-Ca-Cl	431	29000	48100	5980	1000	464	137600	1340	385	<7		0.009738	-3.5	-43				223900
[1]	STGr-2	Sandstone	Na-Ca-Cl	380	36700	51900	7030	1410	611	158500	1550	259	<7		0.009779	-2.9	-34			0.70977	258000
[1]	STGr-3	Sandstone	Na-Ca-Cl	374	27400	42200	6620	899	463	129400	1260	447	<7		0.009737	-4.2	-44				208700
[1]	STGr-4	Sandstone	Na-Ca-Cl	414	34700	49400	6100	981	536	149200	1580	320	<7		0.010590	-2.9	-43				242800
[1]	ST-5	Sandstone	Na-Ca-Cl	292	30500	44500	5830	1010	490	148100	1340	413	<7		0.009048	-4.1	-46	0.78		0.71014	232200
[1]	ST-6	Sandstone	Na-Ca-Cl	408	33700	45200	6210	1040	544	143400	1430	339	<7		0.009972	-3.4	-44				231900
[1]	SGr-7	Sandstone	Na-Ca-Cl	424	33600	50600	5880	1010	530	160800	1510	332	<7		0.009391	-3.3	-43				254300
[1]	SGr-8	Sandstone	Na-Ca-Cl	426	34200	49500	5840	1130	522	164300	1540	345	<7		0.009373	-3.0	-42				257400
[1]	STGr-9	Sandstone	Na-Ca-Cl	522	42100	49700	7500	1260	697	179000	1650	272	<7		0.009218	-2.8	-44				282200
[1]	STGr-10	Sandstone	Na-Ca-Cl	524	45700	58000	8000	1390	784	195800	1970	164	<7		0.010061	-1.9	-42	0.14	0.77		311800
[1]	SGr-11	Sandstone	Na-Ca-Cl	512	44600	58700	7700	1450	745	178300	1870	174	<7		0.010488	-1.7	-41	0.35	1.36		293500
[1]	SGr-12	Sandstone	Na-Ca-Cl	524	26900	38900	5310	878	456	117500	1130	657	<7		0.009617	-3.9	-40				191700
[1]	STGr-13	Sandstone	Na-Ca-Cl	547	31400	45100	5630	877	509	144300	1380	423	<7		0.009563	-3.4	-41	0.35			229600
[1]	STGr-14	Sandstone	Na-Ca-Cl	541	47700	58600	8230	1400	883	207000	2010	123	<7		0.009710	-1.7	-46	0.21	1.35	0.71018	325900
[1]	SGr-15	Sandstone	Na-Ca-Cl	554	34600	46900	6280	930	564	163600	1490	404	<7		0.009108	-3.5	-39				254800
[1]	SGr-16	Sandstone	Na-Ca-Cl	572	28100	45800	4870	911	452	144200	1250	530	<7		0.008669	-3.4	-35			0.71076	226100
[1]	STGr-17	Sandstone	Na-Ca-Cl	544	29100	43300	5070	846	483	142200	1260	450	<7		0.008861	-2.9	-41	0.13			222700
[1]	SGr-18	Sandstone	Ca-Na-Cl	289	39700	22800	6780	664	347	109200	755	560	<7		0.006914	-4.3	-44				180800
[1]	SGr-19	Sandstone	Ca-Na-Cl	335	39800	20900	3540	637	358	119400	694	235	<7		0.005812	-4.5	-44	0.37		0.71092	185600
[1]	SGr-20	Sandstone	Ca-Na-Cl	365	42700	30300	5470	822	481	137400	920	405	<7		0.006696	-3.7	-38	0.50	1.74	0.71036	218500
[1]	SGr-21	Sandstone	Ca-Na-Cl	410	42000	26400	3930	713	426	112600	855	329	<7		0.007593	-3.8	-43	0.50	1.63		187300

Author	Sample Name	Rock Type	Water Type	Depth m	Ca mg/L	Na mg/L	Mg mg/L	K mg/L	Sr mg/L	Cl mg/L	Br mg/L	SO_4 mg/L	HCO_3 mg/L	F mg/L	Br/Cl	$\delta^{18}O$ (VSMOW) (‰)	$\delta^{2}H$ (VSMOW) (‰)	$\delta^{37}Cl$ (SMOC) (‰)	$\delta^{81}Br$ (SMOB) (‰)	$^{87}Sr/^{86}Sr$	TDS mg/L
Early Silurian (Whirlpool)																					
[1]	SW-1	Sandstone	Ca-Na-Cl	361	50400	32400	4250	782	489	158800	1130	320	47	8	0.007116	-3.0	-39	0.86	2.31	0.71103	248600
[1]	SW-2	Sandstone	Ca-Na-Cl	422	47300	29900	3710	763	452	147500	1000	376	60		0.006780	-3.7	-41	0.60	2.11	0.71107	231000
[1]	SW-3	Sandstone	Ca-Na-Cl	422	51100	36400	5500	870	507	171600	1190	375	<7		0.006935	-2.5	-39	0.64	2.13		267500
[1]	SW-4	Sandstone	Ca-Na-Cl	459	43400	28200	4460	770	420	126100	920	433	<7		0.007296	-3.8	-42			0.71112	204700
Late Ordovician (Blue Mountain)																					
[6]	OHD-1 #15	Carbonate	Ca-Na-Cl	173	38600	21800	4520	404	702	118300	1080	120	44		0.009129	-5.6	-46	0.09	1.75		185570
Middle Ordovician (Trenton)																					
[1]	OT-1	Carbonate	Na-Ca-Cl	647	15600	35700	3680	1600	529	98700	578	453	<7	4	0.005856	-2.1	-31	-0.36		0.70978	156900
[1]	OT-2	Carbonate	Na-Ca-Cl	657	16000	35300	3510	1600	540	99800	725	742	34		0.007265	-1.7	-23	0.00		0.70980	158200
[1]	OT-3	Carbonate	Na-Ca-Cl	645	15800	35800	3500	1630	467	101100	563	575	<7	5	0.005569	-1.9	-31	0.30		0.70976	159400
[1]	OT-4	C arbonate	Na-Ca-Cl	738	23300	39800	5480	1970	402	111300	832	630	<7	6	0.007475	-1.7	-30			0.70996	183700
[1]	OT-5	Carbonate	Na-Ca-Cl	743	23500	41400	6130	2120	739	131800	856	152	<7	6	0.006495	-1.9	-29	-0.60		0.70973	206700
[1]	OT-6	Carbonate	Na-Ca-Cl	771	17400	36900	4280	1690	574	103200	550	410	58	4	0.005329	-2.2	-28	-0.30		0.70982	165000
[1]	OT-7	C arbonate	Na-Ca-Cl	790	35200	43600	7410	2310	606	149500	920	263	17		0.006154						239800
[1]	OT-8	Carbonate	Na-Ca-Cl	775	32600	46800	6520	2410	525	148100	1190	353	33		0.008035	-2.1	-30			0.71041	238500
[1]	OT-9	Carbonate	Na-Ca-Cl	786	36500	48800	7410	2270	612	150500	950	263	<7		0.006312	-2.1	-27	-0.59	0.98	0.70900	247300
[1]	OT-10	Carbonate	Na-Ca-Cl	784	36700	48700	7930	2330	633	175900	1170	260			0.006652	-2.3	-31	-0.63	0.87	0.71029	273600
[1]	OT-11	Carbonate	Na-Ca-Cl	804	36730	45700	7270	2320	733	160900	1610	271			0.010006	-1.9	-26	-0.55	0.76	0.71030	255500
[1]	OT-12	Carbonate	Na-Ca-Cl	779	39200	45300	6910	2120	729	166100	1370	321			0.008248	-2.0	-29	-0.49	0.93	0.71030	262100
[1]	OT-13	Carbonate	Na-Ca-Cl	791	32600	55200	7300	2390	578	161200	1150	320	32		0.007134	-2.1	-27	-0.50		0.71007	260700
[1]	OT-14	Carbonate	Na-Ca-Cl	782	33000	48700	6750	2390	548	141400	1170	358	<7	8	0.008274	-2.0	-33	-0.52	0.58	0.71036	234300
[1]	OT-15	Carbonate	Na-Ca-Cl	787	31300	46100	6530	2300	527	149500	1120	380	60	8	0.007492	-2.2	-27	-0.40		0.71023	237800
[1]	OT-16	Carbonate	Na-Ca-Cl	778	32800	46100	6600	2680	529	148600	1220	347	49	13	0.008210	-2.1	-36	-0.55		0.71034	238900
[1]	OT-17	Carbonate	Na-Ca-Cl	781	29700	43200	5960	2150	568	138600	1270	366	<7		0.009163					0.71036	221800
[1]	OT-18	Carbonate	Na-Ca-Cl	786	34100	45400	6700	2310	658	158300	1210	348			0.007644			-0.34	0.62	0.71036	249000
[1]	OT-19	Carbonate	Na-Ca-Cl	844	31100	42000	5440	2190	518	147000	780	393	12		0.005306	-1.8	-24	-0.70			229400
[1]	OT-20	Carbonate	Na-Ca-Cl		27200	46500	5170	2080	467	142300	765	485	45		0.005376	-2.0	-23				225000
[1]	OT-21	Carbonate	Na-Ca-Cl	854	32500	49700	5960	2070	619	150300	1190	335	<7	246	0.007917	-3.1	-32	-0.43	0.18	0.71045	242700
[1]	OT-22	Carbonate	Na-Ca-Cl	1225	21700	41900	4470	3230	493	122700	625	620	49		0.005094					0.70962	195700
[1]	OT-23	Carbonate	Na-Ca-Cl	1140	31000	48000	5450	3390	595	159800	1160	327	86		0.007259	-1.3	-45	-0.65	-0.49	0.70887	249700
[1]	OT-24	Carbonate	Na-Ca-Cl	1247	21800	42300	4270	3130	494	122000	925	402	66	168	0.007582	-1.7	-27	-1.13		0.70958	195300
[1]	OT-25	Carbonate	Na-Ca-Cl	1238	18300	40300	3790	3060	447	117600	797	538	90	160	0.006777	-2.0	-27			0.71000	184800
[1]	OT-26	Carbonate	Na-Ca-CT	1203	19200	41300	4360	3330	490	118500	857	256	81	171	0.007232	-2.1	-27			0.70991	188300
[1]	OT-27	Carbonate	Na-Ca-CT	1287	20500	42500	4620	3490	505	123200	917	312	69	184	0.007443	-1.9	-26			0.70977	196000
[1]	OT-28	Carbonate	Na-Ca-CT	1299	19800	42000	4320	3460	489	119400	650	622	48	8	0.005444					0.70980	190700
[1]	OT-29	Carbonate	Na-Ca-Cl	1278	21400	41200	4670	3490	512	117600	917	418	66	191	0.007798	-1.6	-24			0.70985	190200
[1]	OT-30	Carbonate	Ca-Na-Cl	1280	54900	53200	7790	5250	1060	222000	1780	129	95	10	0.008018	0.4	-35	-0.31		0.70827	346100
[1]	OT-31	Carbonate	Na-Ca-Cl	1279	23800	46200	5070	3960	564	137300	909	411	73	10	0.006621	-1.7	-20	-1.31		0.70992	218200
[1]	OT-32	Carbonate	Na-Ca-Cl	1259	23800	45900	5170	3770	546	134100	890	400	61	708	0.006637	-1.5	-25				214600
[1]	OT-33	Carbonate	Na-Ca-Cl	1289	21600	41900	4110	3890	518	117500	725	460	57	7	0.006170						190700
[1]	OT-34	Carbonate	Na-Ca-Cl	1290	22200	44100	4280	3990	550	133000	911	474	71	6	0.006850	-1.8	-29			0.71027	209500

Author Sample Name		Rock Type	Water Type	Depth m	Ca mg/L	Na mg/L	Mg mg/L	K mg/L	Sr mg/L	Cl mg/L	Br mg/L	SO_4 mg/L	HCO_3 mg/L	F mg/L	Br/Cl	$\delta^{18}O$ (VSMOW) (‰)	$\delta^{2}H$ (VSMOW) (‰)	$\delta^{37}Cl$ (SMOC) (‰)	$\delta^{81}Br$ (SMOB) (‰)	$^{87}Sr/^{86}Sr$	TDS mg/L
Middle Ordovician (Trenton)																					
[1]	OT-35	Carbonate	Na-Ca-Cl	1292	20700	42500	4090	3650	507	126400	872	535	96	8	0.006899	-1.8	-25			0.71010	199300
[1]	OT-36	Carbonate	Na-Ca-Cl	1292	21400	42500	3960	3770	478	126100	650	505	48	8	0.005155						199400
[1]	OT-37	Carbonate	Na-Ca-CT	1288	20900	43000	4130	3760	508	125700	877	491	75	7	0.006977	-1.5	-33			0.71003	199400
[1]	OT-38	Carbonate	Na-Ca-Cl	1293	25300	41800	4720	3300	477	131800	789	507	<7	7	0.005986	-2.4	-34			0.70994	208700
[1]	OT-39	Carbonate	Na-Ca-Cl	637	13100	38800	3670	2010	473	101900	510	415	61		0.005005	-2.7	-26			0.70958	160900
[1]	OT-40	Carbonate	Na-Ca-Cl	308	9850	36400	3720	1840	524	86600	460	66	66		0.005312	-3.0	-28	-1.09		0.70929	139500
[1]	OT-41	Carbonate	Na-Ca-Cl	310	10800	36400	3850	1850	496	87000	440	66	137		0.005057	-2.8	-28	-0.60		0.70938	140900
[1]	OT-42	Carbonate	Na-Ca-Cl	614	10500	37500	3670	1880	567	87500	460	<15	76		0.005257	-2.6	-28			0.70929	142100
[6]	UN-2 #13	Carbonate	Na-Ca-Cl	50	6250	8120	1840	141	277	26975	282	175	53		0.010454	-6.4	-52	-0.32	2.15	0.71057	44113
[6]	OHD-1 #13	Carbonate	Ca-Na-Cl	204	26600	18400	3280	321	515	86700	755	125	41		0.008708	-6.1	-52	0.09	1.93	0.70993	136737
[6]	UN-2 #11	Carbonate	Na-Ca-Cl	85	15100	17900	4080	271	705	63050	635	210	32		0.010071	-5.7	-47	-0.30	2.08	0.71060	101983
Middle Ordovician (Black River)																					
[6]	OHD-1 #7	Carbonate	Ca-Na-Cl	295	58000	37100	7080	636	1210	192045	1555	140	<7		0.008097	-4.8	-41	0.08	1.73	0.70981	297766
[6]	UN-2 #5	Carbonate	Ca-Na-Mg-Cl	175	36000	40800	11200	709	1130	159900	1445	165	26		0.009037	-6.0	-46	-0.13	1.18	0.71042	251375
[6]	OHD-1 #5A	Carbonate	Ca-Na-Cl	326	57800	35700	7100	641	1200	186000	1620	145	29		0.008710	-4.8	-42				290235
[6]	OHD-1 #5B	Carbonate	Ca-Na-Cl	326	59000	38500	7230	651	1220	182000	1595	155	<7		0.008764	-4.6	-42	0.32			290351
[6]	OHD-1 #3	Carbonate	Ca-Na-Cl	353	58500	35100	7150	649	1220	200500	817	150	<7		0.004075	-4.6	-41	0.11	1.78	0.70979	304086
[6]	UN-2 #2	Carbonate	Na-Ca-Cl	210	15000	17400	4090	322	335	59000	619	575	44		0.010492	-6.7	-49	0.01	1.92	0.71027	97385
[6]	UN-2 #4	Carbonate	Ca-Na-Mg-Cl	190	23400	24900	7230	469	488	96000	935	520	45		0.009740	-5.2	-47	-0.14	1.94	0.71038	153987
[6]	OHD-1 #2	Sandstone	Ca-Na-Cl	368	58300	37600	7200	657	1220	189000	1620	155	<7		0.008571	-4.5	-42	0.10	1.76	0.70981	295752
Early Ordovician (Prairie du Chien)																					
[1]	OP-1	Sandstone	Ca-Na-Cl	3425	68000	26700	7200	14200	2350	205000	1930	63	<7		0.009415	-1.6	-50	-0.95	-0.55	0.70930	325400
[2]	LAHAR 1-7	Sandstone	Ca-Cl		89200	30120	7560	12720	3632	245673	1719	83			0.006997			-0.26			390707
[2]	FOSTER 1-21	Sandstone	Ca-Na-Cl		65250	43500	5568	9483	2906	215081	2311	43			0.010745			-0.18			344142
[2]	PRASS 1-12	Sandstone	Ca-Cl		67600	22702	5744	10600	2848	179576	2229	91			0.012413			-0.34			291389
[1]	OP-2	Sandstone	CaCl	3234	87500	22600	8700	18400	2850	249700	1780	<30	<7		0.007129			-1.04	-0.73	0.70923	391500
Cambrian																					
[1]	C-1	Sandstone	Ca-Na-Cl	1217	47900	41000	6750	1410	1210	179000	1680	277	<7		0.009385	-4.0	-29	-0.24		0.71028	279200
[1]	C-2	Sandstone	Ca-Na-Cl	1095	60000	47700	6710	1340	1640	218700	1420	52	21		0.006493	-4.4	-28	-0.16	1.17	0.71002	337600
[1]	C-3	Sandstone	Ca-Na-Cl	1097	60200	48500	6680	1330	1690	205600	1550	47	19		0.007539	-4.6	-28	-0.15	0.93		325600
[1]	C-4	Sandstone	Ca-Na-Cl	1212	57800	49900	7710	1480	1170	186100	1710	96	<7	11	0.009189	-4.6	-35	-0.20	0.72	0.70990	306000
[1]	C-5	Sandstone	Ca-Na-Cl	1070	32100	24900	3240	645	1010	110100	1110	980	<7		0.010082	-4.1	-36	0.19		0.70957	174100
[1]	C-6	Sandstone	Na-Ca-Cl	1011	22400	40100	4380	2060	418	108400	792	645	<7	11	0.007306	-1.4	-28	-0.50		0.71007	179200
[1]	C-7	Sandstone	Ca-Na-Cl	1209	46500	43400	5860	1380	1210	176500	1510	247	<7		0.008555	-3.3	-21			0.70986	276600
[1]	C-8	Sandstone	Ca-Na-Cl	1264	51200	50800	6510	1810	1320	193400	2260	134	<7		0.011686	-3.3	-28	-0.31	1.07	0.70990	307400
[1]	C-9	Sandstone	Ca-Na-Cl	1201	52800	45000	7060	1560	1290	191800	1450	131	17		0.007560	-3.6	-29	-0.12	0.96	0.70980	301100
[1]	C-10	Sandstone	Ca-Na-Cl	1203	50500	43600	6900	1550	1210	183800	1440	169	17		0.007835	-3.8	-32	-0.06			289200
[1]	C-11	Sandstone	Ca-Na-Cl	1149	43600	47700	5340	1570	1130	168700	1610	210	<7		0.009544	-2.0	-24	-0.40		0.71029	269900
[1]	C-12	Sandstone	Ca-Na-Cl	1087	53500	42100	5670	1150	1230	183000	1770	138	<7		0.009672						288600
[1]	C-13	Sandstone	Ca-Na-Cl	887	54800	44200	7180	937	1210	194900	1835	146	<1		0.009415			0.10	1.51	0.70951	305200
Precambrian																					
[6]	OHD-1 #1	Granitic	Ca-Na-Cl	380	68500	32200	5030	499	1400	178400	1635	143	<1		0.009165	-5.3	-44	0.30			287807

Table A2: Geochemical data and stable isotopes of the formation waters in southern Ontario (from Skuce et al. 2015).

Sample ID	Formation of Origin	Ca mg/L	Na mg/L	Mg mg/L	K mg/L	Sr mg/L	Cl mg/L	Br mg/L	SO_4 mg/L	HCO_3 mg/L	Br/Cl	$\delta^{18}O$ (VSMOW) (‰)	$\delta^{2}H$ (VSMOW) (‰)	$\delta^{37}Cl$ (SMOC) (‰)	$\delta^{81}Br$ (SMOB) (‰)	$^{87}Sr/^{86}Sr$	TDS mg/L
Port Dover Quarry	Dundee (subcrop)	190	227	26	7.5	2.3	230	<3	42	168	0.0130	-7.5	-53	0.04	0.07	0.70894	901
T012149 (D)	Dundee (subcrop)	487	846	155	33.1	30.3	2478	20	370.8	145	0.0081	-10.8	-74	-0.26	0.78	0.70863	4678
T012101	Dundee	149	627	99	20.3	–	1128	8	16	–	0.0071	-15.7	-111				2518
T011050	Dundee	140	587	51	55.8	2.7	910	3.3	79.5	522	0.0036	-10.4	-66	0.57	1.06	0.70858	2356
T012150 (D)	Dundee	834	1160	23	101	28.8	3900	24	180	146	0.0062	-13.4	-90	0.91	1.49	0.70833	6385
T009537	Dundee	2050	6850	1460	216	46.3	18000	130	2100	351	0.0072	-8.5	-63	0.25	0.30	0.70829	31260
T008979	Dundee	1110	4830	943	129	29.3	18000	76	540	276	0.0042	-9.2	-65	0.03	1.00	0.70842	25952
F013661	Dundee	255	290	59	10.8	6.8	450	<3	27	365	0.0067	-11	-75			0.70851	1453
F005427	Dundee	649	202	49	8.5	4.5	580	3	320	141	0.0052	-15.1	-105				1963
T012111	Dundee	155	676	82	29	12.9	993	ND	18.9	–	–	-14	-94			0.70866	1976
T012111 (3)	Dundee	144	755	118	28.4	9.7	2600	13	260	3	0.0050	-10.1	-70	0.10	1.89	0.70862	3945
TAQA North battery	Columbus	183	830	149	22.5	23.5	1900	13	13	379	0.0068	-15.7	-115	0.21	0.72	0.70826	3542
T009308	Columbus	388	2410	381	62.3	36.5	5600	33	17	646	0.0059	-14.2	-104	0.15	1.37	0.70812	9618
T007578	Columbus	212	833	150	16.7	16.2	1500	9.8	39	339	0.0065	-15.8	-118	0.22	0.97	0.7083	3133
T012124(L)	Lucas	895	424	0.5	91.1	–	963	5.6	77	–	0.0058	-13.7	-86				2592
T012145 (L1)	Lucas	3060	8312	1540	454	67.1	20077	133	1352.1	159	0.0066	-6.6	-43	0.35	0.58	0.70842	35688
T012145 (L2)	Lucas	1585	7530	1185	136	100	16378	86	1323.6	255	0.0053	-6.6	-39			0.70813	29278
T012146	Lucas	641	3350	459	91.7	60.5	8300	31	640	101	0.0037	-6.8	-51	0.79	0.91	0.70809	13696
Oil Springs 2	Lucas	2854	6474	1674	252	69.3	18680	137	937.2	217	0.0073	-7.2	-46	0.74	1.02	0.70826	32142
Oil Springs 3	Lucas	3473	8316	2071	308	83.3	23556	158	994.9	201	0.0067	-6.5	-44	0.51	0.98	0.70823	40156
Oil Springs 4	Lucas	3248	7811	1890	334	81.6	22938	321	948	210	0.0140	-6.8	-45			0.70818	38663
T012152 (L)	Lucas	743	1247	142	78	18.7	3434	33	56.7	160	0.0096	-15.5	-113	0.14	0.92	0.70921	5944
T009650	Lucas	1880	5080	916	198	30.3	13000	57	1900	241	0.0044	-7	-43	0.92	0.77	0.70827	23328
T005511	Lucas	1440	5770	928	135	30.1	13000	64	1900	308	0.0049	-7	-45	0.81	1.06	0.70824	23601
LAI front battery	Lucas	1490	4630	876	155	25.1	11000	57	1800	250	0.0052	-6.5	-42	0.92	1.49	0.70825	20339
T011323	Lucas	1310	4290	852	122	31.5	11000	58	1900	344	0.0053	-6.5	-41	1.00	1.06	0.70823	19929
T012149 (L)	Lucas	556	301	198	11	14.6	355	1.6	2000	270	0.0045	-13.8	-95			0.70815	4343
McGregor Quarry 1	Lucas	467	204	225	16.6	12.6	380	<3	1690.1	125	0.0079	-16.3	-118	0.23	1.55	0.70836	3769
McGregor Quarry 2-1a	Lucas	350	94	169	6.2	12.8	170	<3	1319.9	242	0.0176	-16.2	-119			0.70844	2792
McGregor Quarry 2-1b	Lucas	353	253	175	–	13.8	301	–	1401	–	–	-16.7	-122				2497
St. Mary's Quarry	Lucas	146	64	32	2.5	16	22	<3	210	85	0.1364	-10.5	-69			0.70815	580
Goderich harbour well	Lucas	519	102	114	1.9	14.9	230	3	1300	183	0.0130	-12.5	-83			0.70807	2474
T012135	Amherstberg	15500	36100	3890	1240	226	80000	658	366	5	0.0082	-6.7	-53	-0.15	0.45	0.70928	138066
T012152 (DR)	Amherstberg	2520	2680	1.1	260	73.3	9700	85	13	50	0.0088	-8.6	-63	-0.04	0.53	0.70925	15342
T012177	BassIslands	629	370	20	10.6	12.2	870	<3	1300	27	0.0034	-11.2	-74			0.70817	3241
T012177 (2)	BassIslands	543	836	45	33.8	16.3	1600	<3	1300	21	0.0019	-10.5	-77			0.70823	4382
T002484	Salina E-unit (subcrop)	799	1320	149	80.7	17	3500	33	56	160	0.0094	-9	-62	0.40	1.69	0.70868	6208
Sulphur Springs C. A.	Salina E-unit (subcrop)	567	7	52	2.1	12.6	8.6	3	1200	212	0.3488	-11.7	-81			0.7085	2070

Sample ID	Formation of Origin	Ca mg/L	Na mg/L	Mg mg/L	K mg/L	Sr mg/L	Cl mg/L	Br mg/L	SO_4 mg/L	HCO_3 mg/L	Br/Cl	$\delta^{18}O$ (VSMOW) (‰)	$\delta^{2}H$ (VSMOW) (‰)	$\delta^{37}Cl$ (SMOC) (‰)	$\delta^{81}Br$ (SMOB) (‰)	$^{87}Sr/^{86}Sr$	TDS mg/L
Brantford spring	Salina A-2 (subcrop)	567	61	28	2.3	0.3	500	0.3	38	284	0.0006	-10.2	-69			0.70881	1488
Goderich salt mine N	Salina A-2 carbonate	84085	31007	15177	7431	1470	240000	3502	89	22	0.0146	4	-41	0.02	0.21	0.7086	383732
T007498	Salina A-2 carbonate	38900	91900	6050	5690	747	245695	1936	200	38	0.0079	-1.6	-37	0.35	0.70	0.70887	391550
T008641	Salina A-2 carbonate	57700	79300	8940	5600	1070	220000	1800	230	5	0.0082	-0.6	-37	0.27	0.79	0.70856	374770
T008633	Salina A-1 carbonate	35982	62939	7680	2660	708	191512	1863	244	<2	0.0097	-1.2	-32	-0.21	0.13	0.70946	303892
T007583	Salina A-1 carbonate	54222	52336	8269	3654	924	207443	2734	150	<2	0.0132	-0.7	-38	-0.40	-1.29	0.70848	330281
T001539	Salina A-1 carbonate	74600	48300	14100	7330	1240	370000	2700	110	<2	0.0073	1.5	-47	-0.23	-0.05	0.7085	518533
T011888	Salina A-1 carbonate	42100	46100	8300	6910	839	180000	1800	250	84	0.0100	-2.7	-49	-0.32	-0.21	0.70879	286440
T008596	Salina A-1 carbonate	39900	79200	9270	4880	946	190000	1300	360	16	0.0068	-4.2	-50	-0.20	-0.13	0.70839	325930
T003536	Salina A-1 carbonate	35600	99600	13500	4130	780	210000	1700	250	5	0.0081	-0.8	-34	-0.28	0.31	0.70928	365643
T008657-1	Guelph	11886	36917	2617	697	185	100904	501	624	–	0.0050	-4.1	-43				154554
T008657-2	Guelph	26665	85500	5874	1623	408	180000	920	330	2	0.0051	-3.2	-41	0.20	0.07	0.70877	301858
T002235-1	Guelph	6780	112000	987	600	143	180000	260	1200	4	0.0014	-11.1	-77	0.31	0.06	0.7088	302015
T002235-2	Guelph	6800	143300	1100	605	161	160000	280	1400	4	0.0018	-2.6	-37				313207
T012124 (G) - A	Guelph	36432	47580	7862	2121	–	169944	1741	203	–	0.0102	-2.5	-36				265883
T012124 (G) - B	Guelph	35863	46874	7707	2033	–	170591	1769	201	–	0.0104	-2.7	-33	-0.24	0.56	0.7092	265039
T012150 (G)	Guelph	20100	98000	4850	2790	403	160000	1200	660	93	0.0075	-1.2	-39	-0.20	-0.49	0.70928	288158
North Seckerton battery	Guelph	43200	56100	6850	3540	1140	170000	1800	340	16	0.0106	-1.3	-33	-0.23	-0.22	0.70928	283048
Corunna battery	Guelph	44700	76600	6700	4100	943	220000	2100	250	<2	0.0095	-0.1	-41	-0.31	-0.77	0.70927	355477
Seckerton battery	Guelph	69600	52700	8210	4810	1210	180000	2800	130	13	0.0156	0.7	-38	-0.30	-0.42	0.70911	319540
Ladysmith battery	Guelph	70300	54896	10620	5550	1310	240000	2600	130	<2	0.0108	2.4	-49	-0.46	-0.52	0.7092	385484
Moore Brine Facility	Guelph	102000	72600	16800	5420	1420	240000	2800	120	3	0.0117	1.9	-43	-0.40	-0.82	0.70937	441259
Den-Mar Brine Facility	Guelph	99500	61700	13700	6020	1550	230000	3000	130	26	0.0130	-0.3	-38	-0.10	0.78	0.71049	415714
T004912	Guelph	91900	71000	5660	1570	2030	190000	1800	100	<2	0.0095	-5.6	-40	0.09	-0.55	0.70917	364171
T004678	Guelph	13800	38000	3120	1190	294	95000	710	1000	70	0.0075	-2.8	-40	-0.03	-0.21	0.7089	153210
T005442	Guelph	30700	106000	5740	3430	817	200000	1300	360	31	0.0065	-6.6	-57	-0.17	0.05	0.70915	348436
Lowrie Dawn battery	Guelph	18700	52000	4360	1730	423	110000	890	140	5	0.0081	-1.3	-52	-0.34	0.08	0.7088	188314
T010097	Guelph	80825	31308	13753	3696	1306	222203	3853	95	<2	0.0173	-6.9	-63	0.02	-0.21	0.70854	358146
T001521	Guelph	21400	83400	4950	2670	415	120000	970	740	<2	0.0081	-3	-36				234622
T008932	Clinton-Cataract	37804	50782	6599	1207	–	152763	1566	421	–	0.0103	-3.2	-47				251142
T008812	Clinton-Cataract	31237	47267	5679	1086	–	135938	1324	458	–	0.0097	-4.1	-38			0.71033	222989
T011830	Clinton-Cataract	29300	48200	5510	765	543	150000	1100	560	<2	0.0073	-4	-39				236120
T010691	Clinton-Cataract	27307	40097	6138	978	–	122542	1133	519	–	0.0092	-3.1	-48				198714
T011549	Clinton-Cataract	30052	45848	6326	1070	–	145041	1408	475	–	0.0097	-2.9	-36				230220
T005741	Clinton-Cataract	33932	48770	5631	1024	–	150503	1511	340	–	0.0100	-3.5	-54				241711
T004185	Clinton-Cataract	35462	50741	6416	1177	–	153560	1562	297	–	0.0102	-0.9	-39	0.29	1.59	0.71045	249215
T003188	Clinton-Cataract	58000	59300	10800	1670	1220	250000	2400	180	<2	0.0096	-1.9	-42	0.25	1.50	0.71036	383666
T011814	Clinton-Cataract	53000	59500	9920	1700	1130	280000	1900	260	<2	0.0068	-1.2	-20	-0.13	0.35	0.71035	407661

Sample ID	Formation of Origin	Ca mg/L	Na mg/L	Mg mg/L	K mg/L	Sr mg/L	Cl mg/L	Br mg/L	SO_4 mg/L	HCO_3 mg/L	Br/Cl	$\delta^{18}O$ (VSMOW) (‰)	$\delta^{2}H$ (VSMOW) (‰)	$\delta^{37}Cl$ (SMOC) (‰)	$\delta^{81}Br$ (SMOB) (‰)	$^{87}Sr/^{86}Sr$	TDS mg/L
T009153	Trenton-BlackRiver	27300	57400	5610	3340	768	180000	1100	330	<2	0.0061	-1.5	-22	-0.45	0.77	0.7103	275902
T010019	Trenton-BlackRiver	27800	79000	6220	3120	871	150000	1200	360	<2	0.0080	-1.6	-20	-0.37	0.43	0.71055	268628
T007330	Trenton-BlackRiver	28500	57500	5710	3120	631	170000	1200	350	<2	0.0071	-1.7	-24	0.31	0.58	0.71042	267071
T007636	Trenton-BlackRiver	28950	62900	5730	3070	634	160000	1300	380	<2	0.0081	-1.5	-22	-0.28	0.89	0.7104	263024
T008358	Trenton-BlackRiver	30100	75700	6620	3200	758	170000	1200	400	20	0.0071	-1.4	-23	-0.41	0.52	0.71038	288050
T009605	Trenton-BlackRiver	32500	89400	7360	3730	965	150000	1200	300	<2	0.0080	-1.4	-21	-0.47	0.29	0.71032	285523
T007954	Trenton-BlackRiver	27400	58100	6067	3100	806	170000	1200	210	3	0.0071	-1.6	-18	-0.44	0.38	0.71034	266940
T008313	Trenton-BlackRiver	27900	61100	6200	3090	686	160000	1200	360	8	0.0075	-0.9	-31	-0.11	0.65	0.71031	260593
T008057	Trenton-BlackRiver	70900	85900	9180	3940	1220	230000	1600	300	<2	0.0070	-1.8	-27	-0.49	0.70	0.71033	403179
T009859	Trenton-BlackRiver	38900	63100	8080	3600	843	190000	1600	250	<2	0.0084	-1.2	-25	-0.16	0.30	0.71011	306446
T007240	Trenton-BlackRiver	42700	71900	7620	2890	1070	230000	2000	200	<2	0.0087	-1.5	-24	-0.19	0.38	0.71008	358453
T006658A	Trenton-BlackRiver	41335	65700	7090	2800	956	182278	1935	197	<2	0.0106	-2.6	-11			0.70991	302689
T007793	Trenton-BlackRiver	1360	1830	321	46	10.1	4143	22	7.2	<2	0.0053	-2	-36	-0.14	0.74	0.70988	7934
T005912	Cambrian	85000	86500	8440	2490	1510	210000	2100	140	3	0.0100	-1.5	-28	-0.22	0.00	0.70951	396232
T001591	Cambrian	37300	90100	8220	4000	766	200000	2000	220	8	0.0100	-3.4	-25	-0.09	1.21	0.7098	342669
T001303	Cambrian	48800	62000	6760	2200	1420	200000	2300	220	<2	0.0115	-2.6	-34	-0.10	1.01	0.70979	323747
T011362	Cambrian	94200	72200	8540	2780	1750	220000	2300	160	<2	0.0105	-2.7	-39				402027
T001343	Cambrian	37600	50400	6240	1950	889	170000	1900	470	<2	0.0112	-3.6	-27	-0.14	0.99	0.70983	269504
T008532	Cambrian	56634	49690	6740	1232	1385	191086	2390	120	<2	0.0125	-4.3	-38	0.30	1.54	0.7093	309954
T008532 (2)	Cambrian	78200	47400	9590	1760	1910	240000	2400	120	<2	0.0100	-3.6	-44	0.27	1.50	0.7093	381499
T007369	Cambrian	47535	50228	5768	1615	1131	180000	1800	200	<2	0.0100	-2	-20	-0.23	0.19	0.71033	288769
T007369 (2)	Cambrian	46700	64300	6250	2390	1170	300000	1800	240	<2	0.0060	-1.9	-24	-0.27	0.45	0.71027	422936
F014364	uncertain shallow aquifer	17	80	9	3.2	0.6	20	<3	22	259	0.1500	-10.2	-70			0.70919	419
F020066 / T012165	uncertain shallow aquifer	615	330	182	18.2	12	760	8.7	1800	81	0.0114	-10.7	-73	-0.01	1.90	0.70895	3814
T012116	uncertain shallow aquifer	637	30	37	3.9	8.1	80	0.7	640	163	0.0088	-10.3	-70			0.70843	1602
Hemlock Creek 1	uncertain shallow aquifer	70	36	27	5.7	1.2	63	0.3	120	166	0.0048	-9.8	-68			0.70894	493
Ancaster sulphur spring	uncertain shallow aquifer	750	1450	182	59	34.3	4000	43	420	181	0.0108	-10.6	-69	-0.11	2.21	0.70995	7130
Church Road Spring	uncertain shallow aquifer	710	461	227	42.3	12.8	960	11	1800	160	0.0115	-12.1	-90			0.70881	4391
Twelve Mile Creek	uncertain shallow aquifer	114	37	39	3.1	1	68	0.5	72	383	0.0074	-10.5	-78			0.71072	724
TAQA North flood water	drift aquifer	77	197	38	4.5	3.6	620	3	2	249	0.0048	-16.5	-121			0.70876	1209
T0121355	probably Dundee/Lucas	192	1320	178	30.3	11.1	1500	11	110	281	0.0073	-14.2	-98			0.70871	3673

Table A3: Geochemistry and stable water isotopes of the porewaters from DGR-3 at the Bruce Nuclear Site. (Due to potential errors in crush and leach preparation the $\delta^{81}Br$ and $\delta^{37}Cl$ isotopic values for DGR-3 are suspect and not used in the discussion)

Note: Geochemical, ^{18}O and ^{2}H analyses are from Clark et al. (2010). The analytical precisions for the $\delta^{18}O$, $\delta^{2}H$, $\delta^{37}Cl$ and $\delta^{81}Br$ isotopic values are ±0.15‰, ±1.50‰, ±0.15‰ and ±0.09‰, respectively.

Borehole	Depth rel. to DGR1/2 (m)	Stratigraphic Unit	Cl (mg/L)	Br (mg/L)	Sr (mg/L)	K (mg/L)	Na (mg/L)	Ca (mg/L)	Mg (mg/L)	SO_4 (mg/L)	HCO_3 (mg/L)	$\delta^{37}Cl$ (SMOC) ‰	$\delta^{81}Br$ (SMOB) ‰	$\delta^{18}O$ (VSMOW) ‰	$\delta^{2}H$ (VSMOW) ‰
DGR3 161.67-4	142.91	Bass Islands	2249		1086	141	2529	3274	1371	13737				-14.3	-107
DGR3 187.72-8	169.72	Salina G	389	1	175	246	874	8256	1833	28530	93			-11.2	-107
DGR3 198.96-8	181.13	Salina F	8984	1	149	704	5862	10260	1322	35350				-8.0	-80
DGR3 207.94-4	190.39	Salina F	20293	19	149	860	12645	8216	812	28242				-7.9	-70
DGR3 248.47-4	230.45	Salina E	45639	41	184	1095	34853	12745	814	50239	158			-10.3	-72
DGR3 270.29-4	250.26	Salina C	138813	117	61	12	345	10581	126	27377					
DGR3 274.38-4	255.66	Salina C	179481	141	166	1408	110789	19678	1184	55715				-11.9	-61
DGR3 298.73-4	285.93	Salina B evap	193254	249							8			-8.3	-67
DGR3 311.79-3	299.70	Salina A2 carb	74870	100	718	821	54762	6853	3621	27953	126	0.86		-9.7	-70
DGR3 348.31-2	333.95	Salina A1 carb	54775	30	1174	1408	62142	43845	9090	190679	821				
DGR3 379.89-2	367.07	Salina A1 carb	173422	1157							2747				
DGR3 399.31-2	385.90	Goat Island	208995	2101	1726	16108	64142	118911	23406	228623	1403		-0.19		
DGR3 417.60-5	404.84	Goat Island-Fossil Hill	577210	2843	3356	6256	243418	80877	32739	73774	652	-0.09	-0.22		
DGR3 432.79-4	420.63	Cabot Head	221439	2482	1700	14818	46532	57071	12590	672	104	0.20	0.85	-2.4	-49
DGR3 445.08-1	432.47	Cabot Head	228204	2952	1709	17320	47727	68974	13854	31316	220	0.12		-3.5	-51
DGR3 453.95-6	442.45	Manitoulin	253808	3187	2173	17281	57107	139512	32277	202687			1.37		
DGR3 462.01-1	452.39	Queenston	227084	2970	1498	16929	52164	75066	12809	44668	510		1.17	-3.1	-46
DGR3 478.13-4	467.63	Queenston	226796	3162	1157	14584	47038	47813	14705	2786		0.07	0.00	-2.8	-49
DGR3 496.75-2	485.24	Queenston	215685	2616	1174	17516	47819	48294	13392	11815		0.47	0.49	-2.6	-48
DGR3 517.30-6	504.67	Queenston	216029	2300	1297	16147	48417	51580	11180	20941		0.03	0.15	-3.2	-49
DGR3 539.46-1	526.26	Georgian Bay	280610	2520	1586	15913	79453	53544	14632	18636		-0.09	1.52	-2.6	-47
DGR3 559.95-5	547.26	Georgian Bay	218713	2279	1533	15483	53498	53143	9285	7012		-0.27	0.43	-3.1	-49
DGR3 581.28-3	569.12	Georgian Bay	212431	2371	1542	16030	54325	50138	12614	25648	5628	0.19	1.59	-3.9	-54
DGR3 604.99-1	593.42	Georgian Bay	205727	2145	1446	13880	51176	49857	8774	20173	2413	0.04	0.57	-3.4	-56
DGR3 629.38-7	617.87	Blue Mountain	216682	2267	1770	15756	64004	65047	10232	19212		-0.26	1.20	-4.5	-59
DGR3 641.00-1	628.76	Blue Mountain	211842	2040	1586	12863	57935	59035	8823	20845	1719	0.19		-4.5	-57
DGR3 651.99-8	639.71	Blue Mountain	207166	1958							2059	-0.03		-4.6	-49
DGR3 662.21-2	649.58	Blue Mountain	205323	1870							5445	-0.25	0.63	-6.0	-68
DGR3 675.69-5	662.27	Cobourg	206372	2083	1770	16265	71775	48454	22142	48126	2370	-0.60	0.70	-5.0	-49
DGR3 685.04-5	671.89	Cobourg	191918	1976	1411	16108	61843	42443	18302	53890		-0.87	0.56		
DGR3 702.54-5	689.73	Sherman Fall	208297	2044	1735	17047	64740	88051	30673	141208	4148	-0.52	1.02	-5.5	-72
DGR3 723.88-1	710.42	Sherman Fall	160726	1486	1016	15366	55958	37232	9528	34293	8113	-1.02	1.06	-6.4	-48
DGR3 737.74-2	724.10	Kirkfield	155745	1322	771	9696	52210	23726	5080	2786	7108	0.23	0.69	-6.3	-55
DGR3 765.95-1	752.34	Kirkfield	147804	1209	789	8875	52279	22684	5858	3650	6605	-0.20	0.52	-7.2	-64
DGR3 783.2-5	769.38	Coboconk	184285	1522	1384	4496	54555	37072	18472	21133		-0.08	0.47	-5.7	-41
DGR3 800.18-1	785.91	Sherman Fall	109780	947	421	6412	51314	16713	6878	16042	35423	-0.57	0.66	-8.3	-50
DGR3 803.14	788.84	Sherman Fall										-1.02	1.03		
DGR3 810.98	796.68	Gull River										-0.36	0.52		
DGR3 814.42-1	800.68	Gull River	158415	1448	815	3206	46325	30259	15312	9126	4671	-0.73	0.99	-6.4	-47
DGR3 818.45	804.82	Gull River										-0.97	0.57		
DGR3 823.95	809.65	Gull River										-0.21	0.83		
DGR3 831.67	817.37	Gull River										-0.96	0.83		
DGR3 838.56	824.26	Gull River										-0.69	0.63		
DGR3 842.74	828.44	Gull River										-0.61	1.31		
DGR3 851.96-6	839.71	Shadow Lake	147272	1111	771	2737	43405	34748	5736	2017		-0.35	1.41	-6.3	-47
DGR3 855.66-5	843.96	Cambrian	166381	1425	929	2541	45658	35108	11423	2113		-0.56	1.34	-5.4	-48